EVALUATION OF THE NUCLEAR DENSITY/MOISTURE GAUGE AND STUDY OF

SOME MATERIAL PROPERTIES AFFECTING ITS PERFORMANCE FOR ROUTINE

HIGHWAY CONSTRUCTION QUALITY CONTROL IN KENYA.

BY

ABDALLA J. M. KULAH

A thesis submitted in partial fulfilment of the degree of

MASTER OF SCIENCE at the University of Nairobi.

1987

DECLARATIONS

This is my original work and has not been presented in any other University.

Signed:

Date:

This work has been submitted for examination with my approval as University Supervisor.

Signed:

Dr. J. P. Patel

Date:

ACKNOWLEDGEMENTS

Table of Contents

Table of contents continued

Table of contents continued

List of tables

List of Tables Continued

List of Figures

List of Figures continued

List of figures continued

List of figures continued

were within the range 0.4-1.1 (% moisture) and 17-46 kg/m^3 respectively.
The investigation shows that after correction for hydrogen contained
in water, density determinations with the nuclear gauge were of
even better accuracy.

It is concluded that recalibration is necessary for every new material
encountered. In addition, it is recommended that specifications
should be drawn based on gauge long term tests to define clearly
the acceptance of the gauge as a routine instrument for density
and moisture determination on roads.

CHAPTER ONE

1.   Introduction

1.1   General

The physical and mechanical properties of soils are primarily dependent on three factors: grain size, density and water content [1].   From these three basic properties, the values of plasticity, deformability, shear resistance and permeability can be determined. In the construction of roads, earth dams, air fields and in the preparation of foundations for buildings and other civil engineering structures and pavements, these data are necessary at all stages to meet the design requirements and stability for their satisfactory performance.   Most specifications in civil engineering now require a minimum degree of compaction and these have to be checked before the quality of the work is accepted.   These require a measurement of bulk density and moisture content which can be obtained by the use of conventional methods or radioisotope density and moisture gauges [2].

In most conventional methods of compaction control of road pavements and bases, some weak points exist.   The sand-replacement (on soils) and core cutting (on asphaltic concrete) methods of measuring bulk density are both subjective, destructive and time consuming, and the conventional methods for measuring moisture content by oven drying are too slow.   The use of gamma radiation attenuation for measuring the bulk density

of materials and slowing down of fast neutrons for determining
moisture content has received much attention. Against this
background, nuclear density and moisture gauges are being
used for the determination of density and moisture of construction
materials. These methods overcome the inadequacies caused by
the conventional techniques because of the following superior
features:-

i)   Non-destructive in-situ measurement;

ii) Measurements can be done on steep embankments, vertical
     surfaces and on materials like sand and course gravel
     where conventional methods are inaccurate;

iii) Testing is physically easier and more rapid; the
     gauges have simple measurement procedures which can
     be followed by relatively inexperienced workers;

iv) A field control strip (which involves the determination
     of the maximum density for a roller type on a particular
     material in the field) provides a basis of comparison
     with the achieved densities on construction site. The
     control strip method eliminates laboratory determination
     of the maximum density of a particular material;

v)   Construction costs are lower to both the contractor and
     the construction authority.

In an attempt to cut down costs, the Kenya Ministry of
Transport and Communications with other local civil engineering

firms have been using the nuclear density/moisture meters
since 1982. For the first time, they were used along Thuchi-
Nkubu road by the contracting firm (Sir Alexander Gibb & Partners)
to test compaction of earthworks and crushrun materials.
The results of these trials indicated accurate results for
density measurements but moisture contents were too erratic
to be of use [3]. Present users of the nuclear gauges in
Kenya have also reported difficulty in distinguishing between
water and air voids in bitumenous materials during density
determination [4].

1.2 STATEMENT OF THE PROBLEM

Despite the highly acceptable level of use of the radioisotope
gauges for highway and building construction quality control,
there still exists a need to study their performance on some
Kenya soils used for road construction. The need arises because
the nuclear gauges were factory calibrated by the manufacturers
on blocks. This consisted of the accumulation of count rate
data on a series of solid homogeneous stone and metallic blocks
of known density for determination of density versus count
rate computations and on a standard density block to verify
calibration accuracy. From these data, an "average soil"
density calibration curve was computed. In order to eliminate
long-term effects of source decay and electronic drift all data
are normalised to the reference standard count and expressed
as a ratio of count rate on material tested to count rate

on reference standard. Hence, gauge calibration on locally
available materials used for road construction and a study
of material properties affecting gauge accuracy are needed.

1.2.1 DENSITY

Soils in nature are heterogeneous. Typical soils have
a bulk density range of 1-2 g/cm^3; the elemental composition
can vary from the simple such as sand, to complex mineralised
soils containing 20 or more constituents. The abundance of
each element contributes to both mass density and the average
electron density of a soil. Both of these factors are of
importance when considering the passage of gamma rays through
a soil medium. In Gardner's report [5] on gamma ray soil
density measurements, three practical sources of error were
identified viz:

1. Inaccurate calibration techniques;

2. Sensitivity to soil composition;

3. Sensitivity to surface roughness.

Other shortcomings of density determination include:-

4. Effect of density difference along the measured depth
   and

5. Poor depth sampling (especially for backscatter mode.)

Although some authors [2], [5] have obtained satisfactory
results, [6], [7]; [9] found that different calibration curves
were required for different soils.

1.2.2 MOISTURE

The nuclear moisture measurement method depends on the moderation (slowing down) of fast neutrons by hydrogen atoms, and the free or easily evaporable water must be controlled in earth construction [10]. However, different soils have varying amounts of other forms of water such as hydrates, interlayer water and hydroxyl water and or high organic matter content. Also, some soils contain elements that absorb the slow neutrons which may affect the soil nuclear moisture test accuracy [11].

In view of the above, the factory calibration of the gauges may not necessarily represent the "true soil types" envisaged in actual road construction in Kenya. Hence, calibrations on sites should be done on each corresponding material encountered. Seemingly, these nuclear results for moisture and density determinations should be compared with those obtained by the conventional sand-replacement and core drilling tests.

1.3 AIM AND SCOPE OF THESIS

The objective of this study therefore was to:-

- investigate the reliability of Troxler model 3411-B surface gamma-neutron gauge for determining bulk densities and moisture contents for routine highway construction control in Kenya.

- to examine the usability of the factory calibration curves for density and moisture determination in various construction materials.

- to perform laboratory calibration for the gauge based on
  model samples prepared from different materials.
- to do field calibrations on various sites.

The investigations to be done are to embrace the comparison
study of eight different soils for use as base and subbase
materials and two asphalt concrete surfacings. The sand-replacement,
oven-dry and asphaltic concrete core cutting methods of determing
bulk density and moisture content are used for calibration of the
nuclear gauge. Also, studies of the effects of the variations
of density differences in the compacted soils, soil type and its
coarseness on the calibration of the apparatus are studied.

1.4 Literature Review

Literature review conducted obtained background information
concerning the factors affecting the nuclear density and moisture
techniques so that remedial measures can be employed for routine
highway construction control in Kenya.

During the mid 1950's most publications were concerned with
moisture and transmission-type density gauges. In 1958, Hoffmeyer
[12] reported that an average accuracy of ± 32 kg/m³ was obtained
by use of a surface density gauge using backscatter of gamma
rays. In 1960, Carlton [13] concluded that the reliability of

such a gauge for compaction control was comparable with that

of conventional methods. In 1965, The Virginia Council of

Highwat Investigation and Research conducted a conference so

that comparative tests could be run among nuclear gauges. Results

of this conference [14] showed standard errors of 176 kg/m^3 for

backscatter geometry gauges using conventional calibration

techniques and 41.6 kg/m^3 using the calibration technique

proposed by Khn [15]. Kuhn suggested that a calibration be

made by plotting the ratio (of the gauge response on surface

to the gauge response when raised to a predetermined height

usually 25 - 75 mm) versus density.

Gardner and Robert [5], proposed a mathematical model (presented

later herein) for density gauge response and used it to study

some of the data from Virginia Council Conference. The result

was that when the model was used to calculate the calibration

curves, 26 of the 42 results had standard errors of less than

38.4 kg/m^3 [16], and he also identified the errors for nuclear

density and moisture gauges. In 1965, Ballard and Gardner [17],

summarised their work which concluded that composition dependence

of density gauge response was the most significant source of

error and stressed that nuclear backscatter density gauge results

were more reproducible and comparable with the results from

conventional techniques. In 1967, Gardner and Roberts [5],

presented a complete analysis of the mathematical model for density

gauges and a thorough summary of the dual gauge studies.

The effect of chemical composition of soil on neutron moisture
calibration has been investigated by various workers. Couchet
[18], McHenry and Gill [19] found that the effect of 10ppm of Boron
in soil was equivalent to 200ppm of Chlorine or Cobalt or 600ppm
of Manganese or 300ppm of iron. Similarly, Jensen and Somer [20]
estimated that for moisture changes from 0 to 40%, an error
of 4.5% was introduced by iron content of 5% in the soils.

Lal [21] studied the effect of soil grain size on neutron
gauge calibration and concluded that for some soils, the grain
size has a significant effect on thermal neutron count rate.
Comparative nuclear moisture and density results of Sherwood [22],
Ahuja and Williams [23] and James [24] also reveal that not all
materials used in construction follow the calibration curves and
therefore give anomalous results.

CHAPTER TWO

2.0   Theory of Nuclear Measurement

2.1   Theory of Nuclear Gauge Determination

The basis of nuclear density determination is the interaction of gamma photons with the matter through which they are passing. For the determination of the bulk density of the soil, gamma radiation passing through the soil is scattered and absorbed by collisions with the electrons of the soil atoms.   The intensity of radiation reaching the detector is a function of the bulk density of the material; the intensity decreasing with increase of bulk density.

In the direct transmission density measurement (Fig. 1a), the intensity I of a monoenergetic collimated beam of radiation transmitted to the detector through a homogeneous soil layer of thickness X (cm) and density D is given by [5]:-

$$I = Io\ e^{-\mu DX} \qquad \text{------------------------------} \qquad (2-1)$$

where Io = photon intensity before interaction

$\mu(E,Z)$ = mass attenuation coefficient (cm^2/g) which is a
function of radiation energy and atomic number
for a particular element.

For broad beam situation, the attenuation is modified by:-

1. "Geometry factor", G which takes into account the source
and detector size since they are not points but displace
somewhat larger volumes.

2. "Build up factor" B, which takes into account secondary
    photons as a result of one or more Compton scatterings
    which reach the detector.

Thus, Eq. (2-1) becomes

$$I = B \, G \, Io \, e^{-\mu DX} \quad \text{-----------------------} \quad (2-2)$$

The intensity of the detected radiation follows an
experimental function as shown in Fig. 1b.

SURFACE

DEPTH

SOURCE

DETECTORS

SOIL

PHOTONPATHS
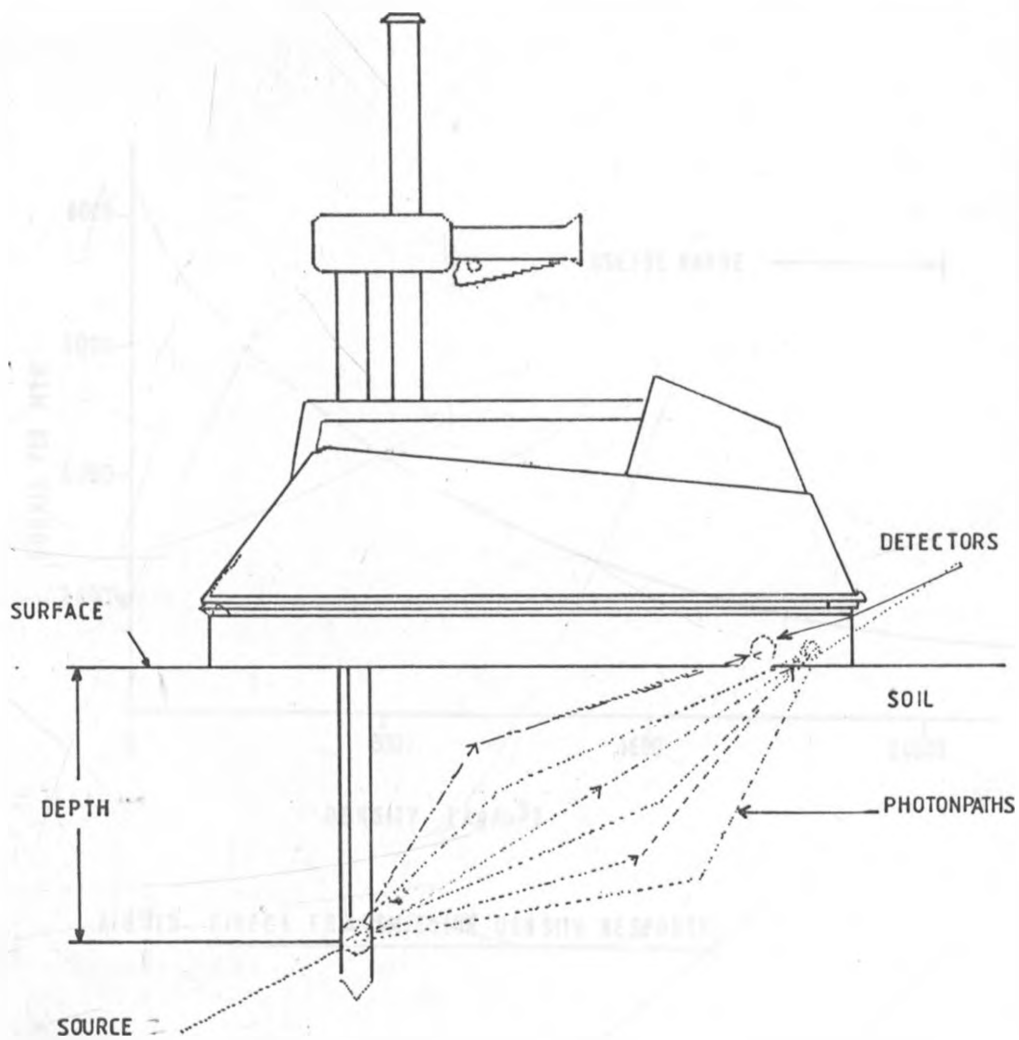
FIG. 10 DIRECT TRANSMISSION GEOMETRY
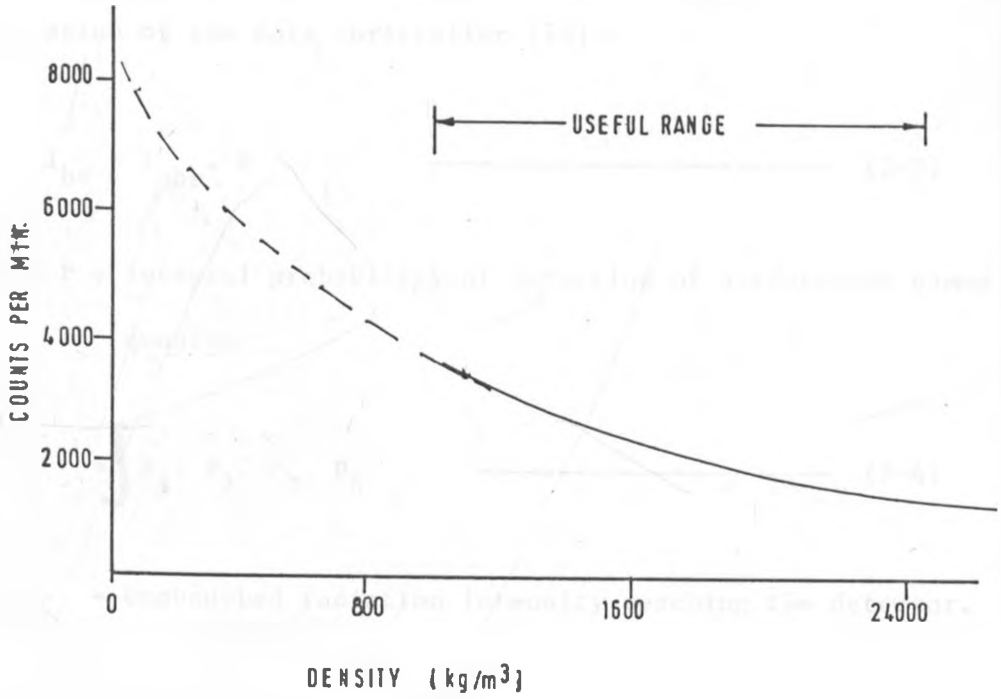
FIG·1b· DIRECT TRANSMISSION DENSITY RESPONSE

In the backscatter mode (Fig. 2a), the intensity I_{bs} of the scattered radiation reaching the detector situated at a distance r from the source is related to the source output by a relation of the form Christaller [25]:-

$$I_{bs} = I_{obs} \cdot P \qquad\qquad\qquad (2-3)$$

Where P = integral probability of detection of a scattered gamma quantum.

$$= \int P_1 \cdot P_2 \cdot P_3 \cdot P_4 \qquad\qquad\qquad (2-4)$$

I_{obs} = Unabsorbed radiation intensity reaching the detector.

Scattering events are characterised by two angles, θ and a rotational angle $\emptyset$. A photon travelling in a direction given by a vector $\overline{U}$ undergoes a scatter at a point given by the coordinates r, θ and leaves the interaction in a direction $\overline{V}$ (Fig. 2b). Scattering angles are determined by examining the probability of scattering into differential solid angle d (Fig. 2c). The probabilities P_1-P_4 are expressed in terms of cross-sections according to the type of scattering involved.
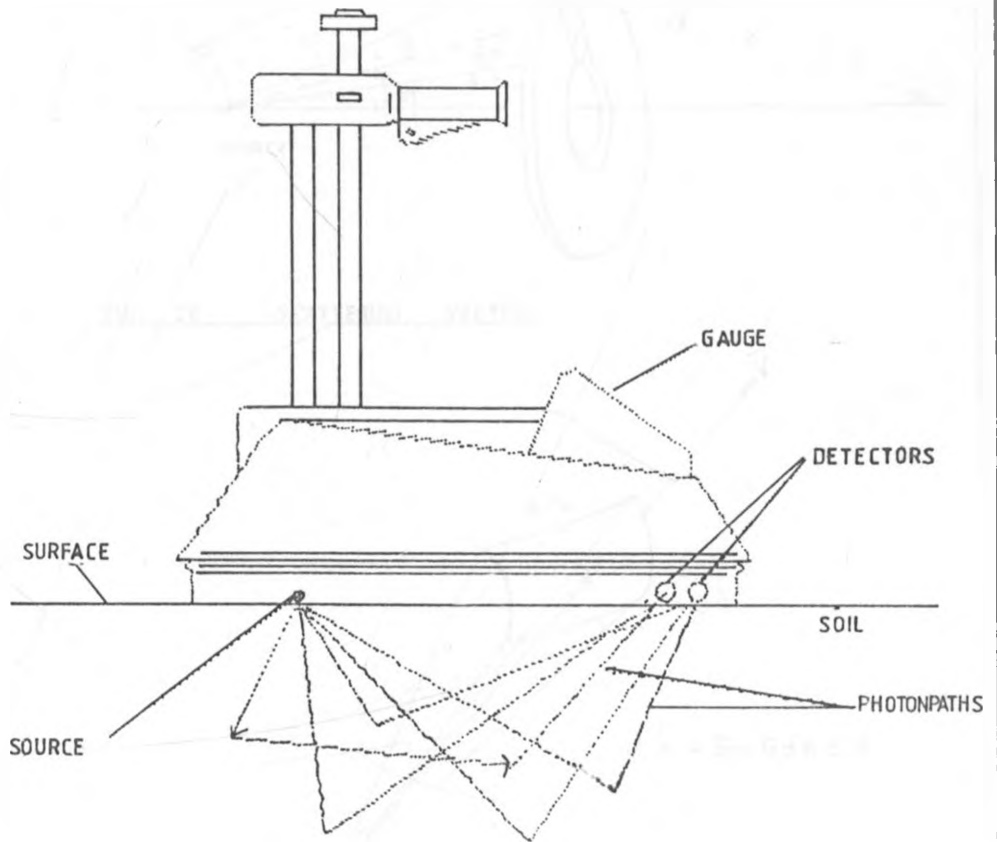
FIG 2a BACKSCATTER DENSITY GEOMETRY

From Eq. (2-2):

$$B_i = \frac{1}{4\pi r^2} \int \rho \, \sigma \, dV \qquad (2-3)$$
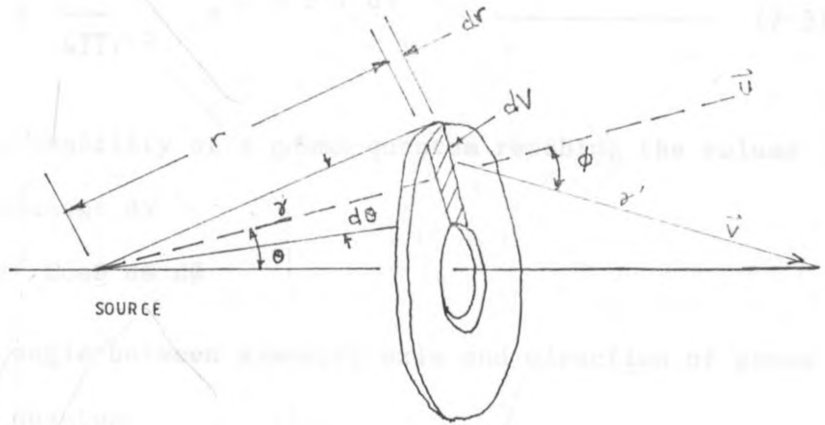
FIG. 2C   SCATTERING   VECTORS

where θ = angle between scattered ray and direction of gamma motion

$$d\Omega = \sin\theta \, d\theta \, d\phi$$
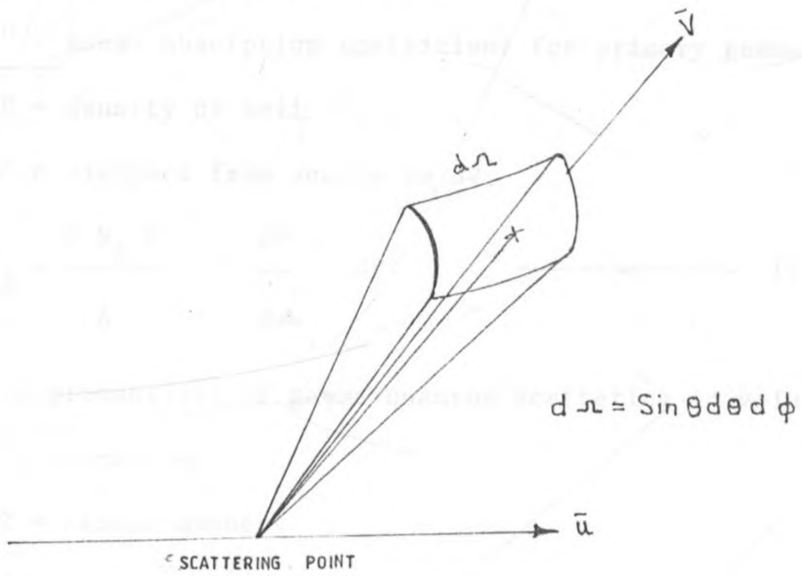
FIG. 2D   DIFFERENTIAL   SOLID   ANGLE   FOR   SCATTERING

From Eqn. (2-4):

$$P_1 = \frac{1}{4\Pi r'^2} e^{-\mu'' D r'} . dV \qquad \text{------------} \quad (2\text{-}5)$$

= probability of a gamma-quantum reaching the volume

element dV

$dV = r^2 \cos\theta \; d\theta \; d\emptyset$

Where θ = angle between symmetry axis and direction of gamma

quantum

$\emptyset$ = azimuthal angle

μ'' = mass- absorption coefficient for primary gamma-energy

D = density of soil

r' = distance from source to dV

$$P_2 = \frac{Z \, N_A \, D}{A} \quad \frac{d\theta}{d\Omega} \quad dr \qquad \text{------------} \quad (2\text{-}6)$$

= probability of gamma quantum scattering in volume

element dV.

Z = atomic number

A = mass number

N_A = Avogadro's number

$d\theta/d\Omega$ = differential cross-section for compton scattering

$$P_3 = e^{-\mu'_{sc} D t'} \qquad \text{------------------} \quad (2\text{-}7)$$

= probability of a scattered gamma-quantum reaching the

detector.

where μ'_{sc} = mass-absorption coefficient for scattered gamma

energy.

t' = distance from dV to detector.

$$P_4 = e^{-\mu'_d d}$$ -------------- (2-8)

P_4 = probability that a scattered gamma-quantum reaching

the detector produces a countable event (detection

efficiency).

where μ'_d = linear attenuation coefficient for the detector

material used.

d = linear geometrical value of the detector (a combination

of diameter and thickness).

To solve Eqn. (2-3), integration has to be done over the entire

volume and energy using complicated mathematical methods like

Monte Carlo calculations. By making simplifying assumptions

and putting all the integrals in a parameterised constant,

Eqn. (2-3) can be written [26] as:-

$$I_{bs} = K (\mu'D\ R) \frac{e^{-\mu'D\ r}}{4\Pi r^2}$$ ------------ (2-9)

where K is a constant and $\mu'(E,Z)$ is the total mass attenuation

coefficient for the scattered radiation and is constant for a

given medium. r is distance from source to detector.

For backscatter geometry, various authors have suggested

different approaches to achieve the best accuracy, starting from

the simple equation as used by Cameron [26], Eqn. (2-9) to more

complex functions suggested by Gardner [5]. This author takes into

consideration two major interactions of gamma rays with matter.

The response of a gamma-scatter gauge is dependent on two major interactions of gamma rays with soil: Compton scattering and photoelectric effect. The compton-scattering and the photoelectric effect cross-sections are respectively given by the proportionalities:-

$$\sigma_c \propto D \sum_{i=1}^{n} \frac{W_i Z_i}{A_i} \qquad\qquad (2-10)$$

and

$$\sigma_p \propto D \sum_{i=1}^{n} \frac{W_i Z_i^5}{A_i} \qquad\qquad (2-11)$$

where D = density of soil

Wi = weight fraction of element i in the soil

Zi = atomic number of element i in the soil

Ai = atomic weight of element i in the soil

 n = total number of elements in the soil

A simple phenomenological response model as given by Gardner [5], based on the above mentioned interactions is:-

$$R = f_1 \cdot (D \sum_{i=1}^{n} W_i Z_i / A_i + f_2 (D \sum_{i=1}^{n} W_i Z_i^5 / A_i) \qquad (2-12)$$

Where f_1 and f_2 are functions that cause this relation to be a definition. R is the gauge response as counts per minute or count ratio (ratio of count rate on material to count rate on standard).

Gauge response data can be taken on various materials of known composition and homogeneous density to determine the f1 and f2 functions of Eq. (2-12) by a least squares method . The resulting relation serves as a refined calibration curve of better accuracy than a calibration curve that contains only density terms (2-13) i.e.

$$R = c \ \exp_{10} \ (a + b \ D + c \ D^2) \ \text{------------------}(2\text{-}13)$$

The refined calibration equation is:-

$$R = (D \sum_{i=1}^{n} WiZi/Ai) \ \exp_{10} \ (a + b \ D \sum_{i=1}^{n} Wizi^5/Ai)\text{----}(2\text{-}14)$$

where a, b and c are constants determined by the least square method.

The physical significance of Eq.(2-13) can be qualitatively made assuming that one "effective path length" (any photon path from source except the one that undergoes no scattering to the detector) must be a direct function of the Compton scattering cross-section; i.e. R $\propto$ c. This proportionality is modified by.the attenuation of gamma rays from the source to the point or points of-interaction and to the detector. Since both the scattering and absorption interactions of gamma rays are exponential, then the right side of the proportionality must be multiplied by the attenuation factor.

The ratio   Z/A in eqn.(2-14) is approximately 0.5 for
most low atomic number elements (Table 1). This means that Compton
cross-section is directly dependent on soil density and essentially
independent of the soil composition. However, hydrogen has a
Z/A value of unity, therefore hydrogen compounds exhibit anomalous
large Compton scattering which can be a source of error in density
determination.

The photoelectric absorption cross-section Eqn.(2-11) is
strongly dependent on soil composition due to the fifth-power
dependence on the atomic number; σ_p is most strongly influenced
by elements of high atomic number. These include iron, calcium
and to a lesser extent other common metals, since they are less
abundant. This strong dependence in terms of density measurement
is detrimental and represents a density measurement interference.

TABLE 1. <u>AVERAGE EARTH CRUST ELEMENTS</u>
Reproduced from [10].

ELEMENTS	WEIGHT FRACTION (%)	AT.NO. Z_i	* μ/D	AV.AT. WT.	Z_i/A_i	Z_i^5/A_i
O	46.6	8	0.0806	16.0	0.0500	0.2048×10^4
Si	27.7	14	0.0805	28.1	0.498	0.1913×10^5
Al	8.1	13	0.0777	27.0	0.482	0.1377×10^5
Fe	5.0	26	0.0762	55.8	0.466	0.2130×10^6
Ca	3.6	20	0.0809	40.1	0.499	0.7984×10^5
Na	2.8	11	0.0772	23.0	0.478	0.6998×10^4
K	2.6	19	0.0787	38.1	0.486	0.6333×10^5
Mg	2.1	12	0.796	24.3	0.494	0.1025×10^5
Ti	0.5	22	--	47.9	0.459	0.1075×10^6
H	0.1	1	0.1600	1	1.000	1.0000
P	0.1	15	--	31	0.484	0.2450×10^5
Mn	0.1	25	--	54.9	0.455	0.1777×10^6
S	0.05	16	--	32.1	0.498	0.3264×10^5
C	0.03	6	--	12.0	0.500	0.6480×10^5

NOTE: * for energy equal to 0.662 Mev.

-- data not available

Table 1 presents some common earth crust elements, and it can
be seen from it that it is the variation of μ/D values by weight
fraction which causes the so called composition error of the
gamma density gauge.

2.2. THEORY OF NUCLEAR MOISTURE DETERMINATION

The nuclear method of determining moisture employs neutrons.
Every neutron gauge contains a source of fast neutrons (with
energy of about 10 Mev) and a detector of thermal neutrons.
The fast neutrons emitted from the source undergo successive
processes of slowing-down, thermalisation and diffusion [27].
Since the slowing down process is governed mainly by elastic
collision of fast neutrons with hydrogen nuclei present in
the surrounding medium, the gauge reading can be related by
proper calibration to the total hydrogen content or moisture
of the medium.

In the slowing down process, the neutrons may engage in
a scattering collision with other nuclei in the soil, or
they may be absorbed by a nucleus.

2.2.1 SCATTERING OF NEUTRONS

Scattering may be inelastic or elastic.

a)   Inelastic Scattering:

This process is only important for fast neutrons. In these
processes e.g. (n,2n) and (n,n), the excited nucleus reaches
the ground state by emitting one or two neutrons of lower
energy than the incident neutron and gamma rays. The
(n,2n) reaction becomes important only at incident neutron

energies above 10 Mev and is not generally involved in moisture
determination.

b) Elastic Scattering:

   Elastic scattering is by far the dominant mode of interaction
   for neutron energies between 1-10 Mev in a non-absorbing
   medium. In this interaction, the kinetic energy of the
   neutron is partially transferred to the nuclei of the
   surrounding medium. The smaller the target nucleus (hence
   small mass), the greater the energy that can be transferred.

   The maximum energy transfer to any nucleus of mass number
A due to head-on collision is given [28] by:-

$$E1 - E2 = \frac{4A}{(1+A)^2} E1 \qquad (2-15)$$

   where E1 and E2 are respectively the energies before and
   after collision.

   The actual energy transfer per collision depends upon the
scattering angle. From the laws of conservation of energy
and momentum, the energy loss is:-

$$E1 - E2 = \frac{2A}{(1+A)^2} (1 - \cos\phi) E1 \qquad (2-16)$$

   where ϕ is the angle in the centre -of-mass coordinate system,
   into which the neutron is scattered.

It follows from Eqn.(2-15) that lighter nuclei are more effective in slowing neutrons than are the heavier nuclei. Thus, the moderation of the neutrons in the medium to thermal energies depends almost entirely on the presence of hydrogen nuclei (which have a mass of similar size to that of the neutron). The average thermal neutron energy is 0.025 eV.

The average number of collisions required to "thermalize" neutrons is given [28] by:-

$$
\text{Av.No. of coll.} = \frac{Ln\ (E1/E2)}{1 + \dfrac{(A-1)^2}{2A}\ Ln(\dfrac{A-1}{A+1})} \qquad\qquad\qquad (2-17)
$$

Thermal neutron scatter cross-sections δ_s and relative effectiveness of slowing down of fast neutrons are shown in Table 2 [28]

TABLE 2.   RELATIVE EFFECTIVENESS OF ELEMENTS IN AN AVERAGE SOIL
IN SLOWING DOWN FAST NEUTRONS.   Troxler [28]

ELEMENT	AT. WT. (A)	WT. FRACTION (Wi)	σ_s	AV. NO. OF COLLISION TO THERMALISATION
H	1.01			19
Li	6.94			69.3
Be	9.65			88.1
B	10.81	*	4.0	109.2
C	12.1	*	4.8	120.6
N	14.01	*	10.0	139.5
O	15.99	0.466	4.2	158.5
Na	22.99	0.028	4.0	224.9
Mg	24.32	0.021	3.6	237.4
Al	26.98	0.081	1.4	262.8
Si	28.09	0.277	1.7	273.3
P	30.94	0.001		300.8
S	32.06	*		311.1
Cl	35.45	*	16	343.3
K	39.10	0.026	1.5	378.0
Ca	40.08	0.036	3.0	387.3
Ti	47.90	0.004		461.6
Mn	54.93	0.001	2.3	528.5
Fe	55.85	0.050	2.6	537.2
Cd	112.4	*		1074.0
Pb	207.2	*		1975.6
U	238.03	*		2268.6

* Note: Weight fraction is less than 0.001

It can be seen from Table 2 that the scattering cross-section (σs) for the elements likely to be found in the soils that the presence of elements heavier than hydrogen is of minor importance in the slowing down of fast neutron scatterings. Nevertheless, in collision with the nuclei of these elements, the neutrons are deflected more than they would be with hydrogen nuclei, and, their migration away from the source is impeded.

c) Absorption:

The flux of thermal neutrons at the detector also depends on the content of the elements in the medium that have high thermal-neutron-capture probabilities such as cadmium, boron, the rare-earth elements, chlorine and iron (see Table 3) [10].

The most common reaction at thermal energies is (n,γ), radioactive capture. The (n,p) and (n,α) reaction probabilities of occurence are relatively low requiring neutrons of high energy. Three exceptions are $^{10}B(n,\alpha)^{7}Li$, $^{6}Li(n,\alpha)^{3}H$, and $^{3}He(n,p)^{3}H$, which have a high probability of occurence at thermal energies.

It follows from Table 3 that the presence of neutron absorbers in the material under test can cause errors since the neutrons would not reach the detector. For construction type soils,

TABLE 3.   RELATIVE ABSORPTION CAPACITY OF SOME ELEMENTS
           FOR THERMAL NEUTRONS (0.025 eV).   Troxler [28]

ELEMENT	ATOMIC WT. (A)	σ_a (barns)
Rare Earths	--	to 46,000
Cd	112.4	2,400
B	10.8	755
In	114.82	196
Au	196.97	98.8
Li	6.94	71.0
Ag	107.87	63.0
Cl	35.45	33.6
Elements Commonly encountered		
Fe	55.85	2.53
K	39.10	2.07
N	14.10	1.88
Na	22.99	0.50
Ca	40.08	0.44
H	1.01	0.33
Al	26.98	0.23
Mg	24.32	0.06
C	12.01	0.004
S	32.06	0.0052
O	15.99	0.0002
P	30.94	0.0002
Si	28.09	0.00016

the first eight elements listed in the Table are likely to be
encountered and could cause large errors. Coastal soils may
also contain significant amount of chlorine, while other soils
containing more than 35-40 percent of iron may cause errors
[29].

CHAPTER THREE

3.0   EXPERIMENTAL

3.1   NUCLEAR EQUIPMENT

The surface density-moisture gauge utilised in the investigation was a Troxler Electronic Laboratorys' model 3411-B.

3.1.1   PRINCIPLES OF GAUGE DENSITY MEASUREMENT

For density measurements, the gauge utilises a 0.03 GBq Cesium-137 source of gamma radiation and two Geiger Mueller gamma ray detectors. The gamma source is permanently mounted on an indexed steel rod. The detectors are placed at a horizontal distance from the source which allows an angular measurement through the material. Density can be measured either in the direct transmission or in the backscatter mode (Figs. 1a and 2a).

In the direct transmission mode, the rod is lowered into the access hole in increments of 50 mm below the surface, down to a depth of 200 mm. The radiation is transmitted through the soil diagonally to the detectors located at the soil surface. So, the density measurement is an average of the material between the source depth and the surface. Since source rod is permanently attached to the instrument base, the geometry relationships between source and detector are fixed for any depth increment.

Using Eqn . (2-1) (Chapt. two), Troxler Electronic Laboratory has found that the relationship between the count ratio (I/Is) and density D for both direct transmission and backscatter geometries is adequately described by

$$\frac{I}{Is} = A e^{-BD} - C \quad -------------------- \quad (3-1)$$

where I = intensity of gamma rays exiting the material

Is = intensity of gamma rays after passing a reference standard.

A,B and C are constants which may be derived from a calibration procedure for each depth. The constant B contains the mass absorption coefficient μ and the material thickness X. A and C are related to source size and detector efficiency. The relationship between A and C determine the degree of deviation from the theoretical function. A plot of Eqn. (3-1) is shown in Fig. 2d.

In the backscatter mode, both the gamma source and the detectors remain on the surface. Gamma rays enter the material and those scattered back into the detector are counted. This mode is generally insensitive to changes in density below a depth of 80 mm which therefore limits its use to thin layers of material. Backscatter is primarily recommended for use on asphaltic concrete. Fig. 2d illustrates
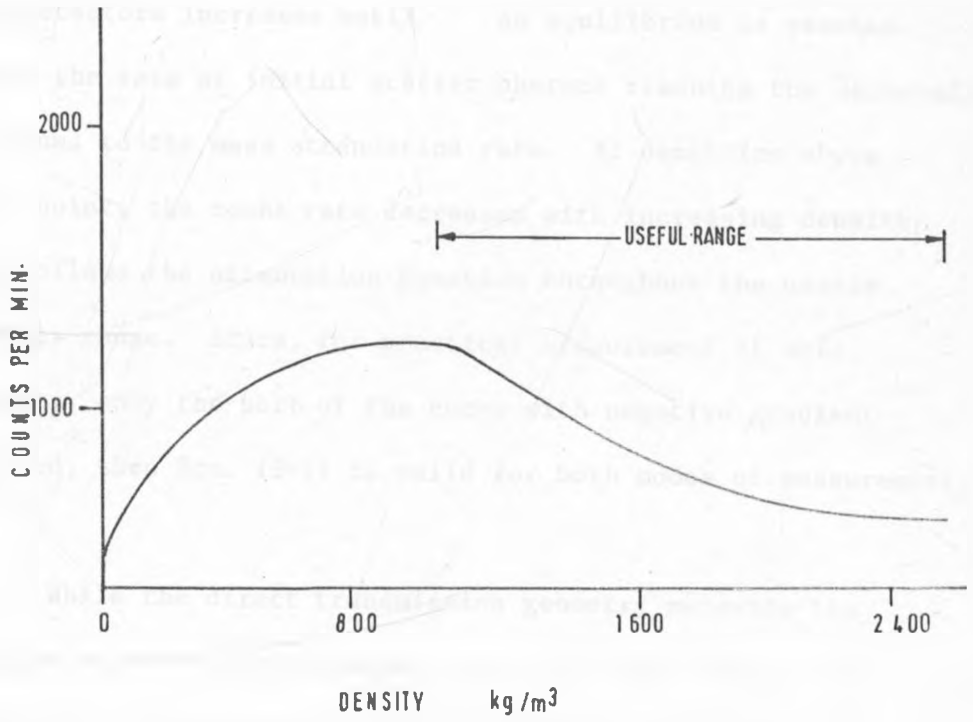
FIG. 2b). **BACK-SCATTER DENSITY RESPONSE**

a typical relationship between count rate and density for backscatter geometry. At very low density, the number of photons arriving at the detectors is very low and represents those that pass through the shielding. As the material density increases, the number of scattered photons reaching the detectors increases until an equilibrium is reached where the rate of initial scatter photons reaching the detectors is equal to the mass attenuation rate. At densities above this point, the count rate decreases with increasing density and follows the attenuation equation throughout the usable density range. Since, for practical measurement of soil density, only the part of the curve with negative gradient is used, then Eqn. (3-1) is valid for both modes of measurement.

While the direct transmission geometry measures the average density from the source depth to the surface, the backscatter measurement yields an average which is heavily weighted by the surface density. It is this phenomenon that causes large error due to surface voids as compared to direct transmission measurements.

3.1.2 PRINCIPLES OF GAUGE MOISTURE MEASUREMENT

Moisture measurements are made utilising a 0.15 Gbq Americum-241/Beryllium neutron source and a ^{3}He slow neutron detector. Both of these are permanently located at the base of the instrument. These are used to measure moisture

content in the surface layer by the backscatter geometry.

The Am-241 emits alpha particles within the sealed capsule which collide with the beryllium atoms. This collision releases fast neutrons according to the reaction as shown below:-

$$^9Be + {}^4He \text{---------------------}{}^1n + {}^{12}C + 5.74 \text{ Mev} \quad (3\text{-}2).$$

With the above activity, the source has a yield of about $7*10^4$ neutrons per second. Neutrons produced by this reaction have a spectrum of energies upto about 10 Mev. The average neutron energy being about 4.5 Mev.

Fast neutrons emitted by the ^{241}Am-Be source are slowed by the hydrogen in the soil and the slowed neutrons are counted by the detector. Counts over a fixed period of time, e.g. one minute, are related to moisture.

The source to detector distance within the instrument has some effect on the moisture calibration curve. In order to obtain maximum sensitivity (thermal neutrons detected per unit water density) the source and detector should be as close as possible. This produces a good linear response

at high moisture contents.   At low moisture contents, since

thermalisation occurs at a large distance from the detector,

the relation is not linear.   This is because of diffusion

of the thermal neutrons, reducing their probability of being

detected.   This response is shown in Fig. 3.
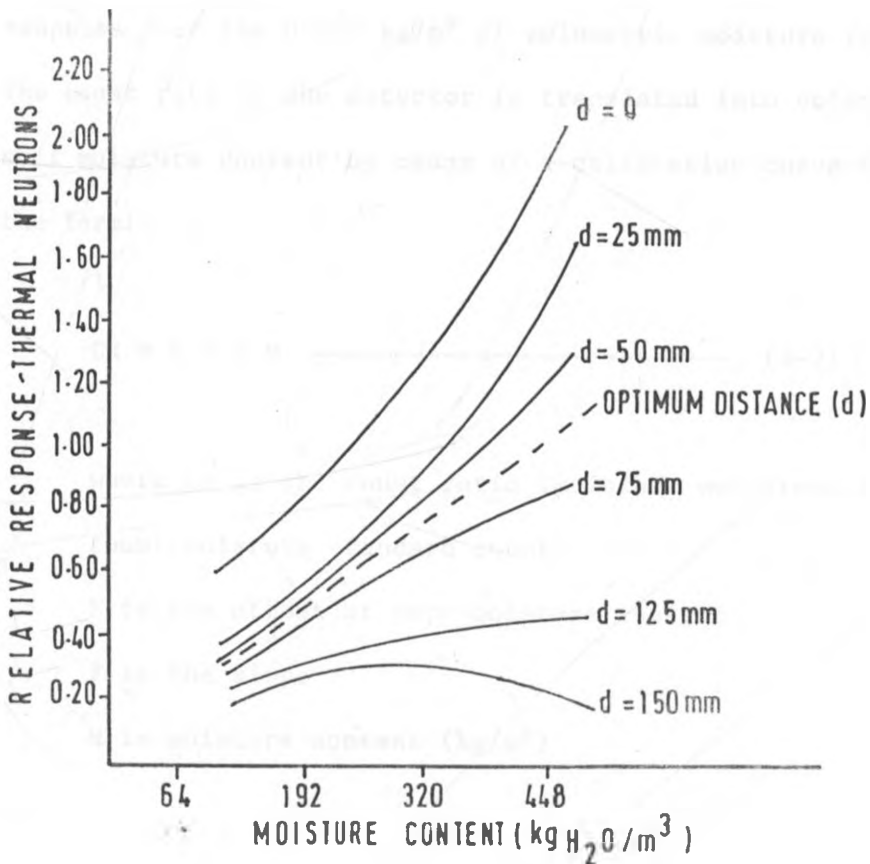
FIG. 3 EFFECT OF SOURCE DETECTOR DISTANCE (d) ON THE SHAPE OF CALIBRATION
CURVE FOR A SURFACE   NEUTRON MOISTURE PROBE [10].

If the source and detector are separated by a large
distance [100-150mm], the linearity at low moisture
contents is very good but not at high moisture contents,
since thermalisation occurs at a point close to the source
but to an increasing distance from the detector.

In the gauge used, the source to detector separation
(which is in the range 50-100 mm) gives an almost linear
response over the 0-650 kg/m³ of volumetric moisture range.
The count rate of the detector is translated into volumetric
soil moisture content by means of a calibration curve of
the form:-

$$CR = E + F M \hspace{2cm} (3-3)$$

where CR is the count ratio (moisture measurement
count/moisture standard count)

E is the offset at zero moisture content

F is the slope

M is moisture content (kg/m³)

3.1.3 EFFECT OF DRY BULK DENSITY ON THE NEUTRON MOISTURE GAUGE RESPONSE

As the neutron flux depends on the dry bulk density of the soil [10], variations in density cause a change in the apparent water content. A small variation of dry density will involve a displacement of the calibration curve. When the calibration curve is a straight line, the slope does not change very much. Fig. 4 illustrates the influence of soil dry bulk on moisture gauge readings [10].
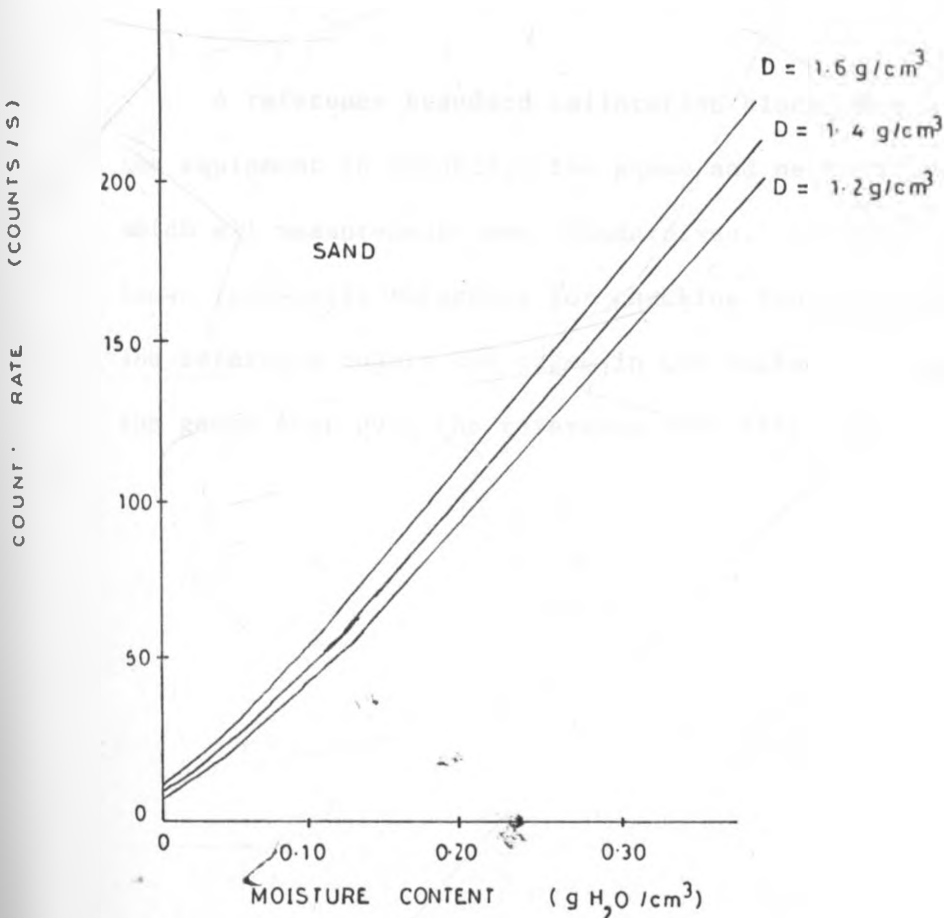
FIG. 4   Effect of variations in dry bulk density on moisture calibration curve: Reproduced from [10].

3.1.4 GAUGE COMPUTATION

The gauge contains a microcomputer which holds all calibration constants and algorithms necessary to compute and display directly density and moisture in either SI or imperial units as chosen by the operator.

If the maximum density has been preset by the operator, the microprocessor can compute percent compaction (% of Marshall or % of Proctor which are respectively the maximum densities for asphaltic concrete and soils as obtained in the laboratory).

A reference standard calibration block is also used with the equipment to establish the gamma and neutron counts against which all measurements are standardised. It also serves as a known repeatable reference for checking long term stability. The reference counts are taken in the backscatter geometry, with the gauge kept over the reference unit (Fig. 5).
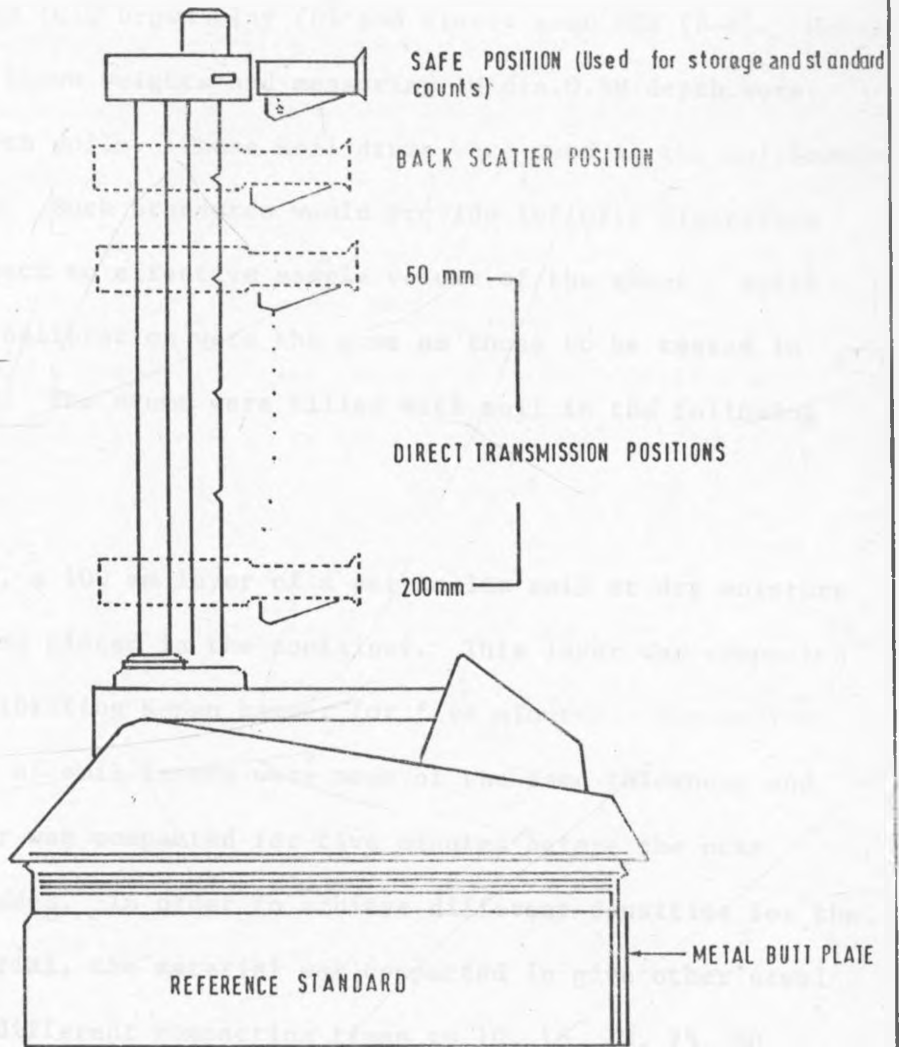
FIG. 5 GAUGE MEASUREMENT POSITIONS

3.2 LABORATORY DENSITY CALIBRATION

Laboratory density calibration was accomplished using
Laboratory standards of four soils viz: natural gravel (B),
silty sand (C), brown clay (D) and clayey sand (E) (B-E). Metal
drums of known weights and measuring 1M dia.0.5M depth were
filled with soils. These soil drums were used as the calibration
standards. Such standards would provide infinite dimensions
with respect to effective sample volume of the gauge. Soils
used for calibration were the same as those to be tested in
the field. The drums were filled with soil in the following
way:-

Initially, a 100 mm layer of a particular soil at dry moisture
content was placed in the container. This layer was compacted
using a vibrating Kango hammer for five minutes. Successive
additions of soil layers were made of the same thickness and
each layer was compacted for five minutes before the next
one was added. In order to achieve different densities for the
same material, the material was compacted in give other steel
drums at different compaction times to 10, 15, 20, 25, 30
minutes for every layer.

For each density test, backscatter and direct transmission

determinations were made with nuclear gauge. Sand replacement
tests were done below the gauge positions. Gravimetric
method of calculating the density of the material from its
volume and weight for each drum was also done. The mean
density gauge results for three positions over the compacted
area were obtained for each drum. Readings were also taken
on the standard block.

The whole procedure was then repeated for the other four
soil types. However, it was not possible to achieve large
density ranges in the laboratory; the calibration curves
obtained are presented in Chapter four.

Laboratory moisture calibrations were not carried out because
of the difficulty involved in obtaining uniform and constant
moisture levels in the soils.

3.3 FIELD DENSITY CALIBRATION

    Field calibration was achieved by selecting an area
on a firm subgrade or sub-base which was rolled with a specified
rolling equipment at optimum moisture content. The rolled
calibration area was a 100-m long section of one-lane
roadway for each material encountered. Density and moisture
tests were randomly carried out at thirty locations after

each rolling until no further increase in density was detected.
The calibration sections became part of the normal construction
although a few test sections were specially constructed
for this purpose. On such sites, the construction of the
calibration bays was done at three moisture contents namely:
optimum moisture content (OMC), 1/2 OMC, and at dry (natural)
moisture content. Both gauge and conventional tests were
done at the same sites. The conventional tests were done
to a depth corresponding to the material layer thickness
under test.   Data obtained from the sites were used to
calibrate the gauge by two methods.

In method one, the manufacturers' calibration method
was used. Each layer tested was treated as a block of the
same material but of different density. Density and moisture
count ratios were obtained and plotted against the sand
replacement density and moisture values for the range of
values obtained in the field. Typical plots obtained are
shown in Chapter four.

In a second method, a procedure described by Ahuja
and Williams [23] was followed. Using their method, bulk
density D for a moist soil is obtained using the following
equation:-

$$D = Ln \left(\frac{A}{[I/Is] + C} \right) / B - 1.05 (M) \text{----------(3-4)}$$

where M is volumetric moisture content and A, B, C are constants. As it is seen from this procedure, moisture content should be known to improve the calibration results.

It is implicitly assumed that the gamma attenuation coefficient of soil water is 1.05 times that of the dry soil. The moisture content M obtained with the surface neutron probe is assumed constant with depth [28].

It is recognised that the gamma attenuation coefficient of soil depends upon the soil composition, especially the fraction of hydrogen contained in materials other than water, as well as the nature of the medium surrounding the beam path [29]. It is better to use separate attenuation coefficients for soil and moisture, and determine them by calibration with in-situ field data, under actual conditions of field operation.

In a moist soil, the attenuation of gamma rays is mainly due to the soil and the water contained in it. Thus,

Eqn. (3-4) for a given location of the gamma source may
be written as:-

$$\frac{I'}{Is} = A\,e^{-(B'\,D'\,+\,Bw\,Dw\,M)} - C \quad\text{----------------} \quad (3\text{-}5)$$

where B' and Bw are the attenuation path-length constants
for soil and for soil water respectively. M is the
average soil moisture content from soil surface to
depth of source. I' is the intensity of radiation
exiting the soil.

Assuming the water to be under standard conditions
of temperature and pressure, the water density can be considered
as one: Dw = 1.
Re-arranging, Eqn. (3-5) thus becomes:

$$Ln\left(\frac{A}{[I'/Is] + C}\right) = B'\,D' + Bw\,M \quad\text{--------------}\quad (3\text{-}6)$$

Both, B' and Bw were obtained by a least-square fit
of Eqn. (3-6) to a set of I' and D' values with the latter
measured by the sand replacement method at each depth of
measurement. From the intercept, Bw was obtained using
the average moisture value obtained by the oven-dry method.

After B' and Bw were determined, the bulk density for each
site was calculated using the measured average gravimetric
soil water content $\overline{M}$, in the specified depth:

$$D = \frac{1}{B'} \left[Ln \left(\frac{A}{[I'/Is] + C} \right) - Bw \, \overline{M} \right] \quad \text{------------} \quad (3-7)$$

    This equation can be used for determining bulk density
    when only gravimetric soil moisture content is measured
    in conjuction with gamma probe reading.

3.4   FIELD TESTING OF MATERIALS

3.4.1 TEST SITES

    Soil bulk densities and moisture contents were measured
on four on-going road construction projects. These sites
were chosen because of their differences in pavement design
and materials used. These were along Lodwar-Kakuma, Nakuru
highway, Nairobi-Thika and Bura-Garissa roads.

    On these sites, eight different soil types and two
asphaltic concrete pavements with different aggregate mixes
and bitumen contents were encountered. Nuclear gauge and
sand replacement test densities and moisture contents were

measured on the soils while gauge and core cutting density
determinations were carried out on the asphaltic concrete
pavements.

3.4.2   TESTING PROCEDURE

After allowing the instrument to warm up for 15 minutes,
the reference standard block was placed in an open area.
Standard counts for gamma photons and neutrons were taken
for four minutes.

At each test site, both backscatter and direct transmission
measurements were taken for 1 minute; at each depth for
the latter. For direct transmission measurements, a 22 mm
diameter access hole was made by hammering the drill rod
into the material under test upto a depth of about 250 mm.
Care was taken to smoothen any rough surface with either
the steel scraper plate or by adding a handful of fine sand.
This was necessary in order to reduce the voids between
the soil surface and the base of the instrument.

The locations of the gauge measurement orientations
in relation to conventional test positions are as shown
in Fig. 6. Both backscatter and direct transmission
measurements were taken at angles of 120° to each other

using the source in the same rod hole. Any material disturbed
by the probe was included in the mass of material removed
from the hole in the sand replacement test.

Immediately after completing the gauge measurements,
sand-replacement test or undisturbed asphaltic concrete
core cutting was done directly under the instrument for
each depth of layer thickness already compacted. These
samples were sealed and carefully taken to the laboratory for
density and moisture determination.

After the completion of the days' gauge tests, standard
counts were taken again. Stability and statistical drift tests
were also done following the manufacturers' procedure.
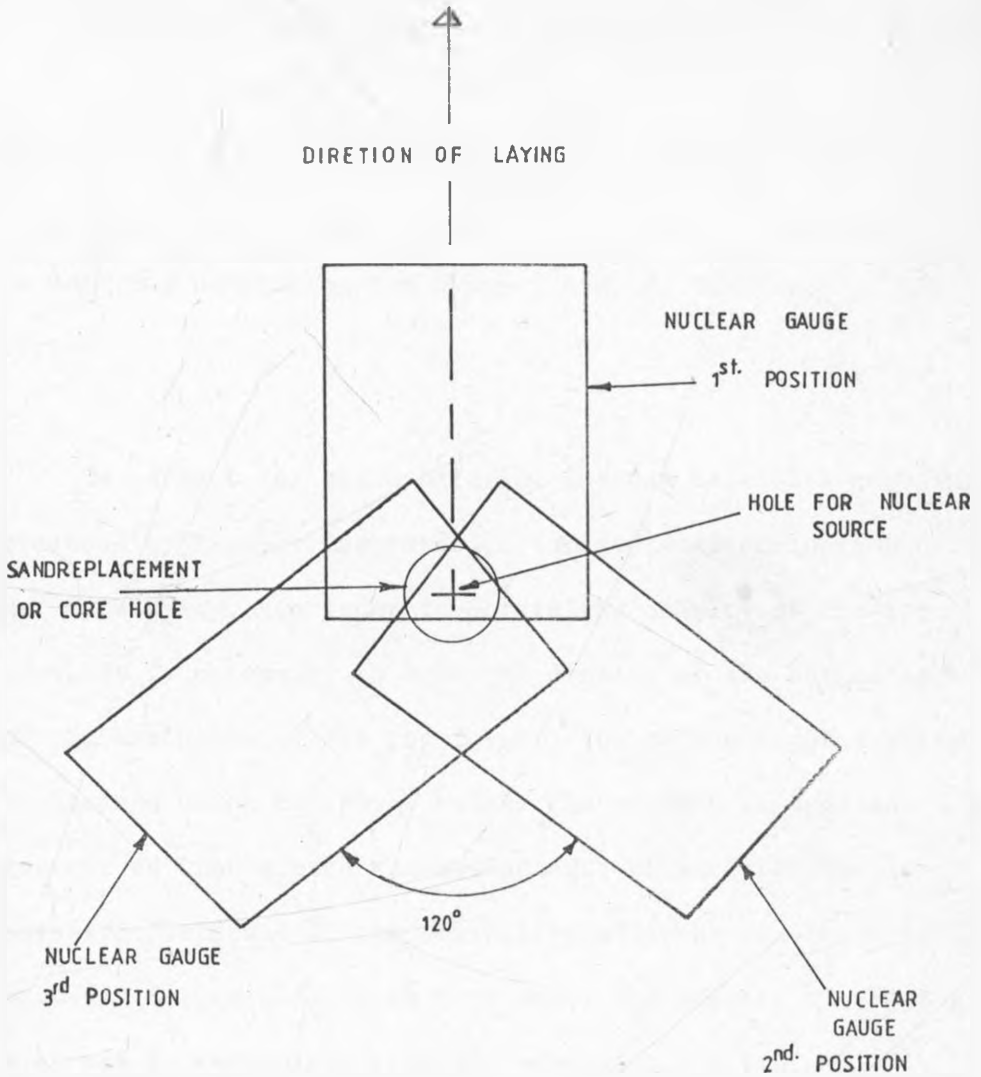
FIG. 5 DIAGRAMATIC REPRESENTATION OF SITE POSITIONS FOR THE IN-SITU MEASUREMENT OF DENSITY AND MOISTURE BY TWO METHODS

3.4.3. Measurement of Thin Lift Overlays

When the nuclear gauge is used in the backscatter mode
on overlays, it has some limitations which must be overcome in
order to obtain correct densities. The problem arises due to
the depth of penetration of gamma rays which is influenced by
the material underlying the overlay and the thickness of the
overlay.

To correct for these effects, use was made of a nomograph
developed by Troxler Laboratories for rapid determination of
overlay density. In order to obtain the density of the top
layer, it is necessary to know the density of the bottom layer
and the thickness of the top layer. The bottom layer density
is obtained using the gauge before the overlay is applied.
Pavement is then placed and compacted. Backscatter density
tests are performed on the top of the pavement and the material
thickness determined. With this data, the density of the top
layer may be determined from the nomograph. A typical
nomograph is shown in Fig. 7.
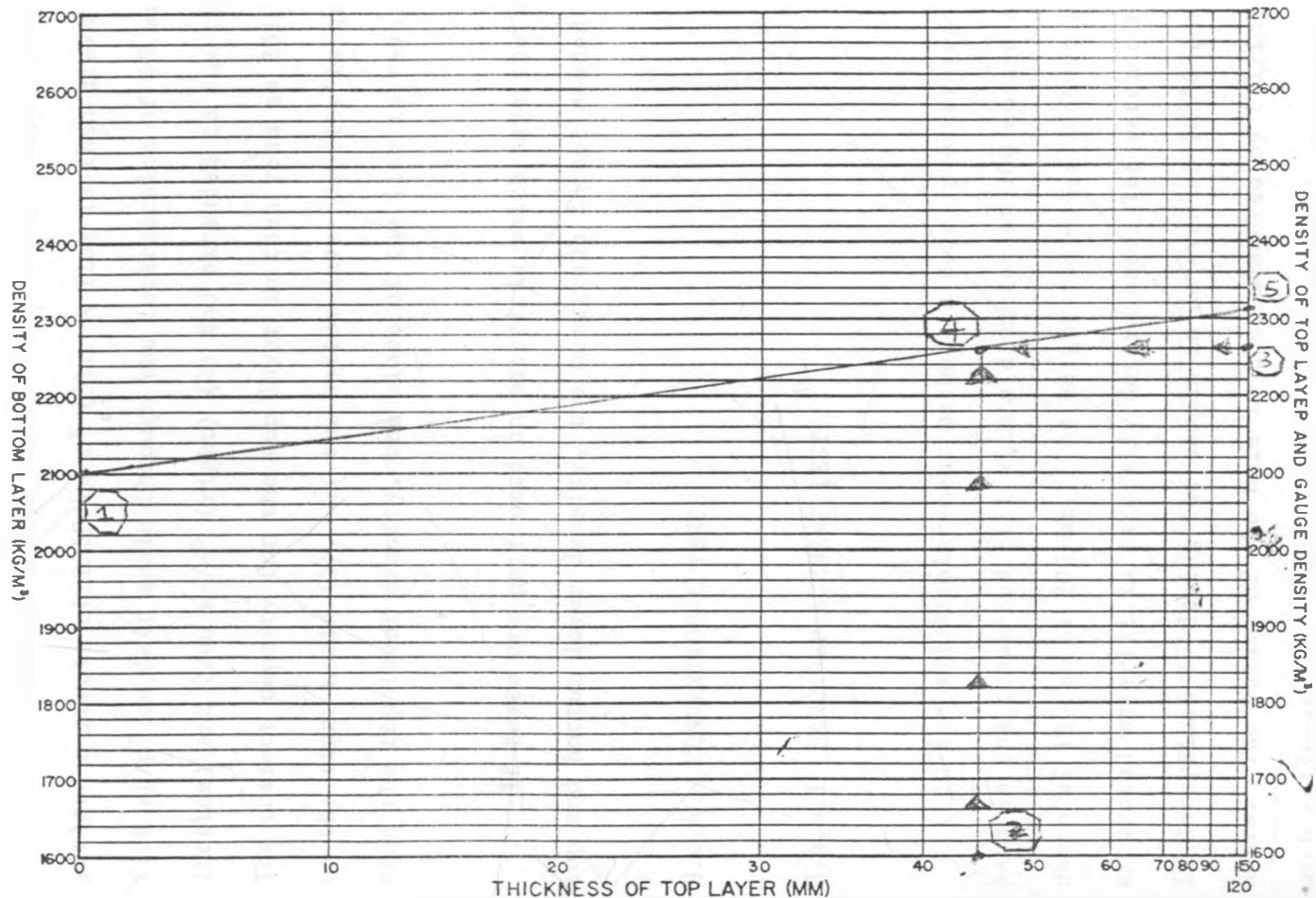
FIG 7.   THIN LIFT OVERLAY NOMOGRAPH   [28]
(SI UNITS)

In this example, the bottom layer density (left scale) is 2100 kg/m^3 (1) with an overlay thickness of 45 mm (2). A backscatter density on the top of the overlay (right scale) yielded a result of 2260 kg/m^3 (3). A line is then drawn from 2100 kg/m^3 on left scale through the intersection of 45 mm (bottom) and 2260 kg/m^3 (right) (4) and extended to the right. The correct density for the top layer is then read as 2310 kg/m^3 on the right scale (5). If the bottom layer density is greater than the top layer density, the slope of the line is reversed.

If tests are performed on materials which have the same top and bottom layer density, the nomograph is not needed.

3.4.4. CONVENTIONAL TESTS

3.4.4.1 SAND REPLACEMENT TEST

In the sand replacement method, a hole is excavated by hand in the compacted fill with a diameter of 100 mm and a depth of 150 mm or 200 mm. The weight and water content of the excavated material is carefully determined. The water content is determined by drying the sample in an oven at 105°C for 24 hours. The volume of the hole is then measured by filling it with calibrated dry sand usually from a special sand-cone cylinder.

With knowledge of the material weight and the volume of the hole, the dry density (DD field) of the compacted fill can be calculated. The degree of compaction is then determined by the formula:

$$\text{compaction} = \frac{\text{DD (field)}}{\text{DD (max.)}} \times 100 \text{ percent} \quad \text{------(3-7)}$$

where DD (max.) is the maximum dry density obtained at the laboratory compaction test.

The sand replacement test method was carried out using BS 1377: 1975 (British Standards Institution) [30].

3.4.4.2 MEASUREMENT OF DENSITY OF ASPHALT CONCRETE CORES

For asphaltic concrete density tests, cores were drilled perpendicular to the surface using a core drilling rig. The drill was kept rigidly positioned during coring to avoid obtaining ridged or curved cores. The samples obtained were then taken to the laboratory for density determination. For smooth and regular core specimens, the procedure used for bulk density determination is as follows:-

a) Weigh the specimen in air (W_1) grams, and if necessary wax the core and weigh again (W_2) grams.

b) Determine the volume of the specimen (V) cm^3 by weighing the

specimen when totally immersed in water at $20 \pm 1°C$ (W_3).

c)   Calculate the density (D) of the core from the following:-

    i)   Unwaxed specimen

$$D = \frac{W_1}{W_1 - W_3} \qquad\qquad\qquad (3-8)$$

        where W_1 is the mass of the specimen in air (in gms)

              W_2 is the mass of the unwaxed specimen in water

              (in gms).

    ii)   Waxed specimen

$$D = \frac{D_5 \, W_1}{D_5 \, (W_2 - W_4) - (W_2 - W_1)} \qquad\qquad (3-8)$$

        where W_2 is the mass of the specimen in air after waxing

              (in gms).

              W_4 is the mass of the waxed specimen in water

              D_5 is the relative density of the wax

    iii)   Determination of air voids in the specimen

From a knowledge of the composition of the specimen and the

relative densities of the constituent materials, the theoretical

volume (the volume the material would occupy if there were no voids)

can be calculated. Hence, the theoretical maximum relative
density D_T of the mixture can be calculated as follows:-

$$D_T = \frac{100}{\dfrac{W'_1}{D_1} + \dfrac{W'_2}{D_2} + \dfrac{W'_3}{D_3} + \dfrac{W_B}{D_B}} \qquad\qquad (3-9)$$

where W'_1, W'_2, W'_3, and W_B represent the respective

percentages by mass of the aggregate/s , filler

and binder used in a particular mix.

D_1, D_2, D_3 and D_B represent the respective relative

densities of the above.

The percentage of voids in the mix (V_m) is obtained from the
relation:-

$$V_m = \frac{D_T - D_m}{D_T} \qquad\qquad\qquad (3-10)$$

where D_m is the relative density of the specimen

$(D_m = W/V)$.

The percentage of voids in the mineral aggregate, V_A, in the
specimen is calculated from:-

$$V_A = V_m + \frac{W_B \times D_m}{D_B} \qquad\qquad\qquad (3-11)$$

The percentage voids filled with binder, V_F, is given by:-

$$V_F = \frac{W_B \times D_m}{V_A \times D_B} \qquad\qquad (3-13)$$

The method of test for the asphalt cores was carried out using BS 598:1985 (British Standards Institution) [31].

CHAPTER 4

4.0   DATA PRESENTATION, ANALYSIS AND DISCUSSION

The bulk density and moisture content results obtained by both the gauge and conventional tests at each site are presented as shown in Tables (7-15) and Tables (24-32) respectively.   In addition, calibration curves of the tested materials relating count-ratios to sand-replacement (SR) dry density are shown Figs. (15-22).   The calibration curves were used to obtain the adjusted gauge values relative to the "true" sand replacement values.   Re-calibration results of density corrected for hydrogen are also reported Tables (7-14).   Results obtained were compared with those from the manufacturer's calibration curves.

An analysis of variance and student's t-test values was undertaken on each group of results (gauge and conventional tests) to assess whether the results were significantly different.   Where the pattern of the difference between gauge and conventional tests were significantly different, a possible cause of the difference was sought.

From the measured data, it was possible to compare the · following results:-

Laboratory density results:

- densities from the sand replacement tests and nuclear
  gauge.

Field results:

1. Densities from sand replacement tests and nuclear gauge.

2. Densities from nuclear gauge and cores.

3. Moisture contents from sand replacement tests and
    nuclear gauge.

4. Analysis of accuracy and repeatability of results.

4.1   LABORATORY DENSITY RESULTS

The materials used in the laboratory for calibration
purposes were four soil types.   They were natural gravel (B),
silty sand (C), brown clay (D) and clayey sand (E).   Material
A (coarse gravel) was not used for laboratory calibration because
of the difficulty involved in maintaining uniform level of the
surface after compaction.   This was caused by the large gravels
(of size 20-60 mm).   This material was however tested in the
field.

The soils were also sieved in the laboratory in order to
know their constituent particle sizes.   The particle size distri-
bution of the materials are given in Fig.8 together with their
physical properties.

The quantitative analysis of the main constituents of the
materials is given in Table 4.   The elements shown were
determined by the energy dispersive X-ray fluorescence
(EDXRF) method.

FIG. 8   PARTICLE SIZE DISTRIBUTION
AGGREGATES

[LAB CALIBRATION MATERIALS]

	B.S. Sieves																						
Non Metric Series	200	150	100	72	52	36	25	18	14	10	7	1/8"	3/16"	1/4"	3/8"	1/2"	3/4"	1"	1½"	2"		3"
Metric Series µm & mm	75		150	212	300	— 425	600			1.18		2.36	3.35	5.0 6.3	10	14	20	28	37.5		63 75

PERCENTAGE PASSING

- 58 -

MAT. TYPE	LIQUID LIMIT	PLASTIC LIMIT	PLASTICITY INDEX	LINEAR SHRINKAGE
Non-Gravel (B)	29	20	9	7
Silty Sand (C)	24	11	8	4
Brown Clay (D)	51	27	24	13
Clayey Sand (E)	27	16	11	9

mm   0.05   0.1   0.2   0.5   1.0   2.0   5.0   10   20   50   100

| Silt | Fine Sand | Medium Sand | Coarse Sand | Gravel |
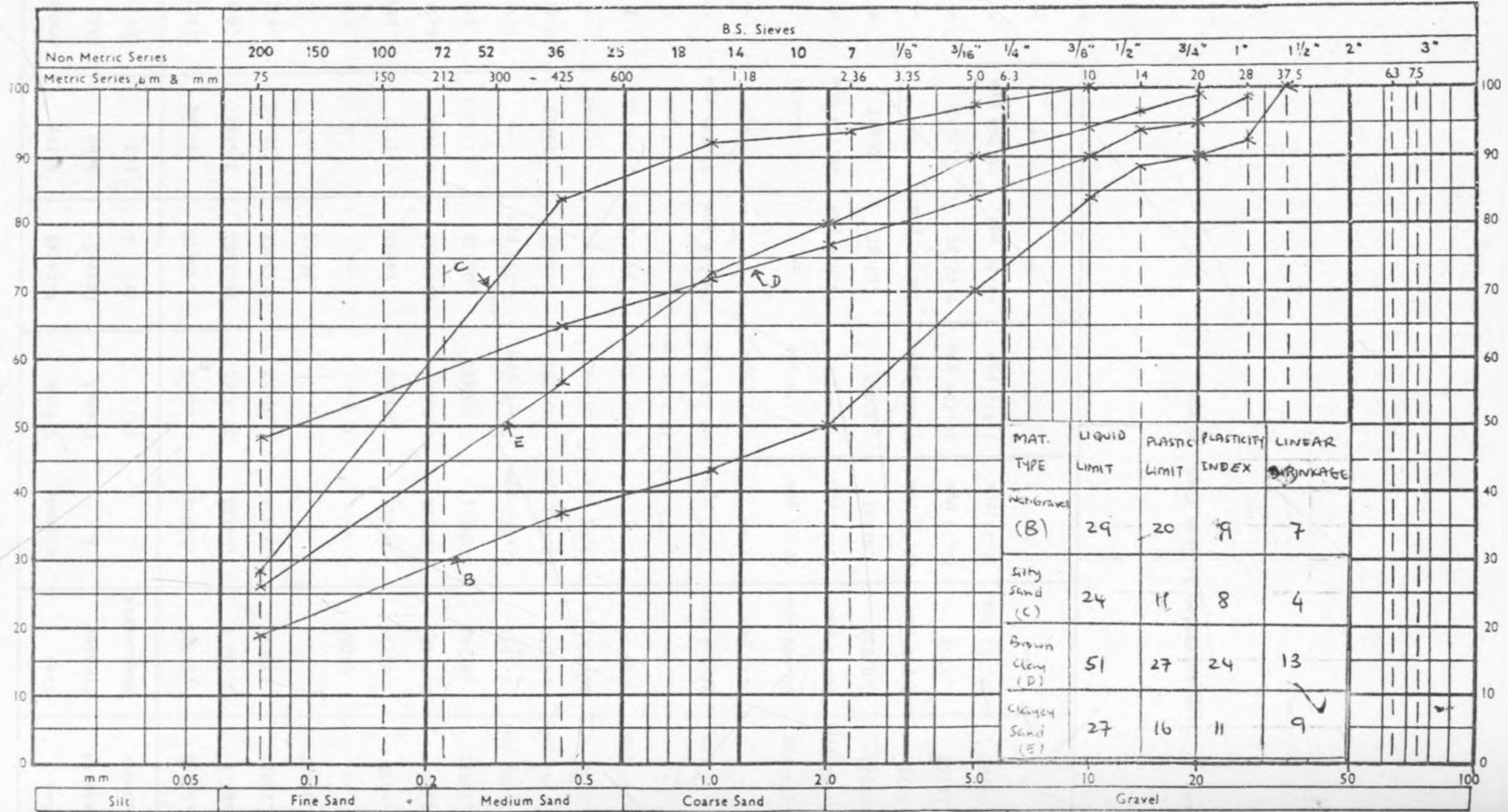
Table 4: Quantitative analysis of the main constituents of the tested material

	lime treated Subbase	lime treated Basecourse	Subgrade 1	Coarse Gravel (A)	Natural Gravel (B)	Silty Sand (C)	Brown Clay (D)	Clayey Sand (E)
K	.4224%	.5192%	.5199%	.4069%	.3093%	.2434%	1.2033%	.7234%
Ca	1.681%	3.792 %	1.6012%	32.539%	14.198%	3.488%	7.840%	5.664%
Ti	.2881%	.2349%	.3782%	.0145%	1.1335%	.5535%	.4334%	.4935%
	.0662%	--	--	--	.0431%	--	--	--
Cr	--	.0106%	--	--	--	--	.0357%	.0180%
Mn	2.455%	.0319%	.05414%	.0569%	.1495%	. 575%	.0846%	.330%
Fe	12.084	2.744%	.1858%	1.858%	6.1565%	3.641%	16.944%	4.293%
Co	.2082%	.0169%	.0817%	.02041%	.0653%	.12335%	.05%	.0867%
Ni	43.860 ppm	0.189%	91.262 ppm	52.20 ppm	9.363 ppm	--	0.195%	.01%
Cu	63.569 ppm	.0155%	73.643 ppm	.01326%	.1240%	.1619%	59.606 ppm	.083%
Zn	.023%	86.73 ppm	93.62 ppm	.01269%	.0118%	.01664%	*	.0114%
Ga	5.538 ppm	4.30 ppm	--	5.674 ppm	6.140? ppm	3.160 ppm	*	2.641 ppm
Ge	--	--	17.713 ppm	11.1351 ppm	--	2.40 ppm	*	1.8842 ppm
Pb	83.72 ppm	42.534 ppm	73.07 ppm	93.149 ppm	38.546 ppm	69.294 ppm	*	*
Se	--	7.22 ppm	--	6.713 ppm	--	--	--	--
Br	6.227 ppm	20.492 ppm	16.85 ppm	44.118 ppm	--	11.290 ppm	*	*
Rb	53.451 ppm	12.13 ppm	59.72 ppm	--	14.626 ppm	18.736 ppm	*	8.64 PR
Sr	.0252%	.0305%	.0125%	.2305%	.0789%	.0487%	*	*
Y	.011%	2.401 ppm	23.48 ppm	9.471 ppm	20.528 ppm	--	--	--
Zr	.1616%	.035%	72.38 ppm	64.759 ppm	0.0233%	0.185%	*	*
Nb	.0378%	24.753 ppm	16.26 ppm	7.972 ppm	48.30 ppm	18.066 ppm	*	9.364 ppm
Mo	--	--	--	--	--	--	--	--

Note * - concentration is less than 1.0 ppm.

Table 5 shows a summary of the density probe readings
(cols. 1 and 2) on the various soil standards constructed.
The true mass density of these materials was obtained from
the sand replacement tests (col.3). Values of dry density read
directly from the gauge are shown in column 4 while those in
column 6 were obtained from the calibration curves. Using
these data, calibration curves were plotted. These are shown
in Fig. 9. The corresponding factory calibration data and
curves are respectively shown in Fig. 10.

Table 5: Laboratory Gauge and SR Readings
Units of Density: Kg/m³

	1	2	3	4	5	6	7
MATERIAL TYPE	COUNTS PER MIN.	COUNT RATIO	SR DENSITY	GAUGE DENSITY (D_g)	$D_{SR}-D_g$ ΔD_1	ADJUSTED GAUGE DENSITY(D_{cc})	$D_{SR}-D_{cc}$ ΔD_2
Natural Gravel (B)	2532	0.847	1750	1845	-95	1750	0
	2254	0.754	1800	1900	-100	1825	-25
	2190	0.732	1875	1920	-45	1850	+25
	2098	0.702	1920	1974	-54	1920	0
	2024	0.677	2004	2020	-16	2000	+4
	1990	0.666	2018	2060	-42	2035	-17
Silty Sand (C)	2816	0.993	1640	1620	+20	1635	+5
	2566	0.905	1675	1690	-15	1680	-5
	2422	0.856	1699	1732	-33	1720	-21
	2456	0.866	1728	1766	-38	1725	+3
	2490	0.808	1874	1780	+94	1860	+14
	2196	0.775	1908	1833	+75	--	--
Brown Clay (D)	3042	1.05	1620	1700	-80	1638	-18
	2775	0.961	1675	1725	-50	1665	+10
	2476	0.857	1715	1756	-41	1720	-5
	2258	0.782	1800	1792	+8	1800	0
	2102	0.728	1856	1893	-37	1863	-7
	1999	0.692	1918	1900	+18	1918	0
Clayey Sand (E)	2984	1.05	1717	1707	-10	1717	0
	2702	0.948	1735	1722	+13	1730	+5
	2289	0.838	1770	1812	-42	1773	-3
	2100	0.737	1811	1836	-25	1818	-7
	1722	0.604	1894	1924	-30	1905	-11
	1634	0.573	1940	1940	0	1940	0

FIG. 9 LAB DENSITY CALIBRATION CURVES FOR FOUR SOIL TYPES (B — E)

O — NATURAL GRAVEL (B)
X — SILTY SAND (C)
△ — BROWN CLAY (D)
□ — CLAY SAND (E)

RELATIVE COUNT RATE

SAND REPLACEMENT DRY DENSITY (Kg/m³)
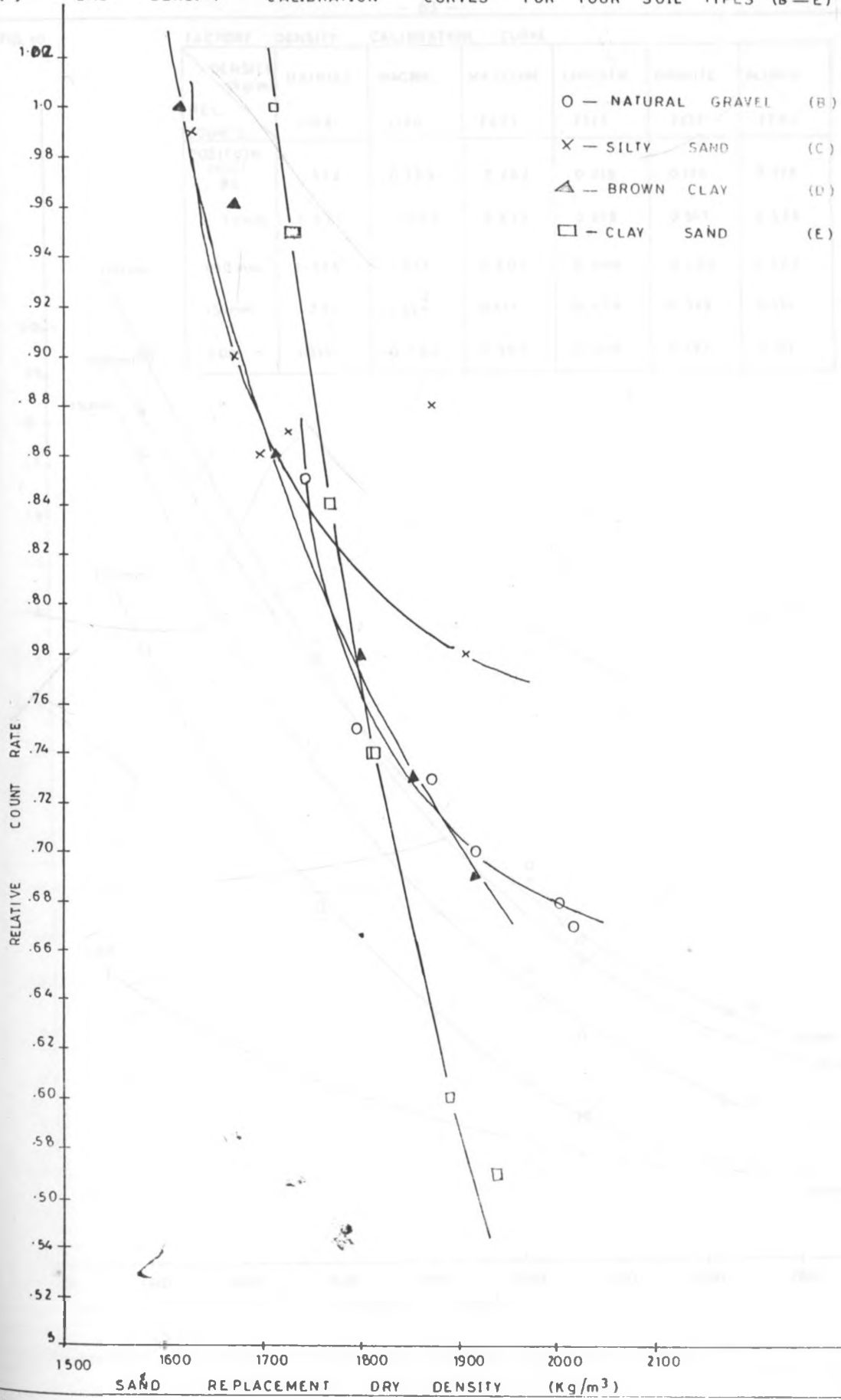
FIG. 10

FACTORY DENSITY CALIBRATION CURVE

DENSITY (kg/m)	MA/POLY	MAGNE.	MA/ALUM	LIMESTN	GRANITE	ALUMIN
REL. COUNTS	1399	1770	2223	2321	2637	2702
POSITION (mm) BS	·572	0·389	0·262	0·215	0·176	0·178
50mm	1·821	1·289	0·839	0·678	0·517	0·528
150mm	1·965	1·326	0·807	0·640	0·465	0·469
150mm	1·731	1·094	0·617	0·478	0·329	0·331
200	1·315	0·764	0·393	0·295	0·197	0·197

RELATIVE COUNT RATE

Density (Kg/m³)
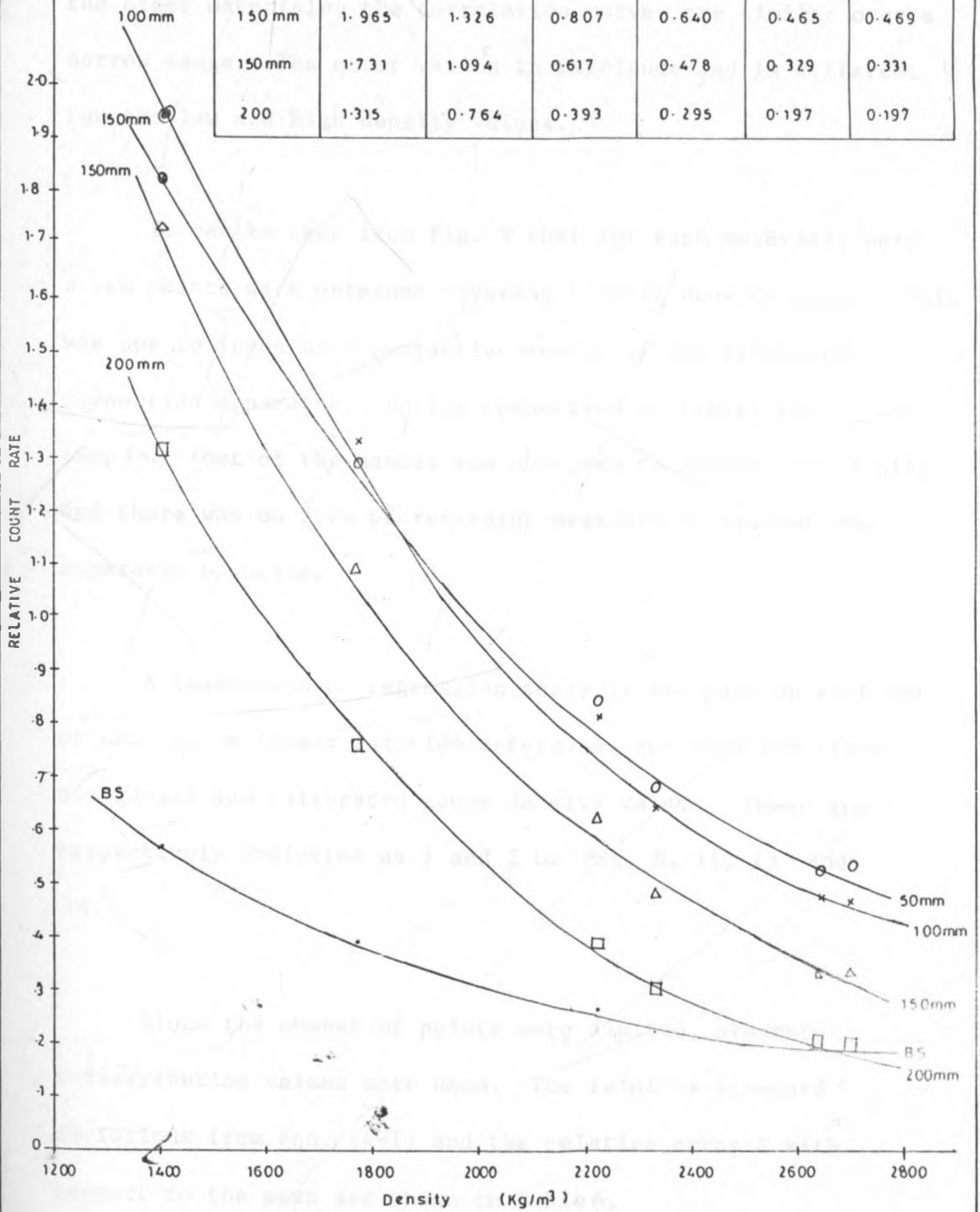
It is evident from Table 5 that systematic errors exist for all the four materials tested. In particular, the error is more visible in clayey sand (E) which is about 20 kg/m^3. For the other materials, the correlation curves are similar over a narrow range. The error varies in magnitude and is different for the low and high density values.

It can be seen from Fig. 9 that for each material, only a few points were obtained covering a short density range. This was due to inadequate compactive energy of the vibratory compaction apparatus. During compaction at times, the tamping foot of the hammer was observed to bounce erratically, and there was no form of retaining pressure to prevent the apparatus bouncing.

A least-square regression analysis was made on each set of data and a linear equation determined for both raw (from the gauge) and calibrated gauge density values. These are respectively indicated as 1 and 2 in Fig. 8, 11, 13 and 14.

Since the number of points were limited, students t-distribution values were used. The relative standard deviations from Eqn. (4-1) and the relative error S with respect to the mean are shown in Table 6.

TABLE 6: <u>RESULTS OF DENSITY DATA EVALUATION (LABORATORY)</u>

SOIL TYPE AND DENSITY RANGE (Kg/m^3)	RELATIVE STANDARD DEVIATION (COUNTING STATISTICS)		ACCURACY $\frac{S}{x} \times 2_t$ REL. STD. DEV. AT 95% CONF.LEVEL
	LOW D	HIGH D (Kg/m^3)	
			(Kg/m^3)
B(1756-2005)	8	85	82.2 (4.3%)
C(1638-1910)	10	65	61.9 (3.6%)
D(1620-1915)	8	33	46.3 (2.3%)
E(1715-1938)	5	30	30.8 (1.7%)

FIG. 11   NATURAL   GRAVEL (B)

LAB.   DENSITY   CORRELATION & CALIBRATION
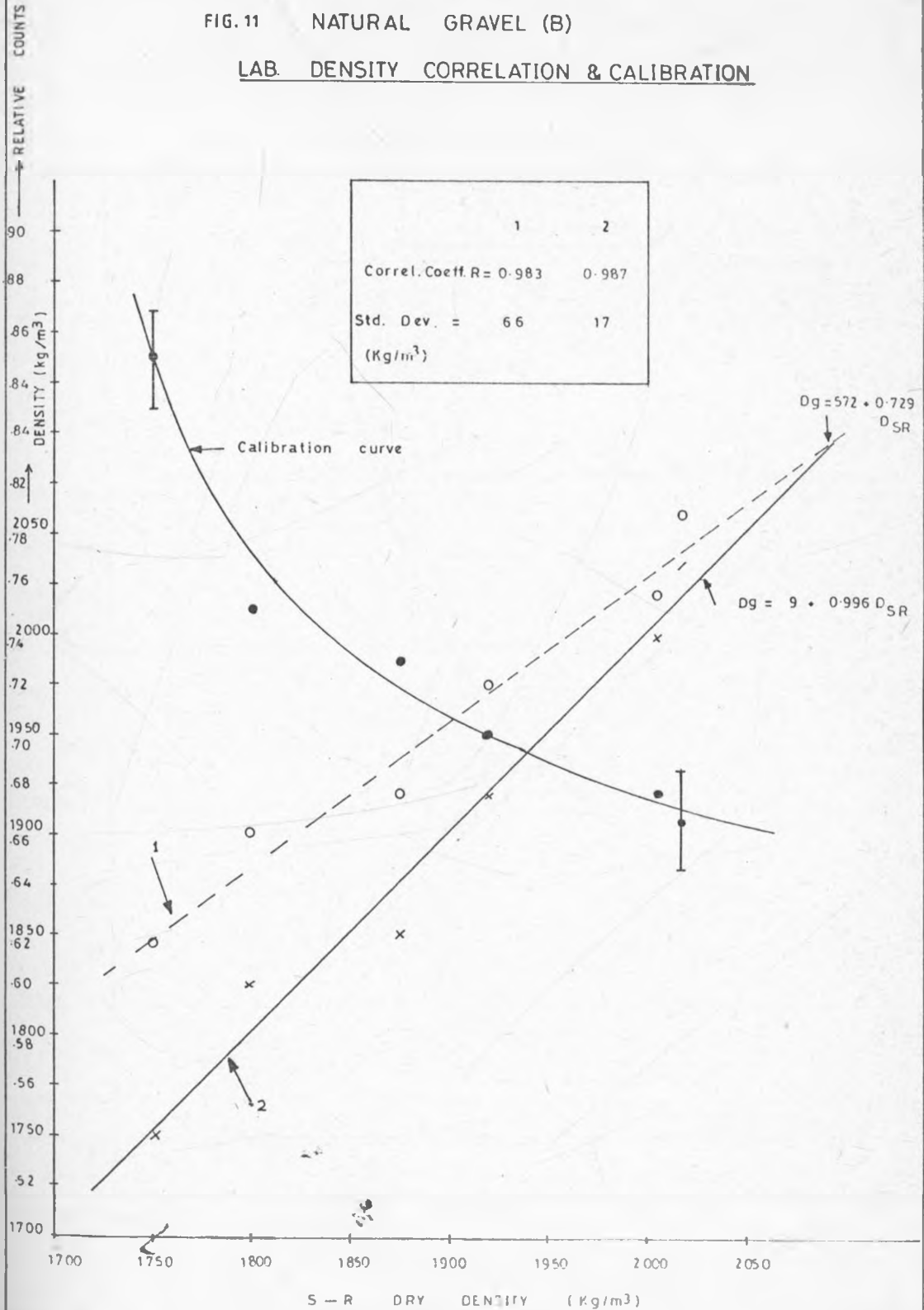
FIG.12 LAB. DENSITY CALIBRATION & CORRELATION CURVES (SILTY SAND (C))
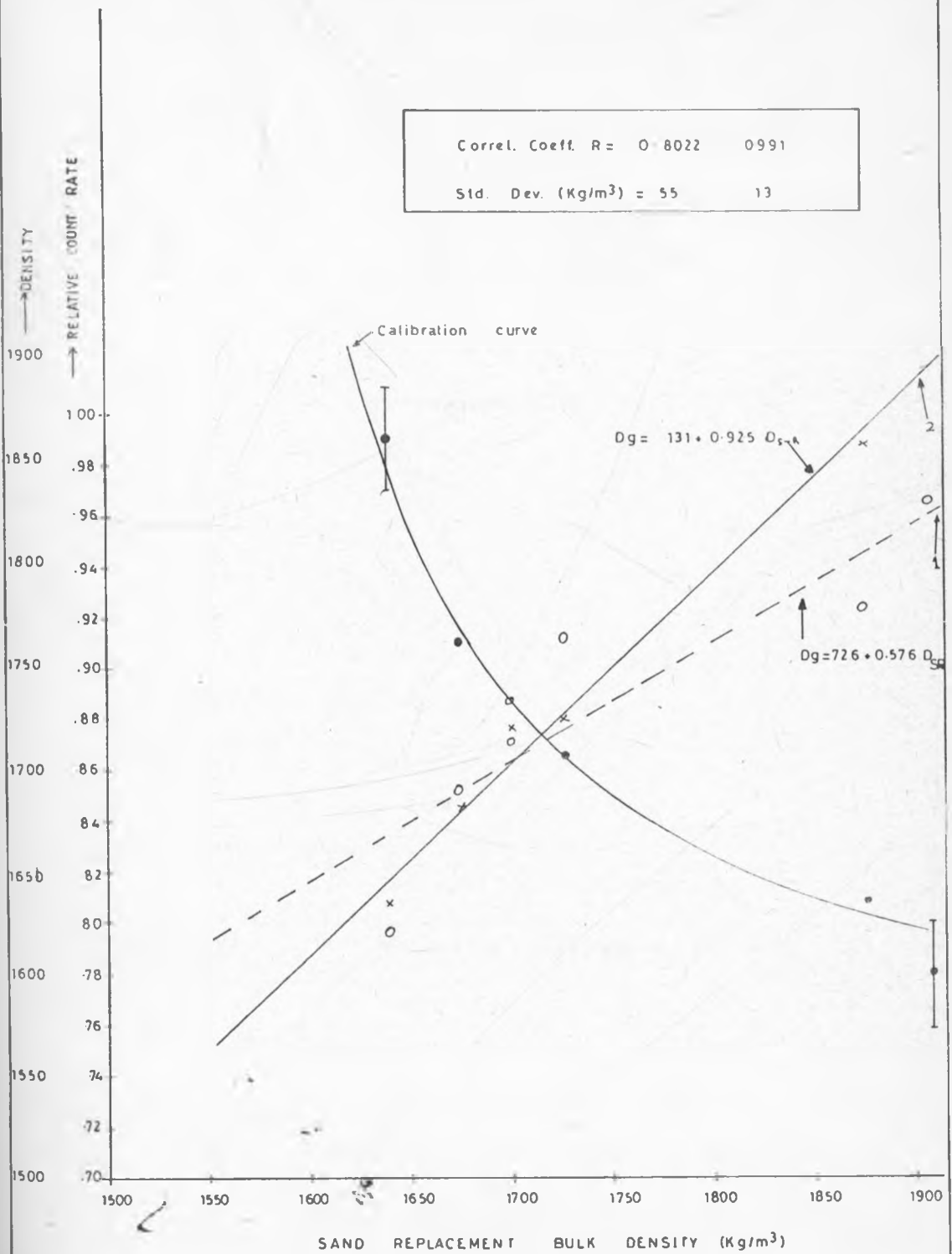
FIG. 13 LAB DENSITY CALIBRATION AND CORRELATION CURVES (BROWN CLAY (D))
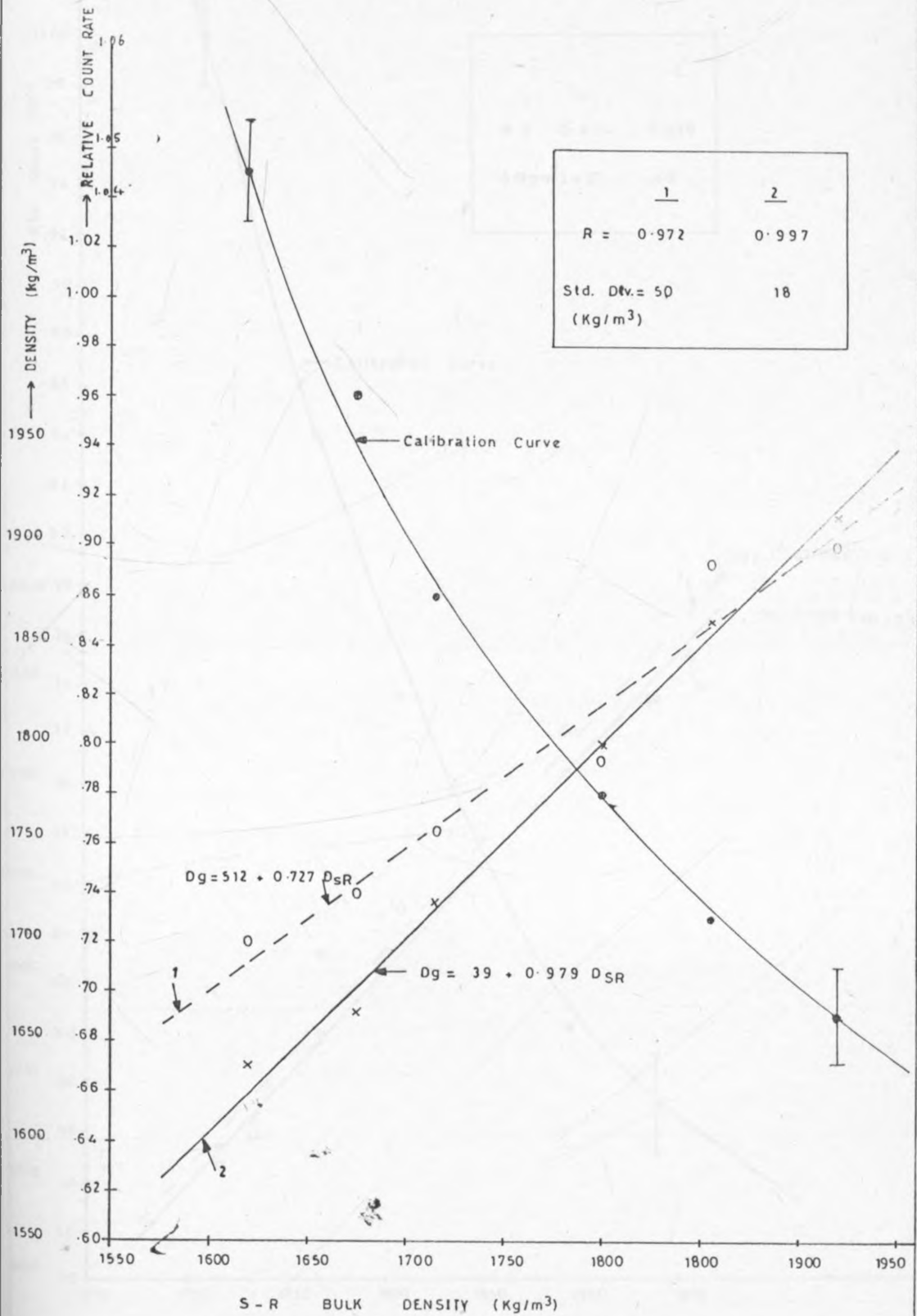
LAB DENSITY CALIBRATION AND CORRELATION CURVES (CLAY SAND (E)) FIG. 14
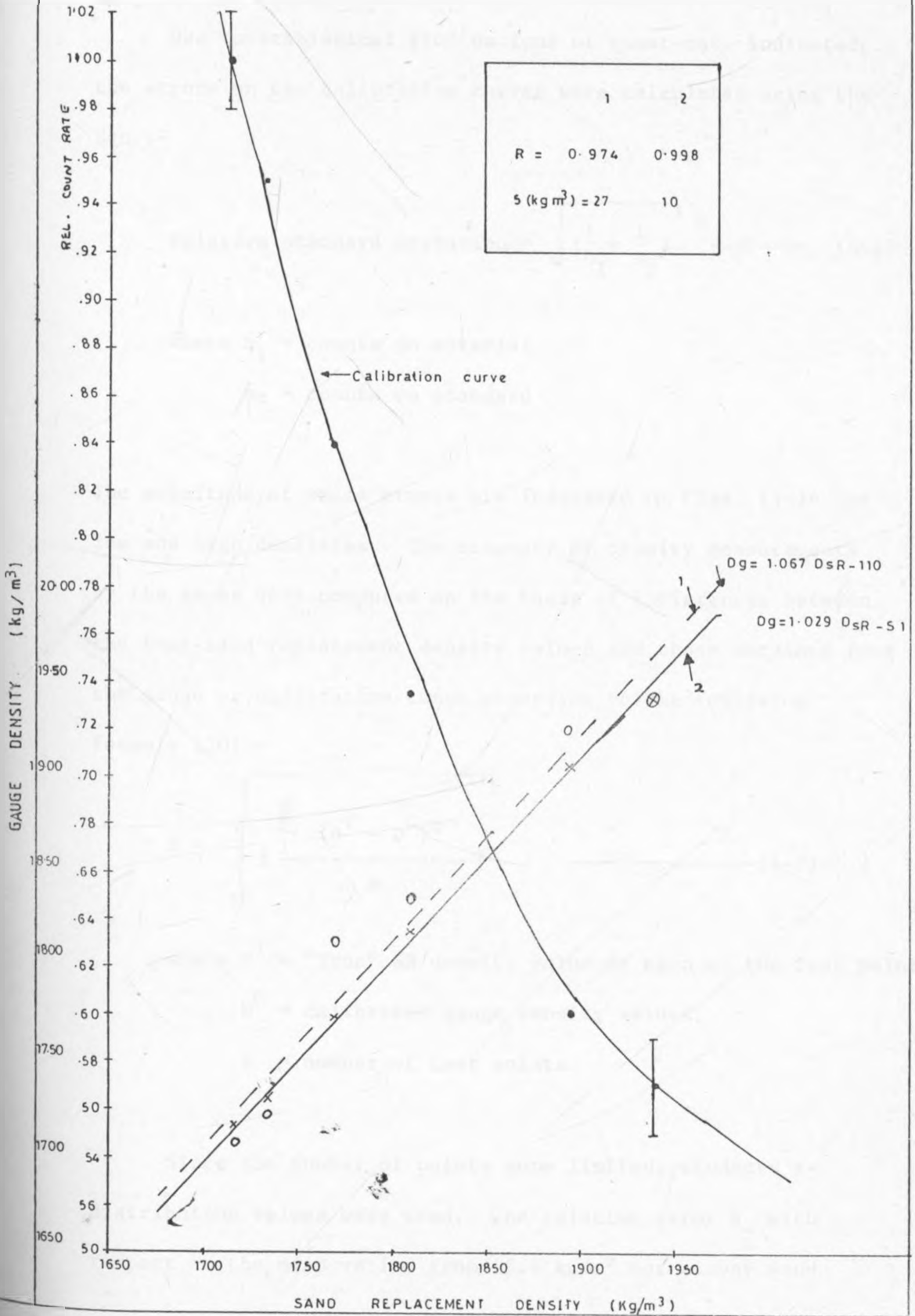
Due to statistical fluctuations of count-rate indicated, the errors on the calibration curves were calculated using the Eqn.:-

$$\text{Relative standard deviation} = \sqrt{\left(\frac{1}{n_1} + \frac{1}{n_2}\right)} \qquad \text{--------} \quad (4\text{-}1)$$

where n_1 = counts on material

n_2 = counts on standard

The magnitude of these errors are indicated in Figs. 11-14 for low and high densities. The accuracy of density measurements by the gauge were computed on the basis of differences between the true sand replacement density values and those obtained from the gauge or calibration curve according to the following formula [30]:-

$$S = \sqrt{\left[\frac{\sum\limits_{1}^{N} (D^T - D^G)^2}{N}\right]} \qquad \text{---------------} (4\text{-}2)$$

where D^T = "True" SR density value at each of the test points.

D^G = calibrated gauge density values.

N = number of test points.

Since the number of points were limited, students t-distribution values were used. The relative error S_x with respect to the mean varied from 15.4 kg/m^3 for clayey sand

(material E) to 46.3 kg/m^3 for brown clay (b) at 95%
confidence level. Since the range of the density values is
narrow, then an average error can be obtained as ± 34 kg/m^3
for all the four materials.

4.1. 1 Discussion of Laboratory results

4.1. 1.1 Comparison of calibration curves

Comparison of the calibration curves (Fig. 9) show that
a single calibration curve could be used for natural gravel, brown
clay and clayey sand in the count-ratio range 0.72 - 0.88. This
curve would cover a density range of 1650 kg/m^3 - 1900 kg/m^3
which may not be of adequate practical use in the field. The
calibration curve for silty sand deviates at densities higher
than 1800 kg/m^3. Generally, the slopes of the calibration curves
are larger for materials with high gravel concentrations [21].
However, from the results obtained, there is no evidence of
consistency of the effect of gravel concentration on density
count ratio.

It was also of interest to assess whether the slopes of
the manufacturer's calibration lines were biased relative to
the slope of the true calibration line linking sand replacement
density values with gauge count ratios.

It can be observed from the calibration curves of Fig. 9 that, except for material E, at low densities, a relatively large change in count ratio corresponds to a small change in density which is less than 10 kg/m^3. However, at high densities (more than 1800 kg/m^3), an equivalent change in count ratio produces a much larger change in density (over 80 Kg/m^3). This reveals that the gauge is less sensitive at high densities.

4.1.1.2 Comparison of regression equations

Consideration of the results obtained in the laboratory (Figs. 11 - 14), show that the gauge density values include, on the average, systematic errors of about 80 kg/m^3 before calibration for materials B, C and D, to less extent material E. These density values are related to the "true" density of the layer as determined from the sand replacement (SR) tests. Nevertheless, no information exists about the accuracy of the sand replacement method.

For each material, the slopes of the regression lines indicated Figs.11 - 14 from the calibration curves were closer to the slope of the equivalence line (slope = 1) than those from the direct gauge data. For clayey sand (E), both slopes of the regression lines were close to unity.

The standard deviations of the density values for the
uncalibrated and calibrated data fall in the ranges of 27-66 kg/m³
and 10-17 kg/m³ respectively. However, the results of suggest
that if the gauge is used on any soil material, the manufacturer's
results can be biased which indicates the importance of
recalibrating the gauge on each material encountered.

4.2 FIELD RESULTS

4.2.1 Comparison of densities from SR tests and nuclear gauge

4.2.1.1 Comparison of Calibration Curves

The types of soils tested in the field were used as base,
sub-base or sub-grade materials for road construction as shown
in the Appendix. The density data obtained consists of density
values read directly from the gauge (Dg) and those obtained from
the calibration curves (Dcc). These curves (Figs. 26-33) were
obtained under field conditions of compaction control. The obtained
nuclear data were compared with the sand replacement test values.
Correction for hydrogen contained in the soil was also done and
the resulting density compared with those of the SR test method.
The results obtained are shown in Tables 7-14 while the corresponding
calibration curves obtained are shown in Figs. 15-22. The density
results corrected for hydrogen content (D_{mc}) are indicated on
column 6 on Tables 7-14.

The ranges of the density values obtained from the calibration curve for each material tested are shown in Fig. 23. The figure shows that the maximum density values for the lime treated sub-base (1), lime treated base-course (3) and the brown clay (7) are lower than the rest of the soils tested. Also evident are the smaller density ranges in these three soil types. A possible explanation for this could be that these materials have small grain size and hence low maximum dry densities.

Table 7: Field Density Data – Nairobi-Thika Road – Lime treated Subbase [depth 200 mm]
Units of Density: Kg/m^3

SIGNAL COUNTS P/MIN. (DC)	RELATIVE COUNT RATE	SAND–REP DENSITY (D_{SR})	GAUGE DENSITY (D_g)	$D_{SR}-D_g$ ΔD_1	DENSITY FROM CALIB. CURVE (D_{cc})	$D_{SR}-D_{cc}$ ΔD_2	DENSITY CORRECTED FOR HYDROGEN (D_{mc})	$D_{SR}-D_{mc}$ ΔD_3
1207	0.422	1783	1750	+33	1760	+23	1752	+31
1228	0.412	1746	1750	-4	1770	-24	1782	-36
1269	0.426	1714	1734	-20	1753	-39	1756	-42
1284	0.431	1745	1730	+15	1745	0	1740	+5
1287	0.432	1756	1709	+47	1740	+16	1744	+12
1399	0.470	1710	1684	+26	1686	+24	1677	+33
1380	0.463	1735	1694	+41	1696	+39	1688	+47
1435	0482	1644	1665	-21	1668	-24	1657	-13
1403	0.471	1708	1691	+17	1684	+24	1675	+33
1239	0.422	1783	1697	+86	1760	+23	1763	+20
1113	0.374	1844	1748	+96	1847	-3	1861	-17
1138	0.390	1826	1807	+19	1816	+10	1827	-1
1249	0.419	1706	2688	+18	1765	-59	1768	-62
1029	0.349	1898	1703	+195	1898	0	1925	-27
1068	0.359	1884	1783	+101	1878	+6	1895	-11
1462	0.491	1697	1615	+82	1634	+63	1642	+55
1175	0.395	1827	1728	+99	1880	-53	1817	+10
1117	0.375	1882	1750	+132	1844	+38	1858	+24
1240	0.416	1730	1753	-23	1770	-40	1774	-44
1212	0.422	1768	1747	+21	1760	+8	1763	+5
1269	0.432	1745	1726	+19	1745	0	1746	-1
1173	0.394	1800	1760	+40	1808	-8	1819	-19
1218	0.409	1738	1766	-12	1782	-44	1789	-51
1299	0.440	1720	1740	-20	1732	-12	1730	-10

Fig.15 NAIROBI - THIKA RD FIELD DENSITY CALIBRATION CURVE
LIME TREATED SUB-BASE .(200mm)

Table 8: Field Density Data (Kg/m^3) [Bura-Garissa Road] – Subgrade I

SIGNAL COUNTS P/MIN. (DC)	RELATIVE COUNT RATE	SAND-REP. DENSITY (D_{SR})	GAUGE DENSITY (D_g)	ΔD_1 $D_{SR}-D_g$	DENSITY FROM CALIB. CURVE (D_{cc})	ΔD_2 $D_{SR}-D_{cc}$	DENSITY CORRECTED FOR HYDROGEN (D_{uc})	ΔD_3 $D_{SR}-D_{mc}$
1548	0.538	2100	2088	+12	2105	−5	2074	+26
2101	0.728	1925	1860	+65	1861	+64	1863	+62
1573	0.511	2097	2105	−8	2145	−48	2108	−11
1749	0.606	1940	1962	−22	2007	−67	1990	−50
1832	0.635	1990	1922	+68	1970	+20	2058	+932
1877	0.601	1980	1900	+80	1951	+31	1941	+39
2123	0.736	1920	1792	+128	1852	+68	1856	+64
1823	0.632	1960	1926	+34	1974	−14	1962	−2
2012	0.697	1850	1843	+7	1895	−45	1893	−43
1937	0.671	1870	1876	−6	1926	−56	1920	−50
2116	0.734	1855	1800	+55	1847	+8	1858	−3
1769	0.613	1935	1949	−14	1998	−63	1982	−47
1686	0.584	2080	1990	+90	2037	+43	2016	+64
2525	0.872	1785	1715	+70	1716	+69	1738	+47
1984	0.688	1825	1852	−27	1906	−81	1903	−78
2010	0.697	1835	1845	−10	1896	−61	1894	−59
2033	0.705	1910	1836	−26	1887	+23	1886	+24
1906	0.661	1915	1890	+25	1938	−23	1931	−16
1598	0.554	2055	2036	+19	2079	−24	2052	+3
2216	0.691	1890	1702	+188	1818	+72	1899	−9
2017	0.699	1880	1842	+38	1893	−13	1891	−11
2188	0.758	1860	1774	+86	1828	+32	1835	+25
2001	0.694	1955	1850	−705	1900	+55	1896	+59
1713	0594	1975	1980	−5	2024	−49	2004	−29

FIG. 16 BURA - GARISSA RD FIELD DENSITY CALIBRATION CURVE
SUB GRADE 1
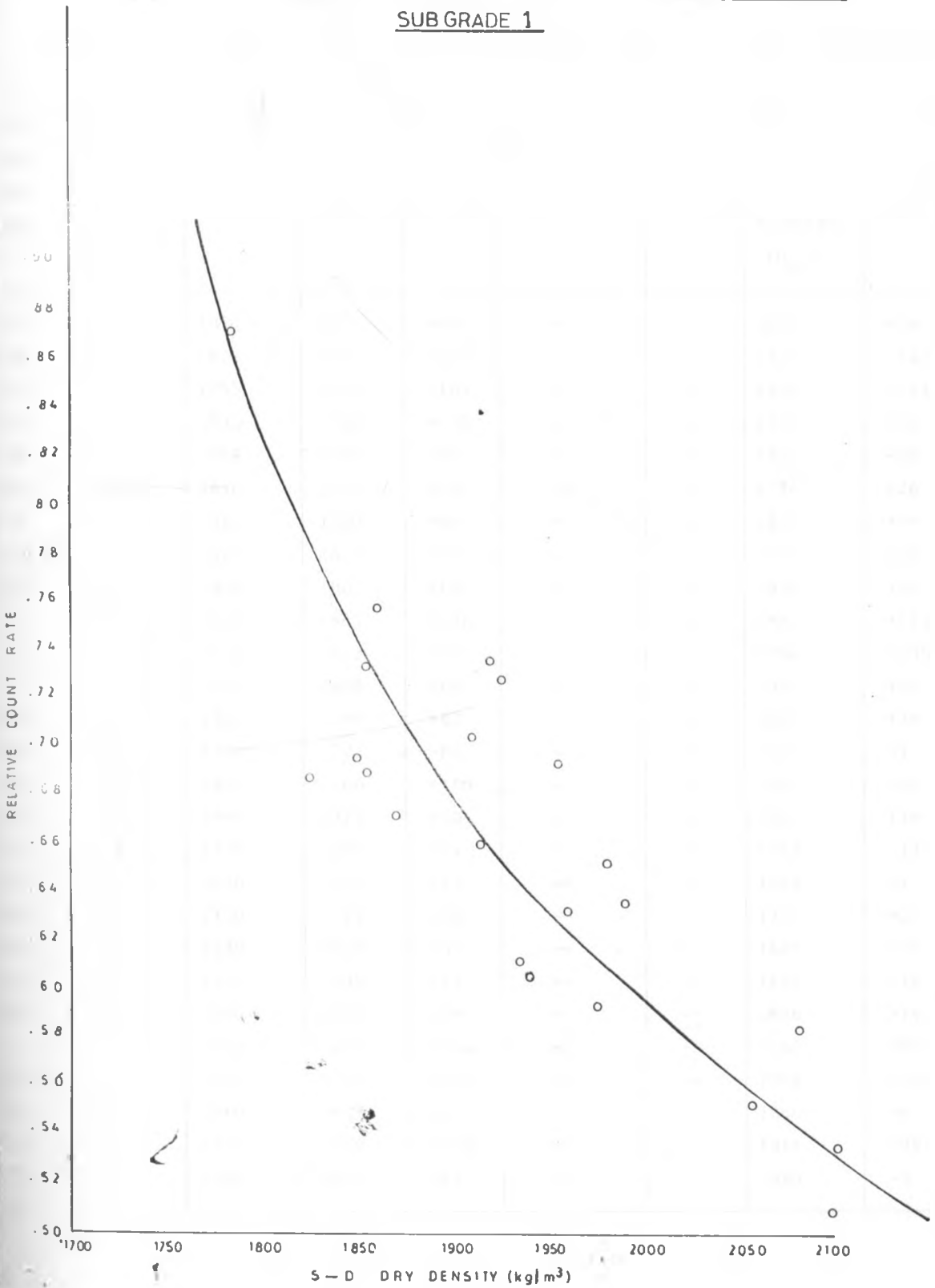
Table 9: Field Density Data (Kg/m³) [Bura-Garissa Road] Lime Treated basecourse

SIGNAL COUNTS P/MIN. (DC)	RELATIVE COUNT RATE	SAND-REP. DENSITY (D_{SR})	GAUGE DENSITY (D_g)	ΔD_1 $D_{SR}-D_g$	DENSITY FROM CALIB. CURVE (D_{cc})	ΔD_2 $D_{SR}-D_{cc}$	DENSITY CORRECTED FOR HYDROGEN (D_{mc})	ΔD_3 $D_{SR}-D_{mc}$
2055	0.723	1934	1871	+63	--	--	1896	+38
2820	0.992	1873	1643	+230	--	--	1721	152
1903	0.669	1755	1920	-165	--	--	1878	-123
2627	0.924	1832	1702	+130	--	--	1777	+55
2228	0.731	1889	1795	+94	--	--	1820	+69
2096	0.781	1810	1752	+58	--	--	1784	+26
2041	0.172	1865	1780	+85	--	--	1820	+45
2602	0.907	1820	1678	+142	--	--	1795	+25
2072	0.723	1870	1802	+68	--	--	1826	+44
1951	0.677	2000	1864	+136	--	--	1887	+113
2220	0.776	1910	1952	-42	--	--	1780	+130
1752	0.708	1950	1890	+60	--	--	1925	+25
2074	0.724	1880	1798	+82	--	--	1804	+76
2169	0.757	1700	1722	-22	--	--	1693	+7
1789	0.624	1860	1700	+160	--	--	1942	-82
1952	0.681	1880	1779	+101	--	--	1861	+19
2343	0.825	1770	1696	+74	--	--	1783	-13
2344	0.825	1690	1701	-11	--	--	1683	+7
2269	0.799	1770	1721	+49	--	--	1743	+27
2490	0.877	1680	1627	+53	--	--	1626	+54
2321	0.817	1710	1699	+11	--	--	1692	+18
1882	0.663	1900	1821	+79	--	--	1886	+14
2153	0.758	1855	1709	+146	--	--	1762	+93
2190	0.771	1870	1739	+131	--	--	1746	+124
1864	0.656	1860	1857	+3	--	--	1866	-6
2030	0.715	1915	1759	+156	--	--	1816	+99
2089	0.736	1880	1819	+61	--	--	1889	-9

FIG.17

Field   calibration curve

Lime   treated   Basecourse   Depth :   150mm.
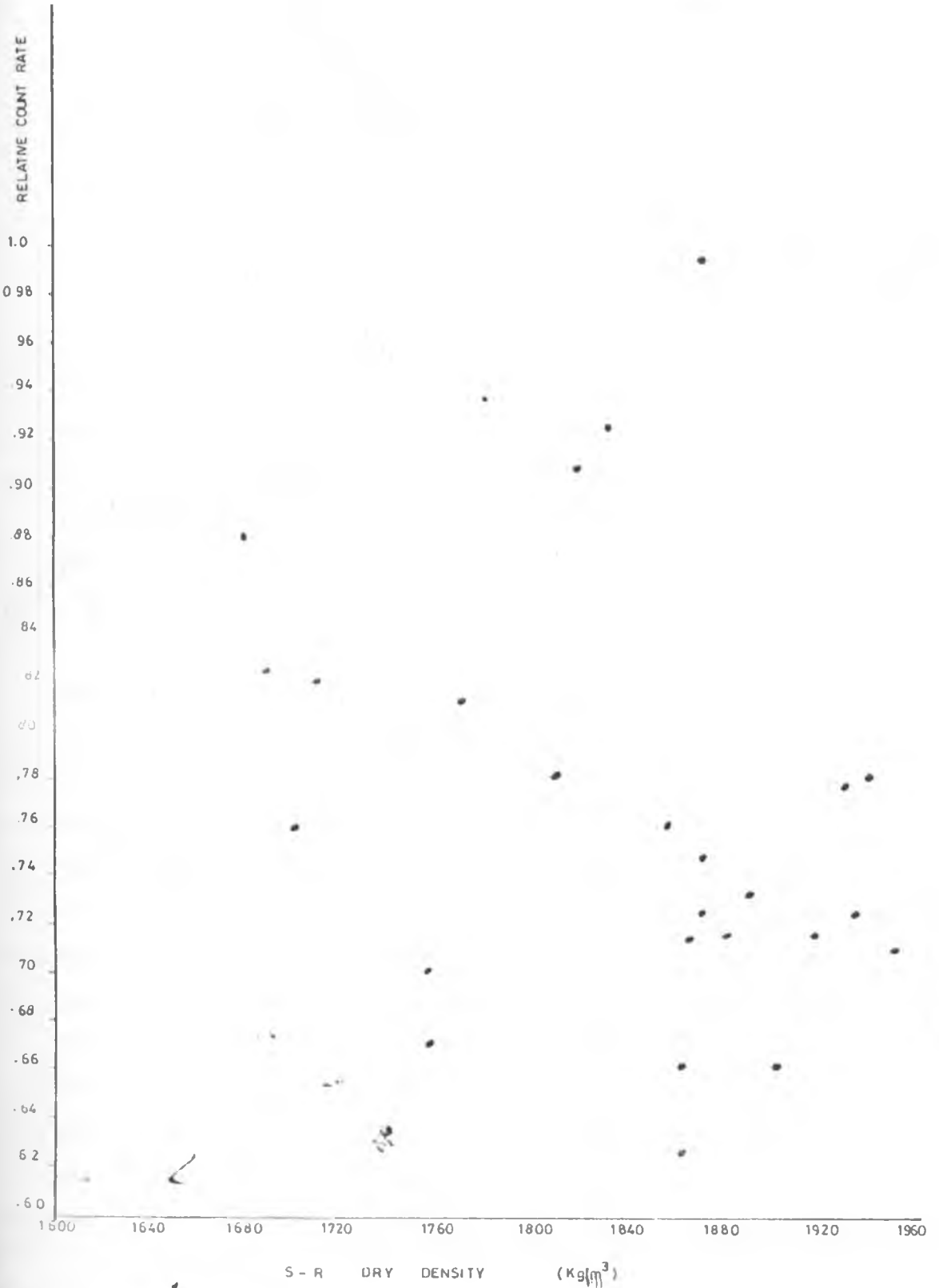
Table 10: Field Density Data (Kg/m^3) - [Lodwar-Kakuma Road] - Coarse Gravel

	SIGNAL COUNTS c/MIN (DC)	RELATIVE COUNT RATE	SAND-REP. DENSITY (D_{SR})	GAUGE DENSITY (D_g)	ΔD_1 $D_{SR}-D_g$	DENSITY FROM CALIB. CURVE (D_{cc})	ΔD_2 $D_{SR}-D_{cc}$	DENSITY CORRECTED FOR HYDROGEN (D_{mc})	ΔD_3 $D_{SR}-D_{mc}$
1	2308	0.789	1770	1861	-91	1760	+10	1761	+9
2	2080	0.701	1996	1932	+64	1960	+36	1990	+6
3	2027	0.693	1928	1931	-3	2010	-82	1922	+6
4	2070	0.708	1814	1924	-110	1920	-106	1920	-106
5	2064	0.706	1917	1939	-22	1930	-22	1918	-1
6	2198	0.692	2007	1893	+114	2024	-17	2015	-8
7	2012	0.688	2066	2058	+8	2070	-4	2056	-10
8	2024	0.692	2047	1998	+49	2030	+17	2028	+15
9	2030	0.694	2014	1997	+17	2005	+9	2010	+4
10	2033	0.695	1977	2003	-26	2000	-13	2001	-24
11	2018	0.690	2070	2002	+62	2050	+20	2048	-22
12	2021	0.691	2024	1963	+61	2030	-6	2018	+6
13	2062	0.705	1924	1901	+23	1930	-6	1932	-8
14	2094	0.716	1876	1933	-57	1890	-14	1881	-5
15	2021	0.691	2070	2008	+62	2035	+35	2000	+70
16	2021	0.691	2052	2008	+44	2035	+17	2040	+12
17	2056	0.703	1950	1962	-12	1945	+5	1952	-2
18	2024	0.692	1973	1967	+6	1980	-7	1970	+3
19	2167	0.741	1800	1822	-22	1810	-10	1814	-14
20	2141	0.732	1831	1798	+33	1825	+6	1828	+3

FIG.18 LODWAR – KAKUMA ROAD
COARSE GRAVEL A DENSITY CALIB (field)
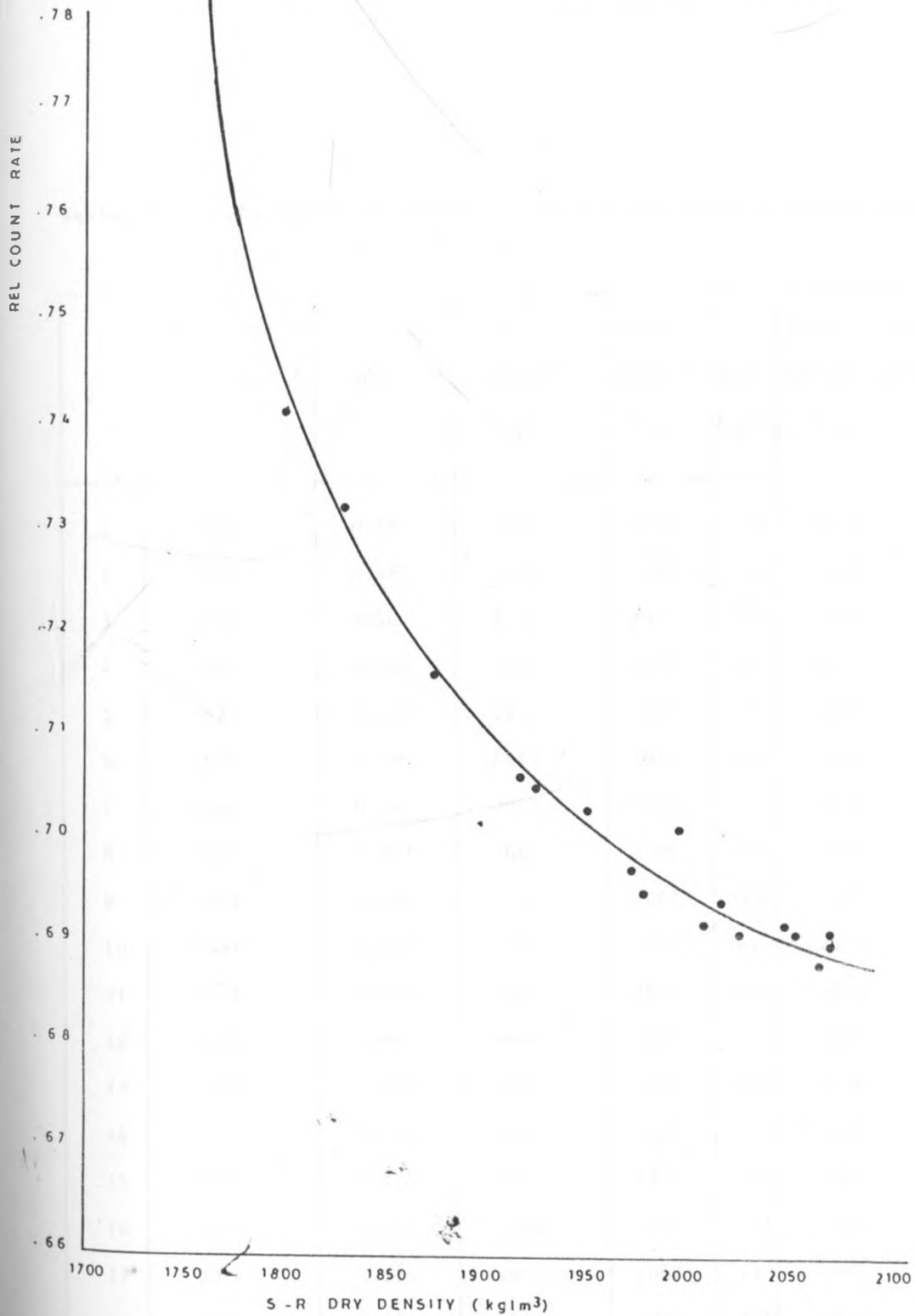
Table 11: Field Density Data (Kg/m^3) [Lodwar-Kakuma Road] - Natural Gravel

	SIGNAL COUNTS PER MIN.(DC)	RELATIVE COUNT	SAND-REP. DENSITY (D_{SR})	GAUGE DENSITY (D_g)	$\triangle D_1$ $D_{SR}-D_g$	DENSITY FROM CALIB. CURVE (D_{cc})	$\triangle D_2$ $D_{SR}-D_{cc}$
1	2501	0.855	1700	1738	-38	1717	-17
2	2010	0.687	1936	1946	-10	1945	-9
3	1919	0.656	2132	2073	+59	2120	+12
4	1942	0.664	2149	2088	+61	2115	+34
5	1925	0.658	2086	2093	-7	2090	-4
6	1948	0.666	1979	2013	-34	2010	-31
7	1948	0.666	2062	2028	+34	2035	+27
8	1936	0.662	2067	2000	+67	2060	+7
9	1948	0.666	1978	2012	-34	2035	-57
10	1931	0.660	2082	2083	-1	2075	+7
11	1948	0.666	2069	1993	+76	2035	+34
12	1936	0.662	2050	2033	+17	2055	-5
13	1919	0.656	2174	2155	+19	2130	+44
14	2141	0.732	1850	1874	-24	1850	0
15	2094	0.716	1865	1830	+35	1867	-2
16	2053	0.702	1906	1920	-14	1910	-6
17°	2094	0.716	1874	1887	-13	1877	-3
18	1972	0.674	2010	1990	+20	1975	+35

FIG.19 FIELD DENSITY CALIBRATION CURVE
(NATURAL GRAVEL (B))
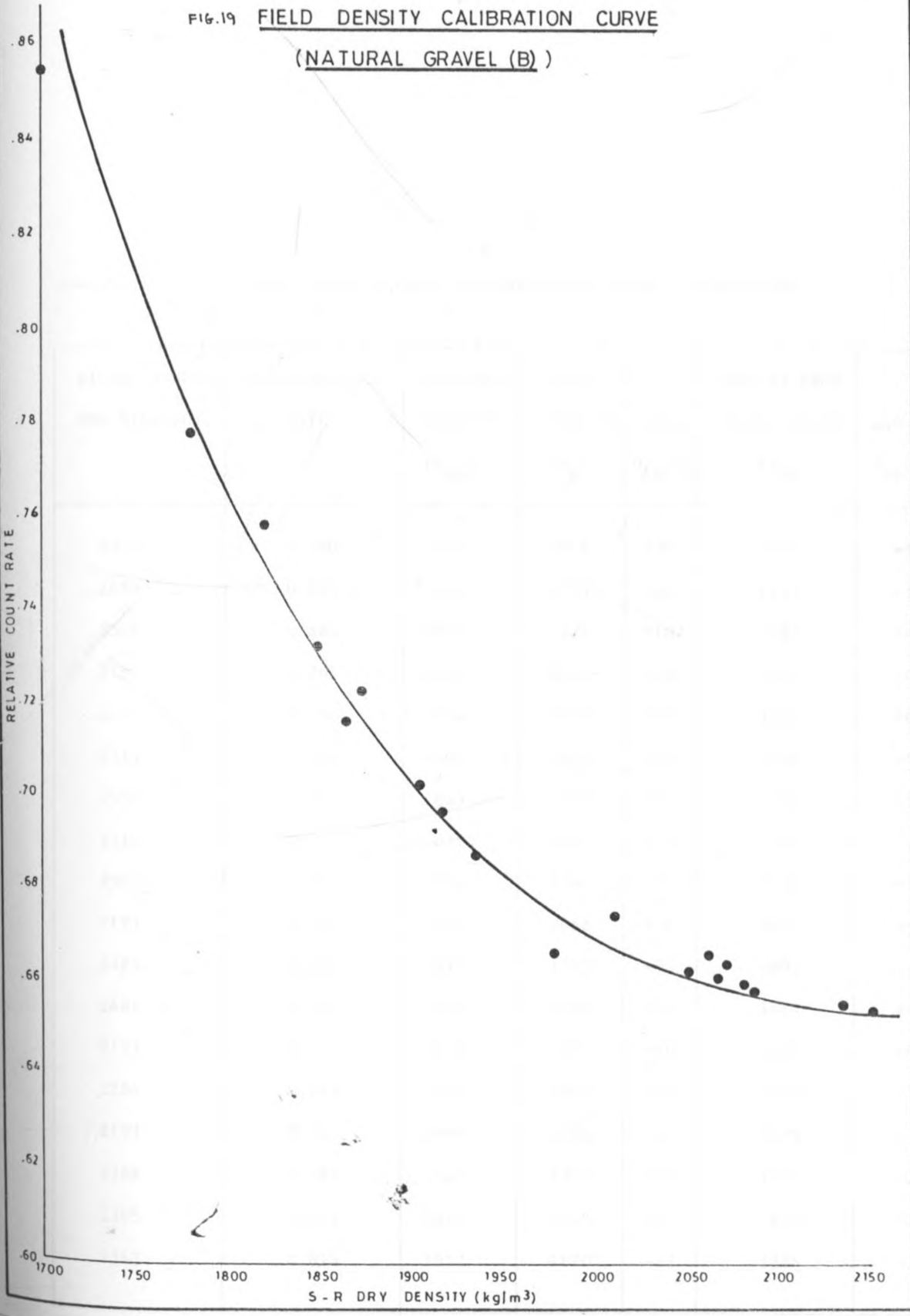
Table 12: Field Density Data (Kg/m^3) [Lodwar-Kakuma Road] - Silty Sand

SIGNAL COUNTS PER MIN.(DC)	RELATIVE COUNT RATE	SAND-REP. DENSITY (D_{SR})	GAUGE DENSITY (D_g)	$\triangle D_1$ $D_{SR}-D_g$	DENSITY FROM CALIB. CURVE (D_{cc})	$\triangle D_2$ $D_{SR}-D_{cc}$
2533	0.880	1846	1816	+30	1795	+51
2659	0.924	1750	1774	-24	1755	-5
2556	0.888	1829	1727	+102	1785	+44
2199	0.764	1975	2043	-68	2020	-45
2245	0.780	2004	1990	+14	1920	+84
2314	0.804	1896	1833	+63	1900	-4
2538	0.882	1805	1760	+45	1790	+15
2210	0.768	2031	1982	+49	2000	-31
2593	0.901	1764	1762	+2	1775	-11
2193	0.762	2074	2058	+16	2025	+49
2325	0.808	1892	1797	+95	1895	-3
2481	0.862	1834	1800	+34	1815	+19
2193	0.762	2031	2005	+26	2025	+6
2254	0.783	1945	1962	-17	1950	-5
2193	0.762	1986	1990	-4	2025	-39
2268	0.788	1920	1952	-32	1940	-20
2395	0.832	1824	1832	-8	1850	-26
2343	0.814	1852	1870	-22	1885	-33

FIG. 20 FIELD DENSITY CALIBRATION CURVE
(SILTY SAND (c))
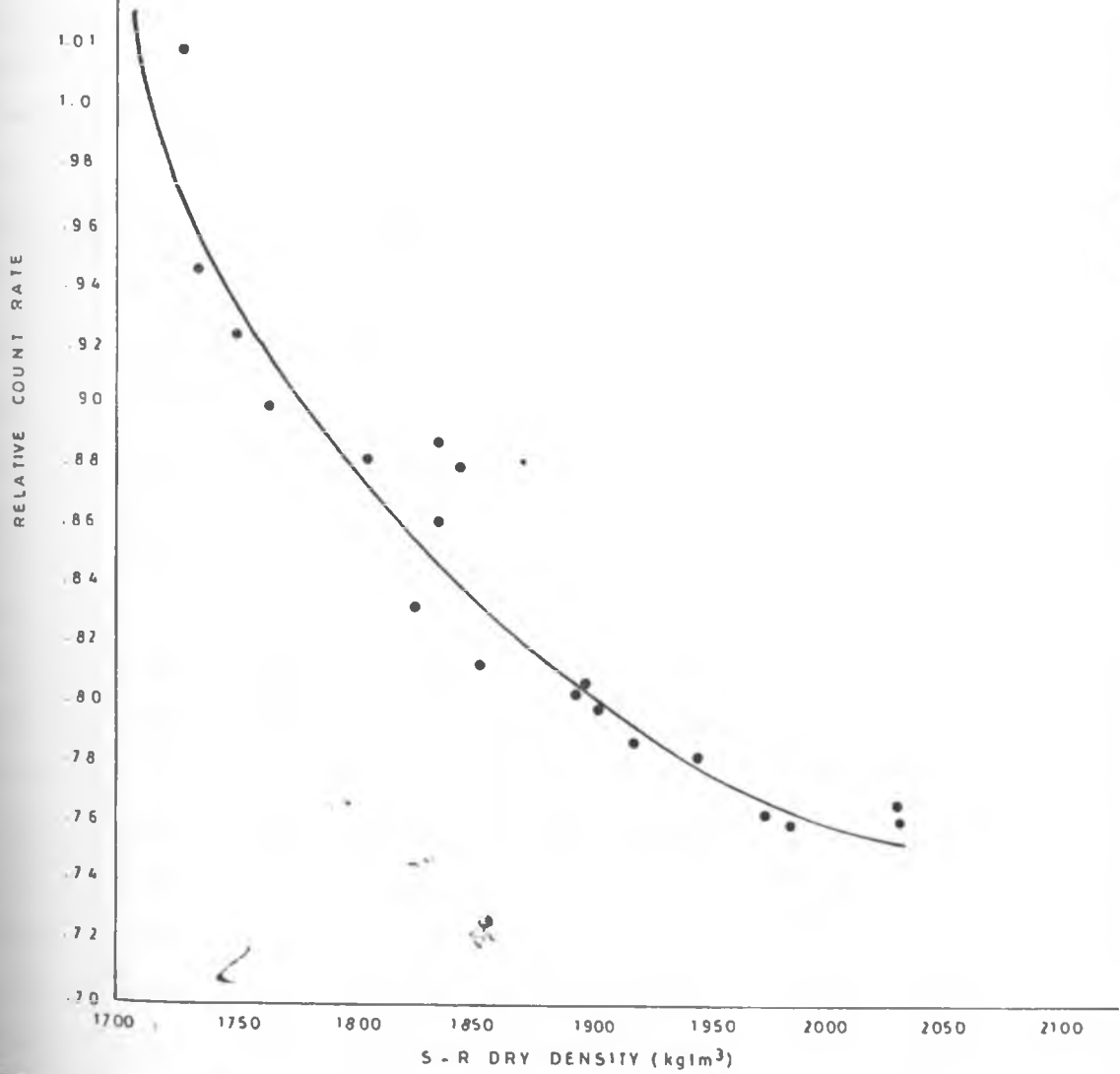
Table 13: Field Density Data (Kg/m^3) [Lodwar-Kakuma Road] Brown Clay

SIGNAL COUNTS P/MIN. (DC)	RELATIVE COUNT RATE	SAND-REP. DENSITY (D_{SR})	GAUGE DENSITY (D_g)	$\triangle D_1$ $D_{SR}-D_g$	DENSITY FROM CALIB. CURVE (D_{cc})	$\triangle D_2$ $D_{SR}-D_{cc}$	DENSITY CORRECTED FOR HYDROGEN (D_{uc})	$\triangle D_3$ $D_{SR}-D_{mc}$
3889	1.351	1595	1654	-59	1605	-10	1590	+5
2728	0.948	1639	1717	-78	1650	-111	1630	+9
3460	1202	1632	1658	-26	1610	+22	1633	-1
2248	1.024	1851	1849	+2	1843	+8	1840	+11
2717	1.443 (.944)	1685	1616	+69	1650	+35	1686	-1
2320	1.143 (.806)	1805	1761	+44	1795	+10	1810	-5
2671	0.928	1750	1740	+10	1663	+87	124	+9
2769	0.962	1635	1650	-15	1640	-5	1647	-12
2383	0.828	1697	1739	-37	1750	-63	1708	-11
2734	0.950	1666	1640	+26	1650	+16	1650	+16
3051	1.06	1597	1649	-43	1615	+18	1600	-3
2475	0.860	1674	1703	-29	1725	-51	1710	-36
2481	0.862	1682	1683	-1	1700	-18	1667	+15
2734	0.950	1630	1680	-50	1650	-20	1620	+10
2331	0.810	1679	1768	-89	1785	-106	168	-2
2475	0.860	1755	1690	+65	1725	+30	1735	+20
2308	0.800	1786	1790	-4	1805	-19	1768	+18
2412	0.838	1722	1744	-22	1750	-28	1729	-7
2625	0.912	1700	1680	+20	1675	+25	1725	-25
2395	0.832	1760	1750	+10	1755	+5	1748	+12

FIG.21 FIELD DENSITY CALIBRATION CURVE
(BROWN CLAY (D))
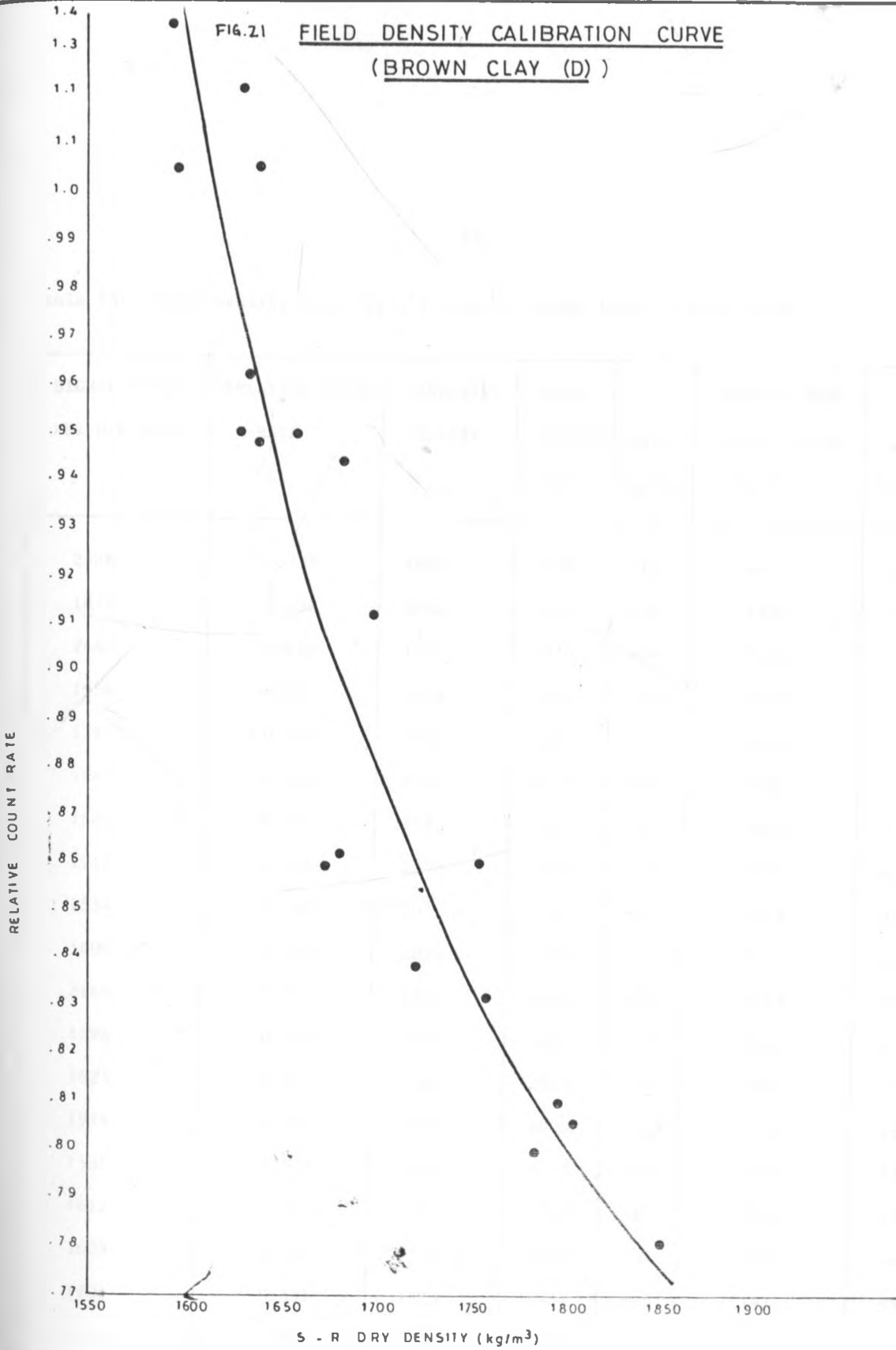
Table 14: Field Density Data (kg/m³) (Lodwar-Kakuma Road - Clayey Sand

SIGNAL COUNTS PER MIN.(DC)	RELATIVE COUNT RATE	SAND-REP. DENSITY (D_{SR})	GAUGE DENSITY (D_g)	$\triangle D_1$ $D_{SR}-D_g$	DENSITY FROM CALIB. CURVE (D_{cc})	$\triangle D_2$ $D_{SR}-D_{cc}$
2588	0.799	1888	1899	-11	--	--
1871	0.650	1892	1930	-38	1900	-8
2440	0.624	1922	1970	-48	1922	0
1956	0569	1994	2094	-100	2000	-6
1795	0.522	2141	2162	-21	2157	-16
1989	0.538	2045	2076	-31	2085	-40
1682	0.584	1982	1977	+5	1975	+7
1917	0.666	1892	1928	-36	1890	+2
1554	0.540	2077	2062	+15	2075	+2
1606	0.558	2030	2028	+2	2026	+4
2164	0.752	1814	1880	-66	1823	-9
1594	0.554	1999	2031	-32	2030	-31
1623	0.564	1987	2020	-33	2007	-20
1974	0.686	1879	2000	-121	1873	+6
1531	0.532	2133	2110	+23	2107	+26
1612	0.560	2010	2018	-8	2015	-5
1629	0.566	956	1990	-34	2003	-47
1701	0.591	1979	1964	+15	1971	+8
1643	0.571	2011	1998	+13	2000	+11
1733	0.602	1967	1944	+23	1950	+17

FIG.22 FIELD DENSITY CALIBRATION CURVE
(CLAYEY SAND (E))

RELATIVE COUNT RATE

D S - R DENSITY (kg/m³)
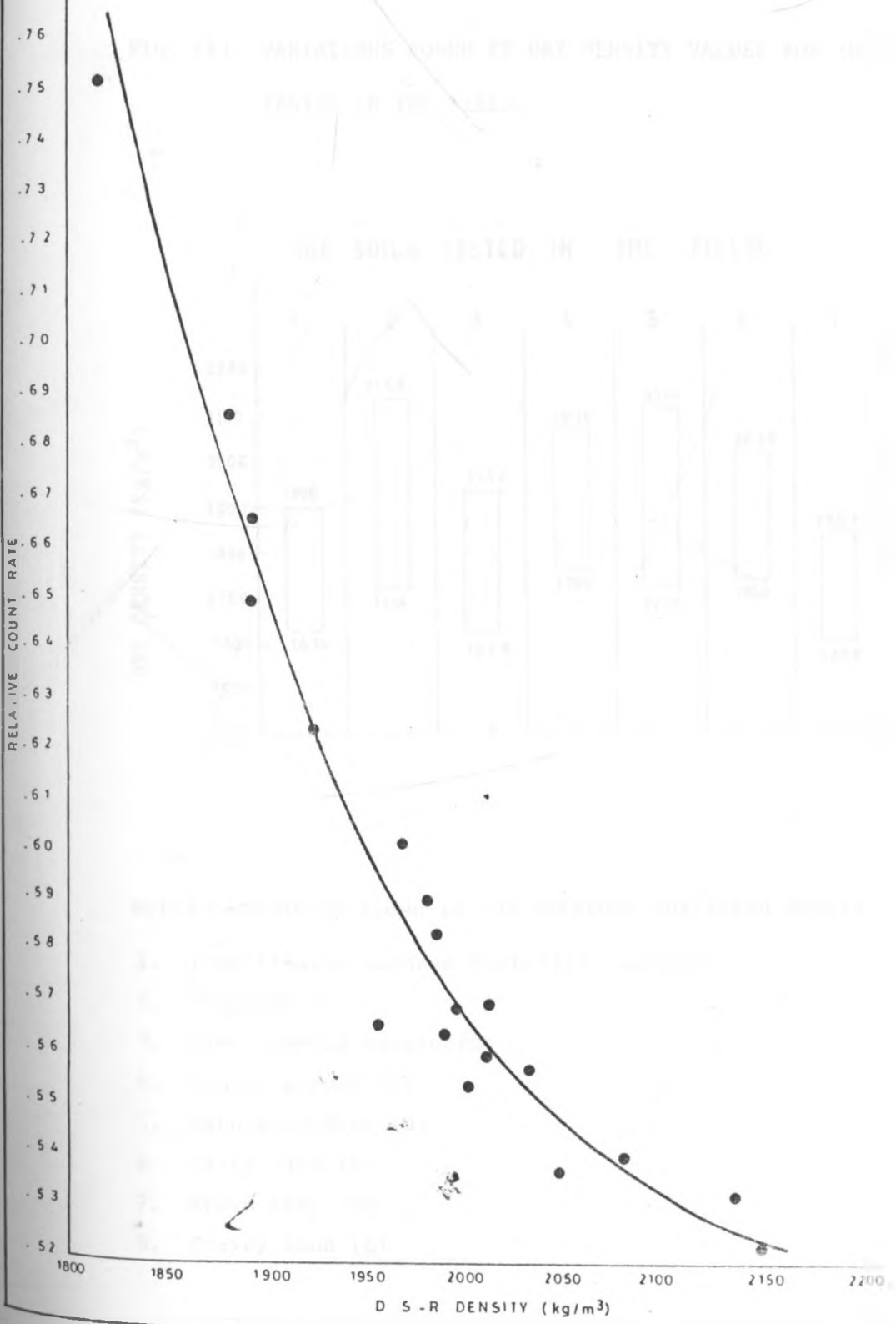
FIG. 23:   VARIATIONS FOUND IN DRY DENSITY VALUES FOR THE SOILS
           TESTED IN THE FIELD.

THE SOILS TESTED IN THE FIELD.
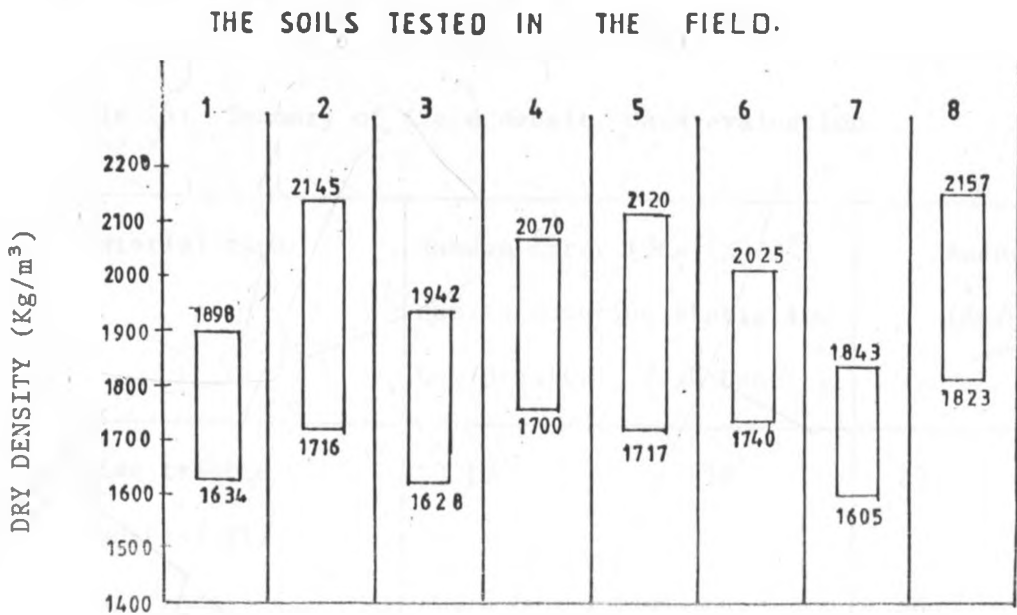
Note: * Variation shown is for moisture corrected density.

1.   lime treated subbase (lateritic murram)

2.   Subgrade 1

3.   lime treated basecourse

4.   Coarse gravel (A)

5.   Natural gravel (B)

6.   Silty sand (C)

7.   Brown clay (D)

8.   Clayey sand (E)

Table 15 shows a summary of the evaluation of the density results obtained. The random error due to counting statistics δcs is indicated for both low and high densities while the accuracies shown are with respect to the mean value of the density range for each material tested.

Table 15: Summary of field density data evaluation

Material type	Random Error (δcs)(Kg/m^3) due to counting statistics		Accuracy (Kg/m^3)	
	Low Density	High Density		
Lime treated Sub-base (1)	10	18	25	(1.3%)
Sub-grade 1 (2)	9	26	46	(2.3%)
Lime treated Basecourse (3)	--	--	--	--
Coarse gravel (4)	10	42	17	(1.1%)
Natural gravel (5)	11	67	24	(1.3%)
Silty sand (6)	12	32	25	(1.3%)
Brown Clay (7)	4	10	27	(1.6%)
Clayey sand (8)	8	30	19	(1%)

Table 16. Variation in density and Relative counts on tested materials.

	Material Type							
	1	2	3	4	5	6	7	8
Relative Count rate difference (Δ CR)	.49-.34 (0.15)	0.87-0.5 (0.37)	* *	0.79-0.69 (0.10)	0.85-0.66 (0.19)	1.02-0.76 (0.26)	1.4-0.78 (0.62)	0.75-0.52 (0.23)
Density difference (Δ D)	264	182	316	310	403	285	238	334

Note: * data obtained were scattered - no correlation between count rate and density was obtained.

1 - 8 are the soil types as indicated on Fig. 23.

Table 15 and the calibration curves obtained indicate that for
all the materials tested, a sensitivity (Δ CR/Δ D) for a given
dry density is affected by the type of material. The use of
a single calibration curve for all the materials could thus
introduce errors. There was some scatter of the points around
the calibration lines, which was more pronounced for soils
1, 3 and 7. The calibration plot obtained from the lime treated
basecourse (3) (Fig. 17) was not suitable for use due to no
correlation between count rate and density. The most probable
cause for adverse scatter in soil 3 could have been due to
non-uniform mixing of the lime with the soil on site which was
carried out by inexperienced operators who were on training.
The only results that could be obtained for this material were
read directly from gauge and calibrated density could not be
compared with sand replacement results. The results obtained
are thus not discussed. It is felt that the pronounced scatter
of the results for soils 1, 3 and 7 was partly due to soil type effect
(that is, composition and texture), due to moisture content,
and also the different depths of soil sampled by the apparatus
as compared with the sand replacement test. The errors due
to counting statistics, and gauge sitting position also
contributed to the scatter of points.

The variation of density due to changes in moisture

content can be explained by considering Eqn. (3-1) of Chapter 3.
It can be seen from the equation that the nuclear gauge
essentially measures the bulk density of the soil. The
difference between the bulk (wet) density (WD) and dry density
(DD) gives the volumetric moisture content. No information
is available about hydrogen correction for density determination
by the gauge electronics. However, it is known that soil
contains hydrogen from organic matter and/or crystallization
water. Figure 24 reveals that hydrogen has a mass absorption
coefficient that differs widely from those of all the other
elements over a wide range of gamma radiation energy. Thus,
the gauge reading for a given dry density would be affected
by the hydrogen content of the material. This leads to the
conclusion that correction for soil hydrogen could be made
to improve the density results. The correction can be done
using Eqn. (3-6). The results obtained are discussed later
in section 4.2.2.
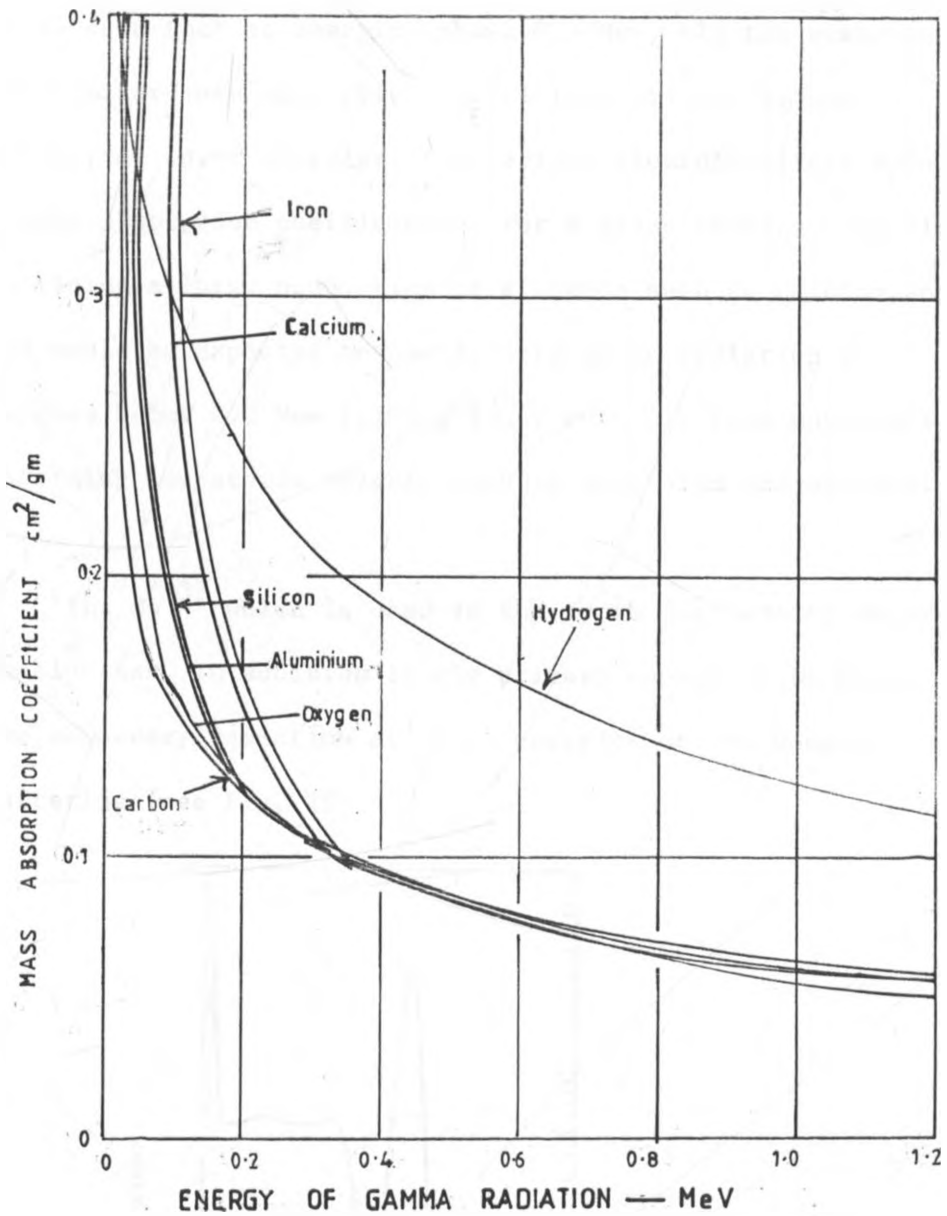
Fig. 24. Relations between mass absorption coefficients and the energy of gamma radiation for elements commonly found in soils (21)

The influence of soil chemical composition on the counting rate at a given density can also be explained using Fig. 24.   It can be seen that at energies above 0.3 Mev, all the elements have similar mass absorption coefficient (except hydrogen). However, at lower energies, the various elements differ widely in mass absorption coefficient.   For a given density, materials containing a large proportion of elements such as calcium and iron would be expected to absorb more gamma radiation at energies below 0.3 Mev (giving lower counts), than materials containing low atomic weights such as aluminium and silicon.

The Cs^{137} which is used in the gauge for density determination has, in addition to the primary energy (0.66 Mev), some secondary radiation at lower energies due to Compton Scattering (see Fig. 25)
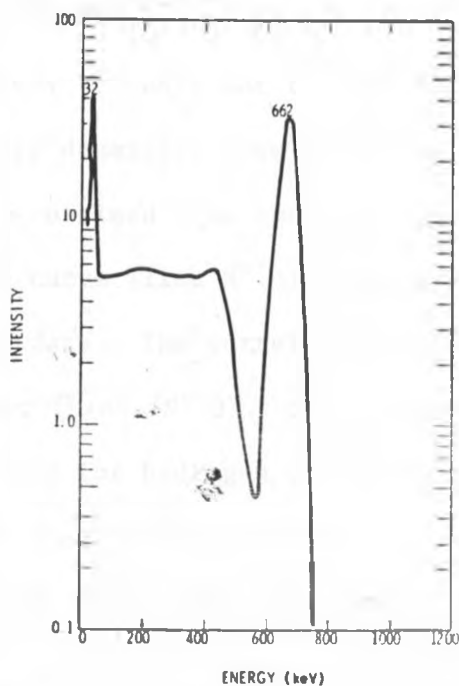
Fig. 25:   Spectrum for ^{137}Cs as a function of energy in KeV [32].

If this Compton scattered radiation is detected, the effect of small variation in the composition of a soil material may lead to appreciable errors in density determination.

The results of quantitative analysis as given in Table 4 show that iron contents for brown clay (D), natural gravel (B), coarse gravel (A) and lime treated sub-base (1) are higher than for the other types of soil. Calcium contents are also higher for coarse gravel (A) and natural gravel (B).

The effect of soil composition (iron and calcium influence) can be directly seen from the calibration graphs (Figs. 15-22) where for soils 1, 4, 5 and 7 the count rates for a given density are lower.

4.2.1.2   Comparison of regression equations

In order to check for the validity of the method used to obtain dry densities from gamma-ray attenuation measurements, the results obtained from the gauge (line N°.1) and from the calibration curve (line N°.2) were correlated with the sand replacement data. The correlation lines were also drawn for the results, (Line N°.3), obtained using the density gauge data corrected for hydrogen contained in the soils (hydrogen contained in soil in forms other than water). Graphs showing the regression lines are presented in Figs. 26-33.

NAIROBI THIKA RD. FIELD DENSITY CORRELLATION
Lime treated subbase (200)

FIG. 26
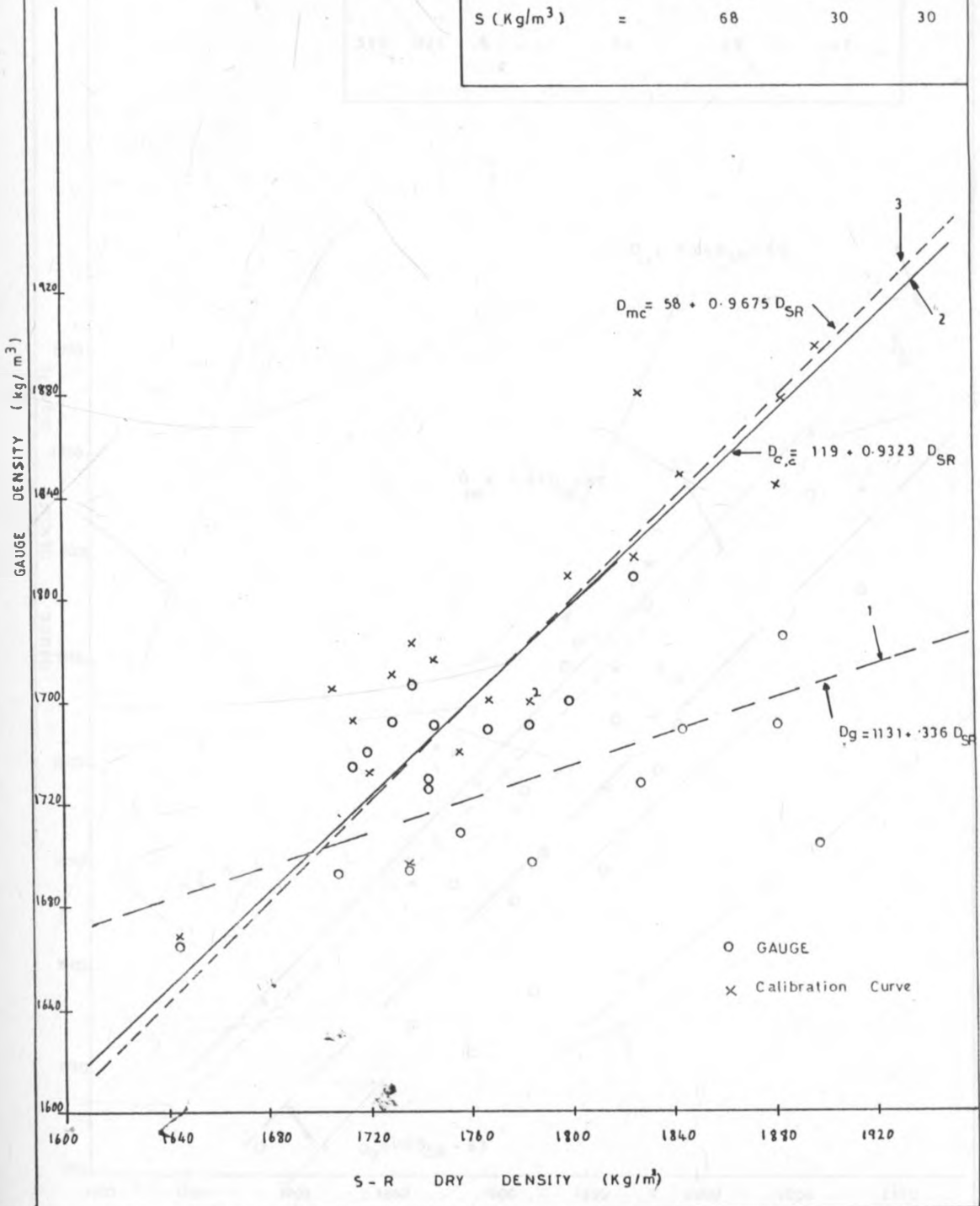
FIG.27 BURA - GARISSA RD. DENSITY CORRELATION CURVES.

(SUBGRADE 1. (150mm))
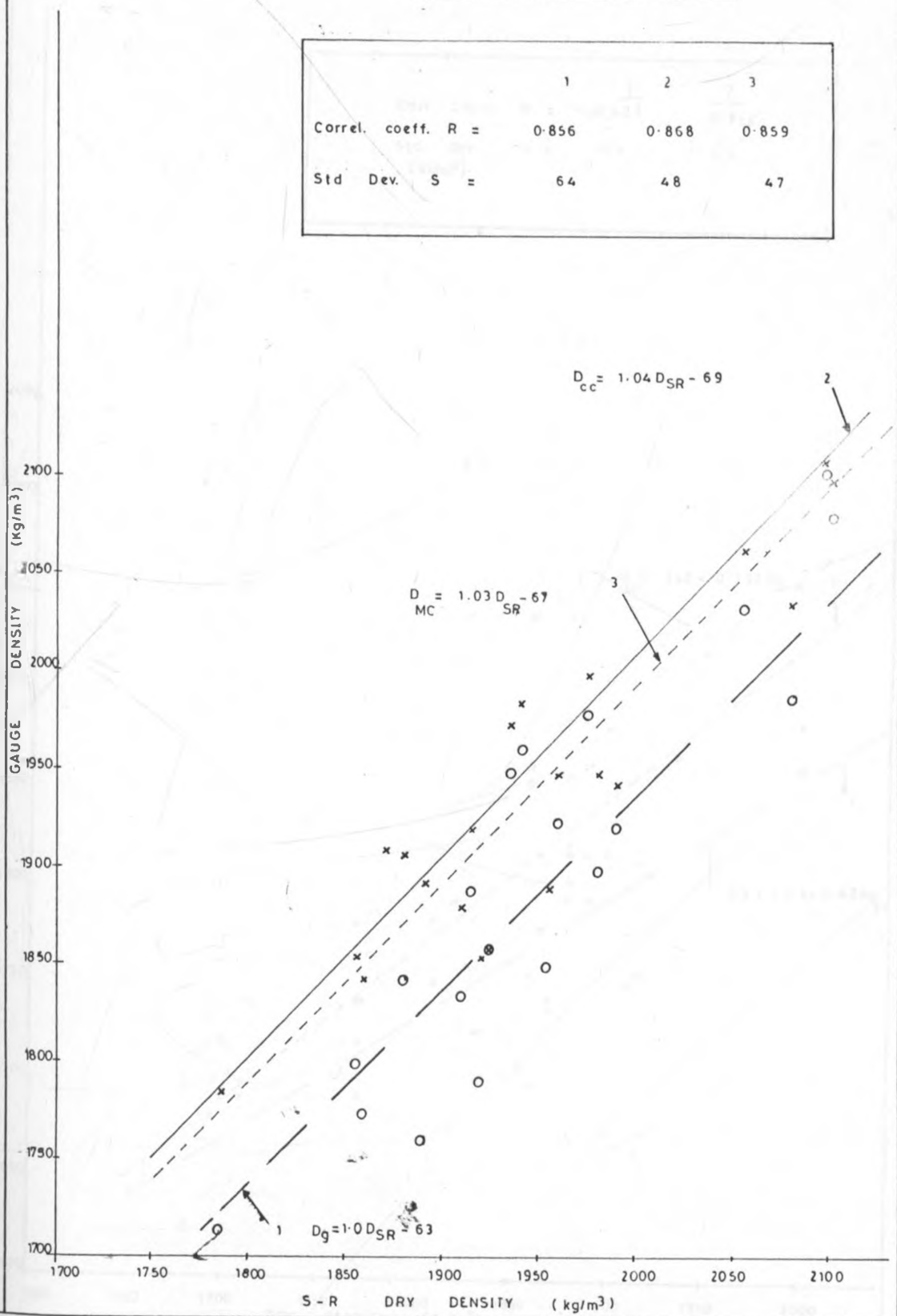
Fig.28 BURA GARISSA RD. DENSITY CORRELATION CURVES (Lime treated base course) depth 150mm
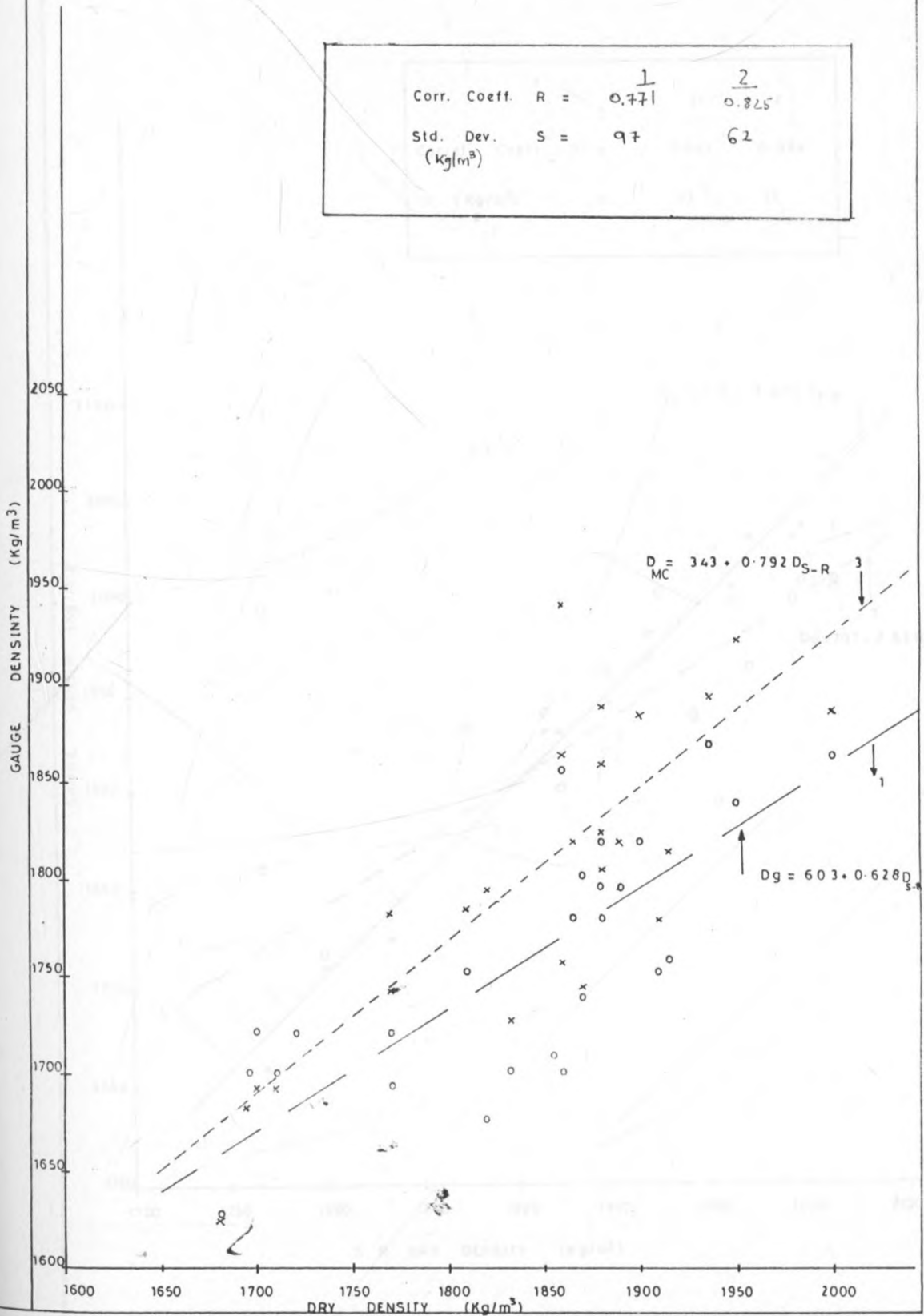
FIG. 29 LODWAR KAKUMA RD. DENSITY CORRELLATION CURVES.
(COARSE GRAVEL (A))
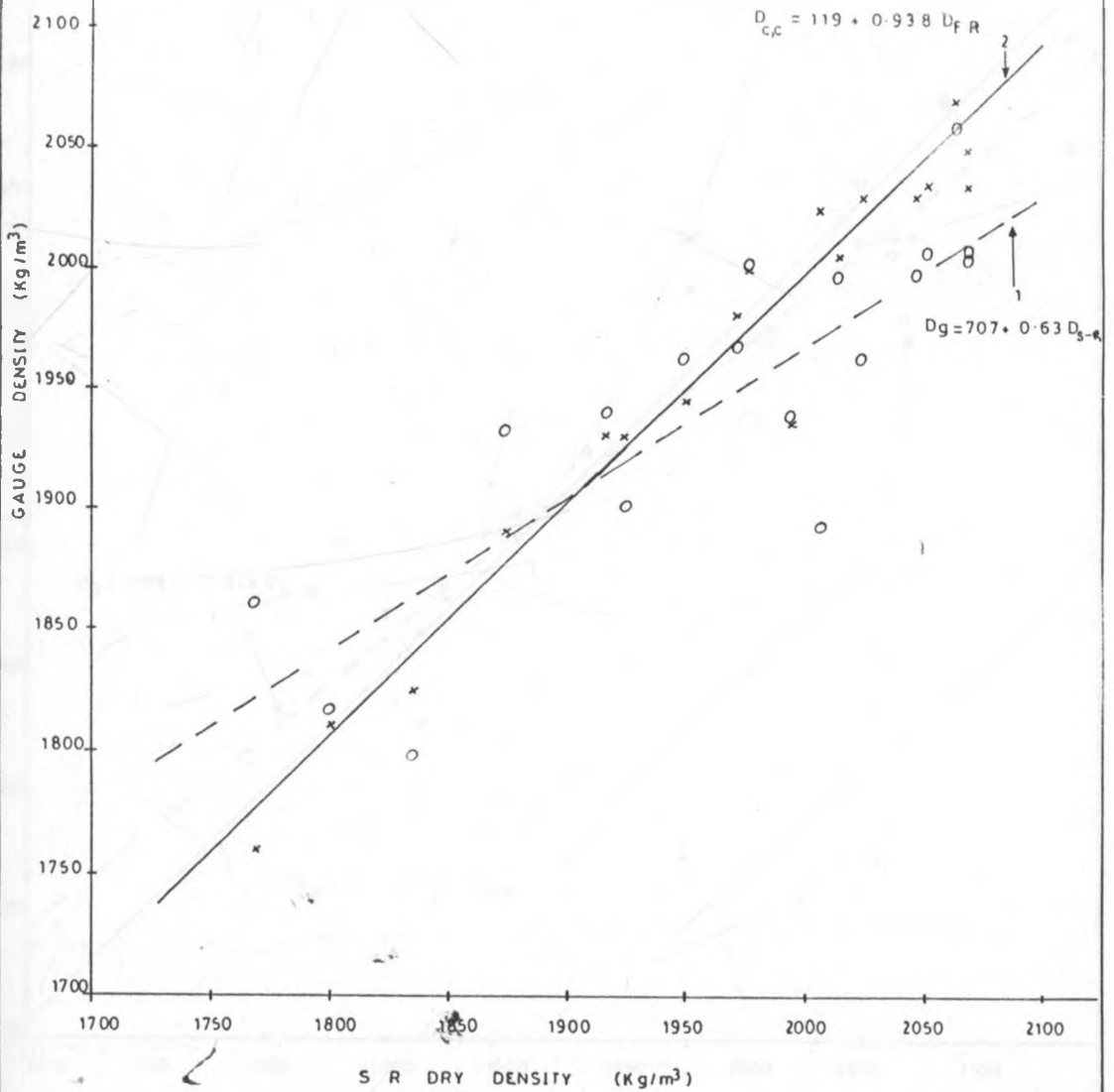
FIG.30 LODWAR KAKUMA RD. FIELD DENSITY CORREL. CURVES. (NAT. GRAVEL (B))
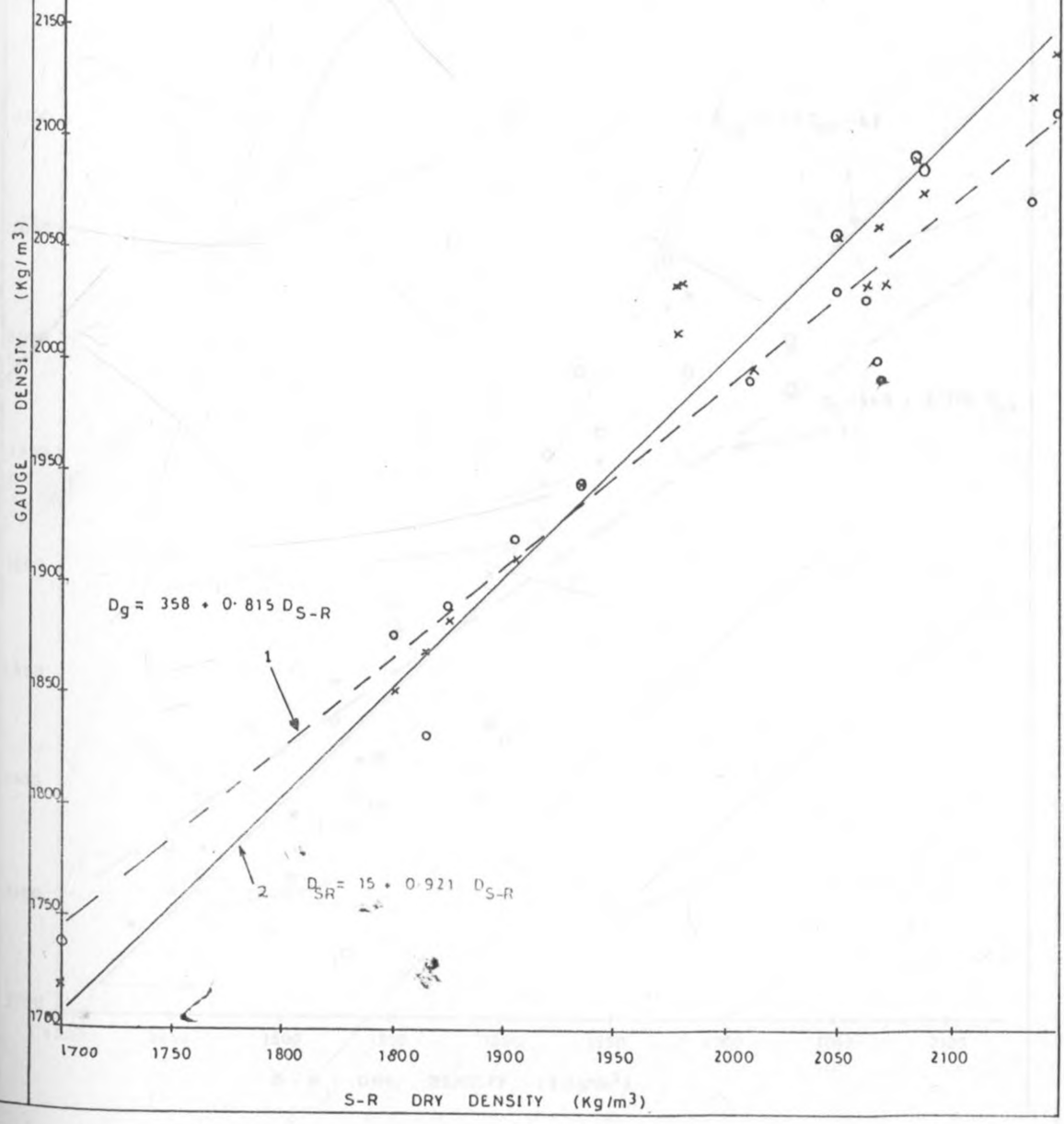
FIG.31 FIELD DENSITY CORRELLATION CURVES (SILTY SAND (C))

Correl. Coeff. R =			0.617	0.962
Std. Error, S =			84	25

$D_{SR} = 1.03\, D_{SR} - 62$

2

$D_g = 548 + 0.705\, D_{SR}$

1

GAUGE DENSITY (Kg/m³)

S - R DRY DENSITY (Kg/m³)
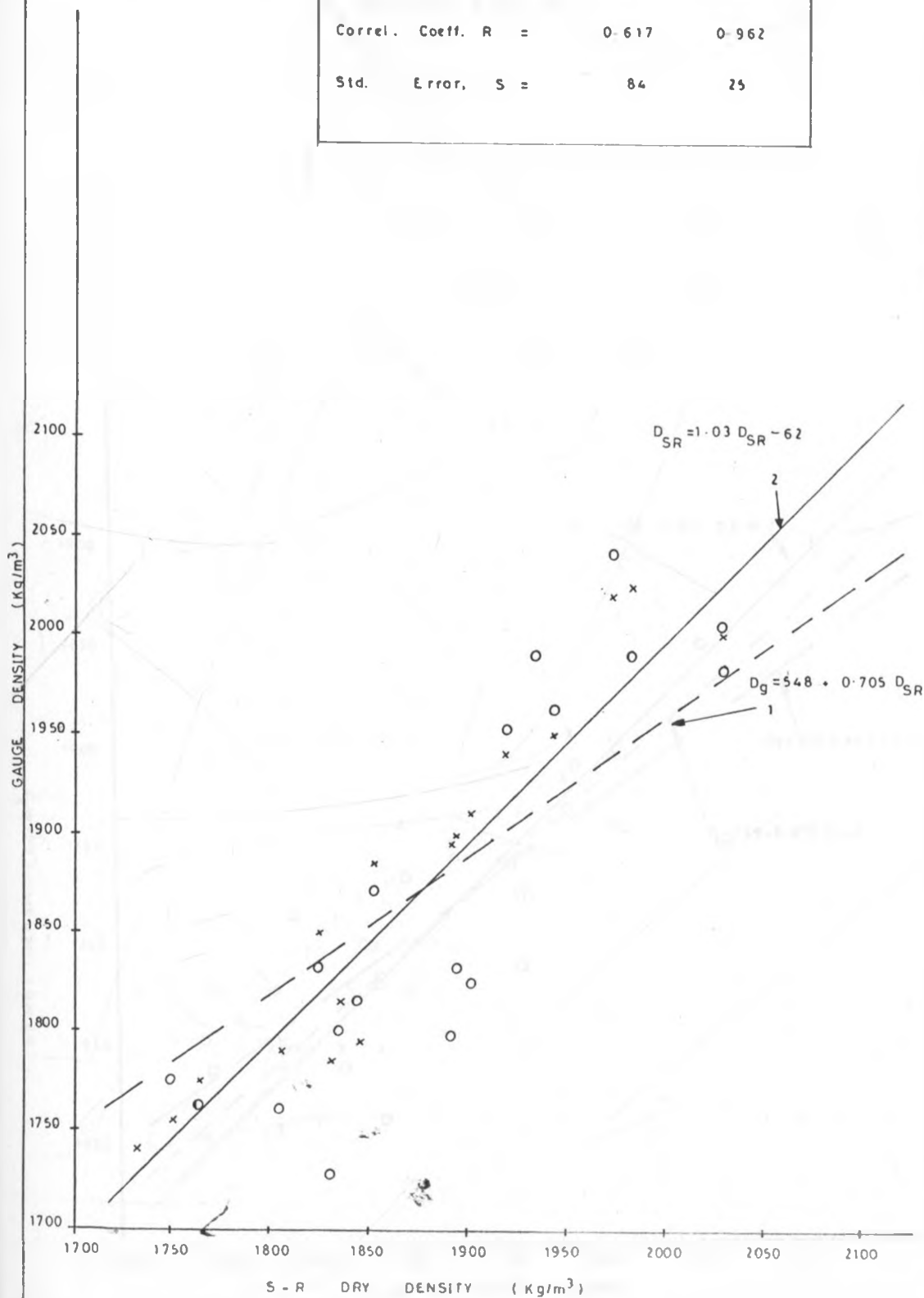
FIG 32   LODWAR - KAKUMA RD FIED DENSITY CORRELATION CURVES
(BROWN CLAY D)
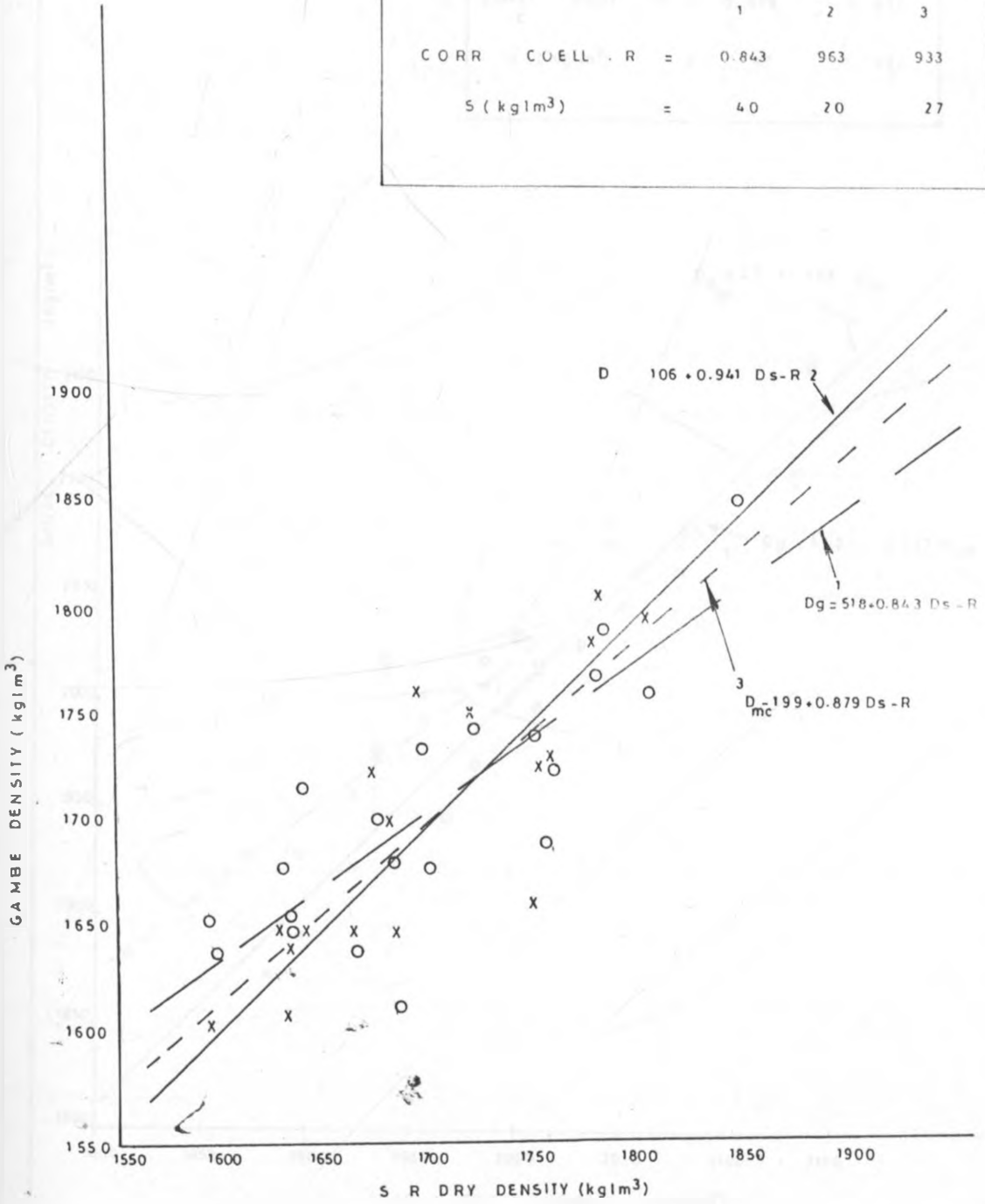
FIG.33 LODWAR KAKUMA RD. FIELD DENSITY CORRELATION CURVES
(CLAYEY SAND (E))

	1	2
Correl. Coeff. R =	0·879	0·975
S (Kg/m^3) =	47	19

$$Dg_{cf} = 27 + \cdot 989 \, P_{SR}$$

$$Dg = 547 + 0.737 \, D_{SR}$$

GAUGE DENSITY (Kg/m^3)

2150

2100

2050

2000

1950

1900

1850

1800

1800   1850   1900   1950   2000   2050   2100   2150

S R   DRY   DENSITY   (Kg/m^3)
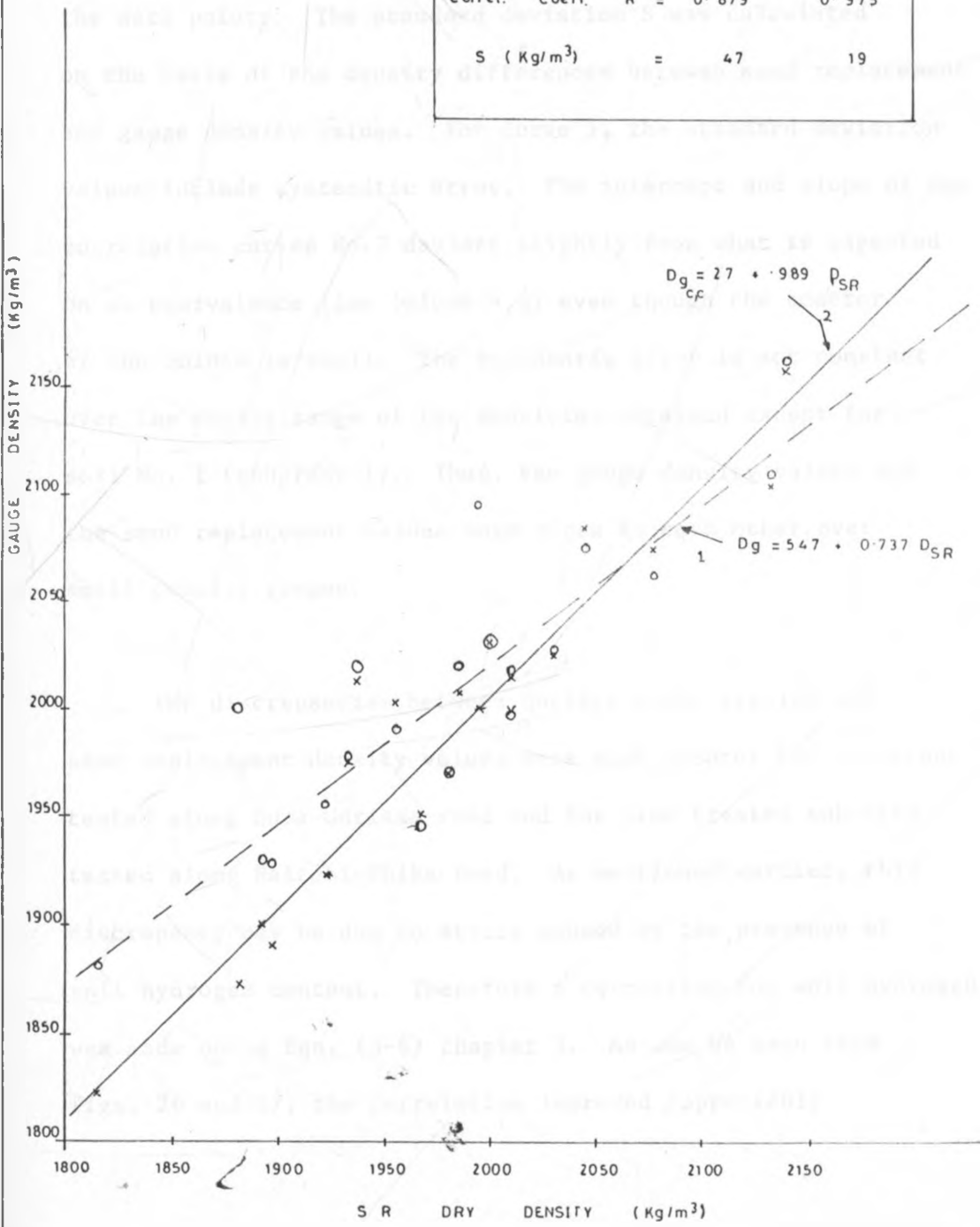
It can be seen from the correlation curves that before
calibration, gauge density values are generally smaller than
the sand replacement values and there is larger scatter of
the data points. The standard deviation S was calculated
on the basis of the density differences between sand replacement
and gauge density values. For curve 1, the standard deviation
values include systematic error. The intercept and slope of the
correlation curves No.2 deviate slightly from what is expected
on an equivalence line (slope = 1) even though the scatter
of the points is small. The systematic error is not constant
over the entire range of the densities obtained except for
soil No. 1 (subgrade 1). Thus, the gauge density values and
the sand replacement values were close to each other over
small density ranges.

The discrepancies between nuclear probe results and
sand replacement density values were much greater for sub-grade 1
tested along Bura-Garissa road and for lime treated sub-base
tested along Nairobi-Thika road. As mentioned earlier, this
discrepancy may be due to errors caused by the presence of
soil hydrogen content. Therefore a correction for soil hydrogen
was made using Eqn. (3-6) chapter 3. As can be seen from
Figs. 26 and 27, the correlation improved appreciably

(line No. 3). However, correction for soil hydrogen does
not seem to improve the results for brown clay. Correction
for soil hydrogen could not be calculated for the other soil
types because their moisture results were not available, and
as it can be seen from Eqn. (3-6), moisture value is needed
for the calculation in the correction.

From Eqn. (3-6) (indicated below Table 17), the constants
B' and B_w which were determined by the least squares method,
and the constants A, B and C for the gauge produced by Troxler
calibration were used to calculate the density values corrected
for hydrogen. These constants are presented in Table 16.

Table 17. B' and B_w Values for different soils and Troxler

A, B and C values

Material Type	Location of gamma source (mm)	B' $(\times 10^{-3})$		B_w $(\times 10^{-3})$
Lime treated subbase	200	1.29843		3.95506
Subgrade 1	150	1.16843		2.90377
Brown clay	150	1.62316		3.0492
Troxler calibration		A	$B(\times 10^{-3})$	C
for all soils	150	11.37646	1.32849	0.02566
	200	12.70263	1.01613	‾0.00984

$$L_n \left(\frac{A}{[I^1/I_s] + C} \right) = B'\, D' + B_w\, D_w \qquad \text{---------------} \quad (3-6)$$

It can be seen from Table 17 that the least squares values

of constants B' and B_w for a given soil and location source

varied with the material type. The soil attenuation factor

B' was highest for brown clay and lowest for lime treated

base course, whereas, the soil water attenuation factor

B_w was highest for lime treated subbase and lowest for subgrade 1.

For soils indicated in Table 17 , B' values were within

12 - 22 per cent of the corresponding Troxler B values.

Thus, a large error would be introduced if the factory B

value is used for hydrogen correction of the density values.

4.2.2 Comparison of Density values from nuclear gauge and

asphaltic concrete cores.

The cores tested were obtained from two different

roads under construction, and thus, had different properties

in order to meet their pavement performance. Along Nakuru

highway, the tested asphalt concrete consisted of two layers:

50 mm thick wearing course (WC) and 100 mm thick dense bitumen

macadam (DBM) below it. Nuclear backscatter density tests

were carried out to determine the density of the thin layer

(WC). Direct transmission measurements were carried out

to check on the gauge response on density variation within

the same material.

Use of the nomograph (as explained in Chapter 3) for

backscatter density determination of the wearing course

was not possible along Nakuru highway since at the time

of test, both the 100 mm DBM and the 50 mm WC had already

been laid and compacted.

However, the use of the nomograph was made using the

test data obtained from Nairobi-Thika road. The laboratory

results together with the core properties from the two roads
are shown in Tables 18 (a,b) and 19. As it can be seen
from these Tables, the heights of some cores were smaller
than recommended, such cores did not represent the full
thickness of the compacted layer.

It was not possible to test all the cores obtained
from the areas where the nuclear density readings had been
made, because of some financial limitations involved with
laboratory tests.

TABLE 18a: SUMMARY OF TEST RESULTS - ASPHALT CONCRETE - NAKURU HIGHWAY

Wearing Course (70 mm)

CORE NO.	MARSHALL TEST PROPERTIES		BITUMEN TEST RESULTS												FIELD DENSITY TEST		
	BULK SP. GRAVITY Kg/m³	AIR VOIDS %	% MATERIAL PASSING SIEVE (mm)												BITUMEN CONTENT %	THICKNESS MM	COMPACTION DEGREE (%)
			28	20	14	10	6.3	4	2	1	0.425	0.300	0.150	0.075			
1	2316	6.8		100	97	88	72	66	49	33	22	19	14	10	6.6	50	96.2
2	2316	6.0		100	97	86	70	65	50	34	23	20	14	11	6.6	50	97.0
3	2309	7.3		100	95	86	75	70	50	33	20	17	12	9	6.8	50	95.4
4	2322	8.0		100	97	86	73	73	67	49	22	18	13	10	6.4	50	95.2
5	2325	9.1		100	96	84	71	64	47	32	20	17	12	9	6.3	50	94.2
6	2313	6.8		100	97	89	70	65	46	30	19	16	11	8	6.7	50	96.0
7	2325	8.3		100	98	85	70	63	47	33	21	18	13	10	6.3	50	95.0
8	2313	5.0		100	95	84	64	56	41	29	20	18	13	10	6.7	50	98.0
9	2306	6.6		100	95	88	73	68	51	33	21	17	13	9	6.9	50	96.0
10	2322	6.2		100	97	87	71	64	48	32	20	17	11	9	6.4	50	96.9
11	2313	10.0		100	95	86	72	66	48	31	19	16	12	8	6.7	50	93.2
12	2309	10.8		100	96	86	72	64	46	30	20	17	12	9	6.8	50	91.8
13	2332	5.2		100	95	87	75	66	48	32	20	17	11	9	6.1	50	98.6
14	2309	4.0		100	98	88	74	67	48	32	20	17	11	8	6.8	50	98.8
15	2322	7.0		100	99	90	72	64	46	31	20	17	12	9	6.4	50	96.3
16	2300	4.4		100	99	88	70	63	44	30	19	16	12	9	7.1	50	98.0
17	2313	5.4		100	96	85	74	68	49	32	20	17	12	9	6.7	50	97.5
18	2322	6.0		100	96	84	68	61	44	29	19	16	11	8	6.4	50	97.3

TABLE 18b: SUMMARY OF TEST ESULTS – ASPHALT CONCRETE – NAKURU HIGHWAY

Wearing Course – Base Course (150 mm)

CORE NO.	MARSHALL TEST PROPERTIES		BITUMEN TEST RESULTS												FIELD DENSITY TEST		
	BULK SP. GRAVITY Kg/m³	AIR VOIDS %	% MATERIAL PASSING SIEVE (MM)												BITUMEN CONTENT %	THICKNESS MM	COMPACTION DEGREE %
			28	20	14	10	6.3	4	2	1	0.425	0.300	0.150	0.075			
1	2347	10.4	100	97	91	84	70	65	48	29	16	13	9	7	5.6	150	93.6
2	2351	10.1	100	100	89	77	67	62	46	28	16	12	8	6	5.5	150	94.2
3	2335	10.6	100	99	95	86	74	67	48	29	16	12	8	6	6.0	150	93.0
4	2351	10.7	100	95	91	81	70	64	46	28	16	13	9	6	5.5	150	93.5
5	2367	11.7	100	98	88	75	71	64	47	30	16	12	8	6	5.0	150	93.2
6	2363	13.6	100	96	92	82	72	65	47	29	16	12	8	6	5.1	150	91.0
7	2371	9.2	100	99	92	81	69	62	44	27	16	12	9	7	4.9	150	96.0
8	2355	10.0	100	97	94	85	73	66	47	29	16	13	9	7	5.4	150	94.4
9	2359	9.5	100	100	90	79	66	59	40	23	13	10	7	5	5.3	150	95.1
10	2375	8.1	100	95	82	70	59	53	39	24	14	11	7	5	4.8	150	97.3
11	2347	11.4	100	97	91	83	74	67	48	29	16	13	9	7	5.6	150	92.3
12	2364	9.6	100	97	90	80	65	57	41	26	15	12	8	6	5.1	119	95.2
13	2351	11.9	100	100	91	80	70	63	45	28	16	12	9	6	5.5	101	92.3
14	2367	10.4	100	97	90	79	70	62	43	26	14	11	7	5	5.0	137	94.5
15	2335	10.3	100	100	93	84	73	64	45	28	16	12	9	6	5.4	114	94.1
16	2359	10.6	100	97	93	84	74	67	48	29	16	13	9	6	5.3	125	94.0
17	2361	9.8	100	90	84	75	63	56	39	25	15	12	8	6	5.2	110	94.9
18	2347	8.4	100	98	91	78	65	55	39	25	15	13	9	7	5.6	152	95.8
19	2361	8.5	100	95	89	75	65	55	39	26	16	13	9	7	5.2	166	96.3
20	2367	9.3	100	92	84	76	63	54	38	24	15	12	8	6	5.0	160	95.6

CORE №	MARSHALL TEST PROPERTIES		BITUMEN EXTRACTION TEST RESULTS													BITUMEN CONTENT %	FIELD DENSITY TEST	
	BULK SP GRAVITY g/cc	AIR VOIDS %	% MATERIAL PASSING SIEVE mm														THICKNESS mm	%
			2 8	20	14	10	6 3	4	2	1	0 425	0 300	0 150	0 075				
1	2192	4·7			100	85·1	69·7	60·9	44·1	29·1	17·9	15·1	11·0	8·3		6·83	40·1	98·4
2	2166	5·9			100	82·5	66·9	57 7	42·1	27·8	16·4	13·7	10 0	7 7		6·73	47·3	98 7
3	2237	2·6			100	87·4	70·7	61·4	44·9	29·4	17·1	14·3	10·1	7·6		6·90	38·2	56·6
4	2233	2·3			100	85·6	69·6	60·0	42·6	28·1	17·0	14·4	10·5	8·0		7·0	43·7	57·2
5	2175	5·4			100	88·0	71·5	61·6	44·0	28·3	16·3	13·3	9·2	6·6		5·83	42·9	96·0
6	2110	5·1			100	86·4	72·0	60·9	43·7	27·6	16·4	13·0	8·9	6·5		6·90	43·0	96·3
7	2190	4·3			100	87·6	70·9	60·0	43·0	28·0	17·1	14·0	9·0	7·0		7·12	44·0	98·0
8	2233	3·0			100	88·1	74·8	64·3	46·9	31·0	18·8	15·8	11·5	8·5		6·73	58·1	97·9
9	2188	5·9			100	81·7	63·1	53·6	40·2	27·0	16·2	13·6	9·9	7·3		6·16	49·5	199·0
10	2198	4·7			100	85·0	70·9	60·1	45·1	30·1	18·8	15·8	11·9	9·2		6~77	46·4	98·4
11	2213	4·7			100	84·6	68·2	58·6	42·4	27·5	15·9	13·2	9·1	6·6		6·08	45·7	97·7
12	2207	3·5			100	87·7	70·3	61·2	44·3	29·4	18·2	15·6	11·9	9·5		7·19	54·3	99·2
13	2189	4·0			100	84·9	67·2	57·4	42·1	27·4	16·4	13·8	10·0	7·5		7·42	41·6	98·2
14	2224	3·9			100	88·5	68·2	60·2	45·4	30·0	18·2	15·2	11·2	8·5		6·34	45·7	97·2
15	2207	3·9			100	86·4	67·2	54·3	41·8	28·6	18·3	15·9	12·0	9·5		6·91	43·2	97·7
16	2214	3·4			100	87·4	69·4	59·3	43·3	28·8	16·6	13·8	10·0	7·3		7·04	49·8	95·0
17	2199	3·6			100	90·9	75·3	66·0	48·6	32·3	20·0	17·2	12·9	10·1		7·40	48·8	97·5
18	2203	3·6			100	85·3	68·8	57·5	43·5	28·7	16·9	14·3	10·1	7·4		7·25	44·0	99·1
19	2224	3·4			100	87·1	68·8	57·7	41·3	26·7	16·0	13·5	9·6	7·1		6·72	49·9	95·9
20	2187	5·3			100	86·9	72·8	63·6	46·4	30·1	18·0	15·3	11·2	8·5		6·48	53·3	98·0

The densities of all the cores shown in the above Tables (18-23) were determined in the laboratory by the method described in BS 598 [British Standards Institution] [32]. These densities were compared with those obtained with the nuclear gauge. Calibration of the gauge was done on the test sites for the data obtained along Nakuru highway. These data together with their calibration curves are respectively shown in Tables 21 and 22 and figures 34 and 35. From the calibration curves, it can be noticed that there is much scatter of the points. The data from both wearing course and dense bitumen macadam layers exhibit a very small density range. Table 20 shows the evaluation of the density data obtained.

Table 20: Summary of field density data evaluation (asphalt-concrete)

Parameter layer Type	Random error due to counting statistics (δcs) (Kg/m^3)		Accuracy
	Low Density	High Density	(Kg/m^3)
Wearing Course (50 mm) (Calibration) 7	7	18	33 (1.6%)
Nairobi-Thika Road (nomograph)	--	--	27 (1.2%)

From the correlation results, Tables 21 and 22 and
figures 36 and 37, it is noticed that the results from the
nuclear gauge are generally higher than the corresponding
core results. The comparison of nuclear gauge and core
densities from Nakuru highway show that the correlation
between the two sets of results for the backscatter (50 mm)
measurements was poor.

Considering the transmission (150 mm) density results,
it was found that the correlation between gauge and core
density values was also poor. The direct transmission results
are not reliable because the 150 mm thick material consisted
of two layers (150 mm WC and 100 mm basecourse) with different
aggregate mix and bitumen content. These differences in
properties of the two layers (hence density difference)
could possibly have been the cause of the unreliable transmission
results. These results are thus not discussed in detail.

From the correlation results obtained along Nairob-Thika
road (Table 23 and fig. 38), it can be seen that there was
a noticeable improvement of the results when the nomograph
was used. It is felt that these results would have been
improved considerably-using the data of a wider density
range.

Table 21: Field Density Data [Nakuru Highway] - Wearing Course (50 mm)
Density Units: Kg/m^3

SIGNAL COUNTS PER MIN. (DC)	RELATIVE COUNT RATE	CORE DENSITY (D_c)	GAUGE DENSITY (D_g)	$\triangle D_1$ (D_c-D_g)	DENSITY FROM CALIB. CURVE (D_{cc})	$\triangle D_2$ (D_c-D_{cc})
2578	0.861	2159	2127	+32	2159	0
2579	0.861	2177	2128	+49	2159	+18
2656	0.882	2141	2100	+41	2144	-3
2626	0.895	2137	2110	+27	2142	-5
2828	0.964	2114	2021	+93	2114	0
2544	0.867	2155	2121	+34	2155	0
2591	0.883	2131	2105	+26	2150	-19
2581	0.814	2198	2087	+111	2196	+2
2442	0.833	2151	2156	-2	2180	-26
2581	0.880	2179	2108	+71	2150	+29
2486	0.848	2159	2140	+19	2166	-9
2504	0.790	2212	2067	+145	2142	+70
2480	0.846	2216	2040	+176	2166	-50
2604	0.860	2160	2067	+93	2142	+22
2504	0.854	2198	2134	+64	2166	+32
2514	0.854	2216	2104	+112	2150	+66
2528	0.860	2160	2130	+30	2162	-2
2387	0.812	2198	2178	+20	2196	+2
2376	0.812	2188	2174	+14	2196	-8
2322	0.793	2183	2162	+21	2200	-17

NAKURU HWY   A C   (Wearing course - 50mm) Calib. curve
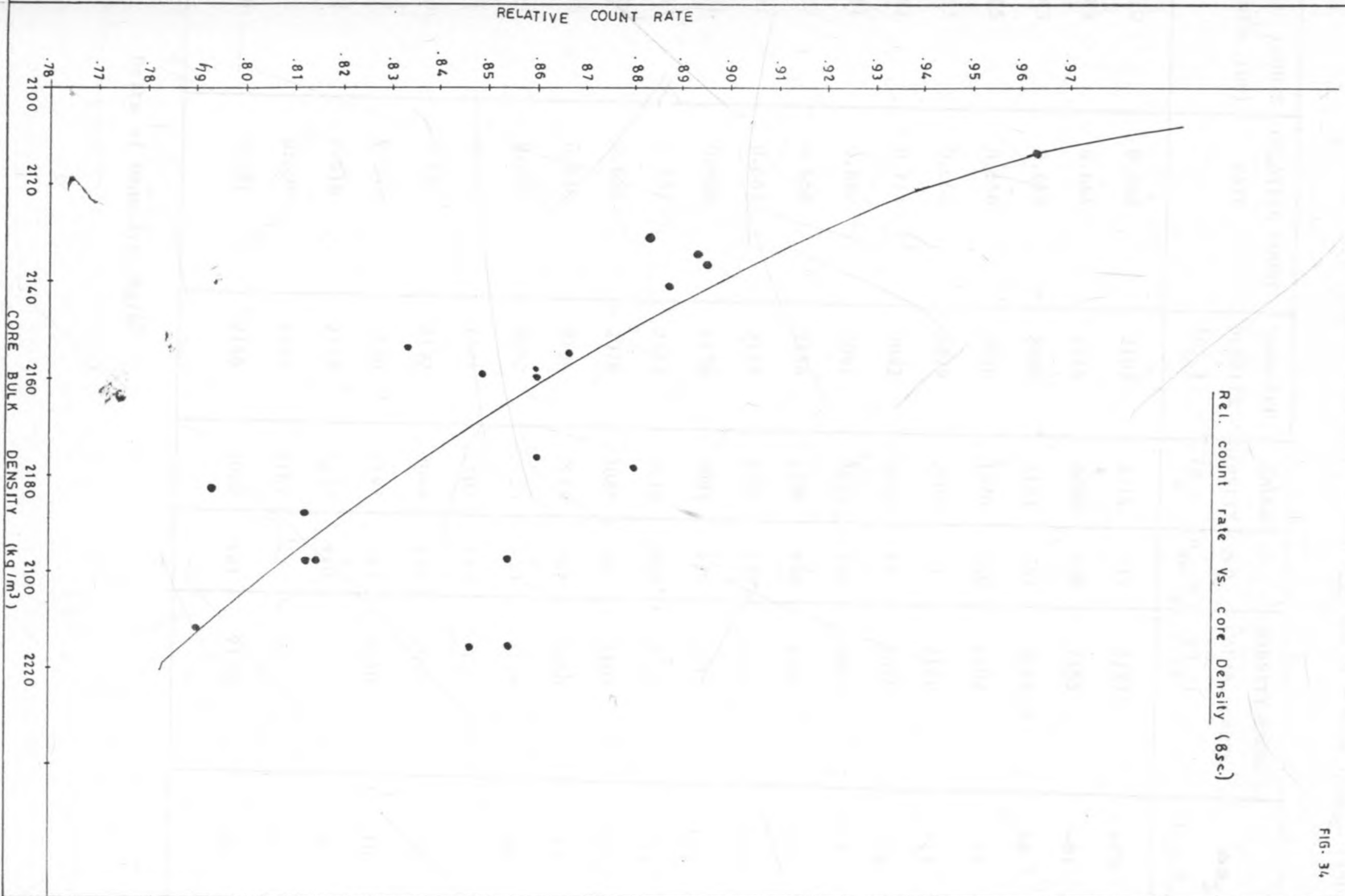
Rel. count rate vs. core Density (8se.)

FIG. 34

Table 22: Field Density Data [Nakuru Highway] — Wearing Course + Base Course [150mm]

SIGNAL COUNTS PER MIN. (DC)	RELATIVE COUNT RATE	SAND-REP. DENSITY (D_{SR})	GAUGE DENSITY (D_g)	ΔD_1 $D_{SR}-D_g$	DENSITY FROM CALIB.- CURVE (D_{cc})	ΔD_2 $(D_{SR}-D_{cc})$
1910	0.638	2102	2114	−12	2122	−20
1989	0.664	2114	2088	+26	2195	−81
1843	0.675	2086	2143	−57	2178	+8
1965	0.656	2030	1980	+50	2102	−72
1953	0.652	2099	2102	−3	2120	−21
2141	0.715	2042	2035	+7	2076	−34
2081	0.680	2091	2035	+56	2082	+9
1902	0.649	2154	2106	+48	2126	+28
1941	0.662	2119	2088	+31	2109	+10
1931	0.658	2134	2095	+35	2112	+22
1867	0.637	2183	2118	+65	2150	+33
1952	0.666	2079	2085	−6	2105	+74
1866	0.636	2136	2119	+17	2150	−14
1848	0.680	2072	2125	−53	2170	−98
1902	0.648	2121	2102	+19	2126	−5
2014	0.686	2112	2064	+48	2090	−78
1889	0.641	2130	2147	−17	2140	−10
1818	0.618	2149	2139	+10	--	--
1741	0.595	2160	2167	−7	--	--
1848	0.681	2146	2025	+21	2170	−24

Units of Density: Kg/m^3

FIG. 35   NAKURU   HWY.   A C   DEPTH: 150mm

DENSITY   CALIB. CURVE

Rel. count Rate   Vs. Core Density
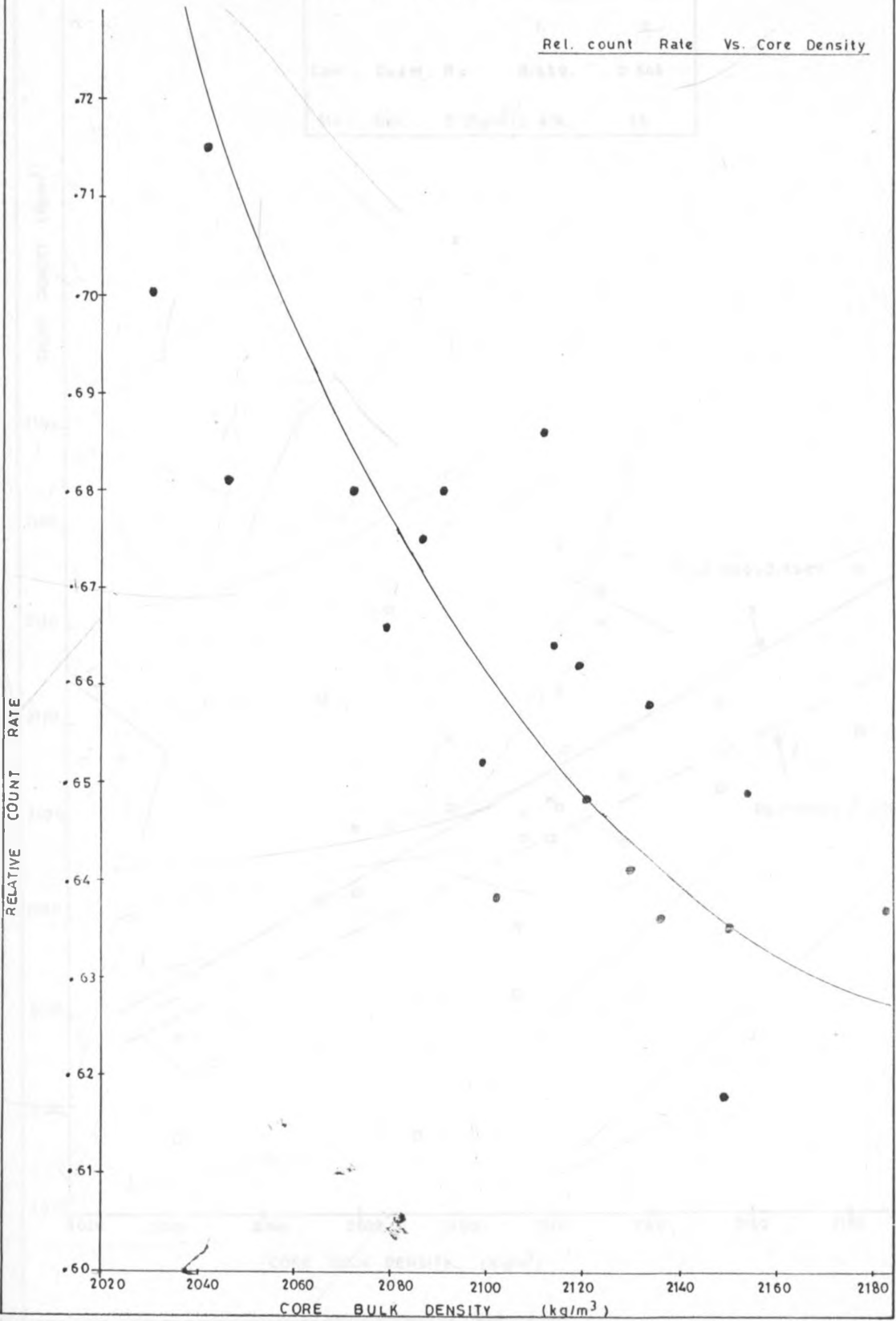
ASPHALT DENSITY CORRELLATION CURVES   Depth : 150mm   FIG. 36
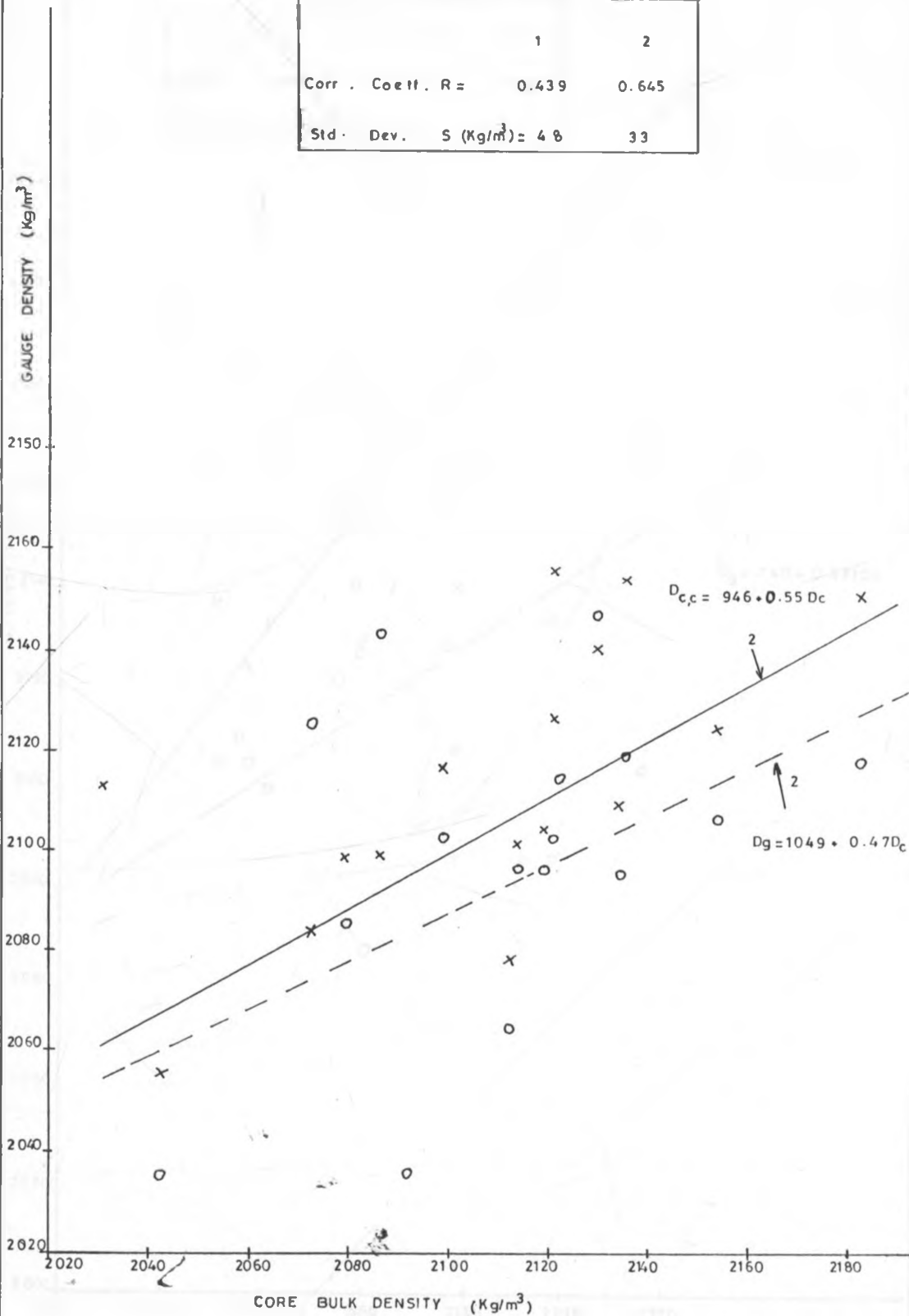
NAKURU HIGHWAY A C   DEPTH. 50mm   FIG. 37
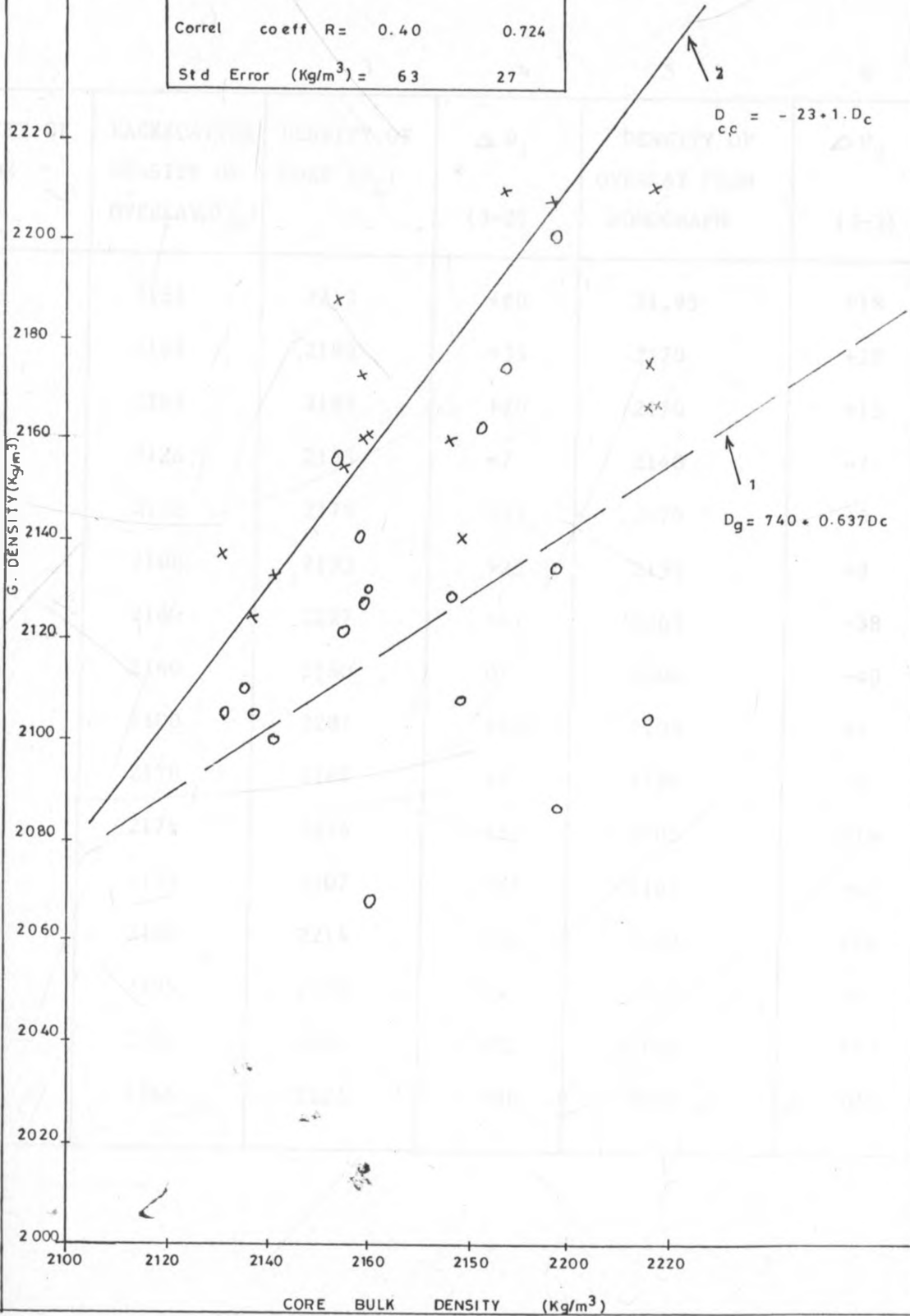
TABLE 23: NAIROBI-THIKA ROAD - SUMMARY OF DENSITY RESULTS (KG/M^3)

ASPHALT CONCRETE, TYPE 1, WEARING COURSE (50 MM)

1	2	3	4	5	6
DENSITY OF BOTTOM LAYER	BACKSCATTER DENSITY OF OVERLAY(D_{OV})	DENSITY OF CORE (D_C)	ΔD_1 (3-2)	DENSITY OF OVERLAY FROM NOMOGRAPH	ΔD_2 (3-5)
1930	2153	2213	+60	21.95	+18
2121	2163	2198	+35	2170	+28
2112	2163	2183	+20	2170	+13
2067	2126	2133	+7	2140	-7
2053	2142	2175	+33	2170	+5
2041	2108	2133	+25	2130	+3
1927	2180	2227	+47	2265	-38
2026	2160	2160	0	2200	-40
2120	2100	2207	+107	2203	+4
2155	2178	2187	+9	2190	-3
2055	2171	2224	+53	2205	+19
2110	2152	2207	+55	2165	+42
1978	2150	2214	+64	2190	+24
2164	2195	2199	+4	2205	-6
2131	2151	2203	+52	2160	+43
2053	2166	2224	+58	2200	+24

Density   Correlation   Curve

(Wearing   Course)(50 mm)

	1	2
R =	0·400	0·690
Std Dev =	53	30
(kg / m^3)		

Gauge Density (kg/m^3)

$$D_n = 546 + 0.735 \ D_c$$

$$D_g = 1236 + 0.41 \ D_c$$

2260

2240

2220

2200

2180

2160

2140

2120

2100

2100   2120   2140   2160   2180   2200   2220   2240

CORE   BULK   DENSITY (kg/m^3)
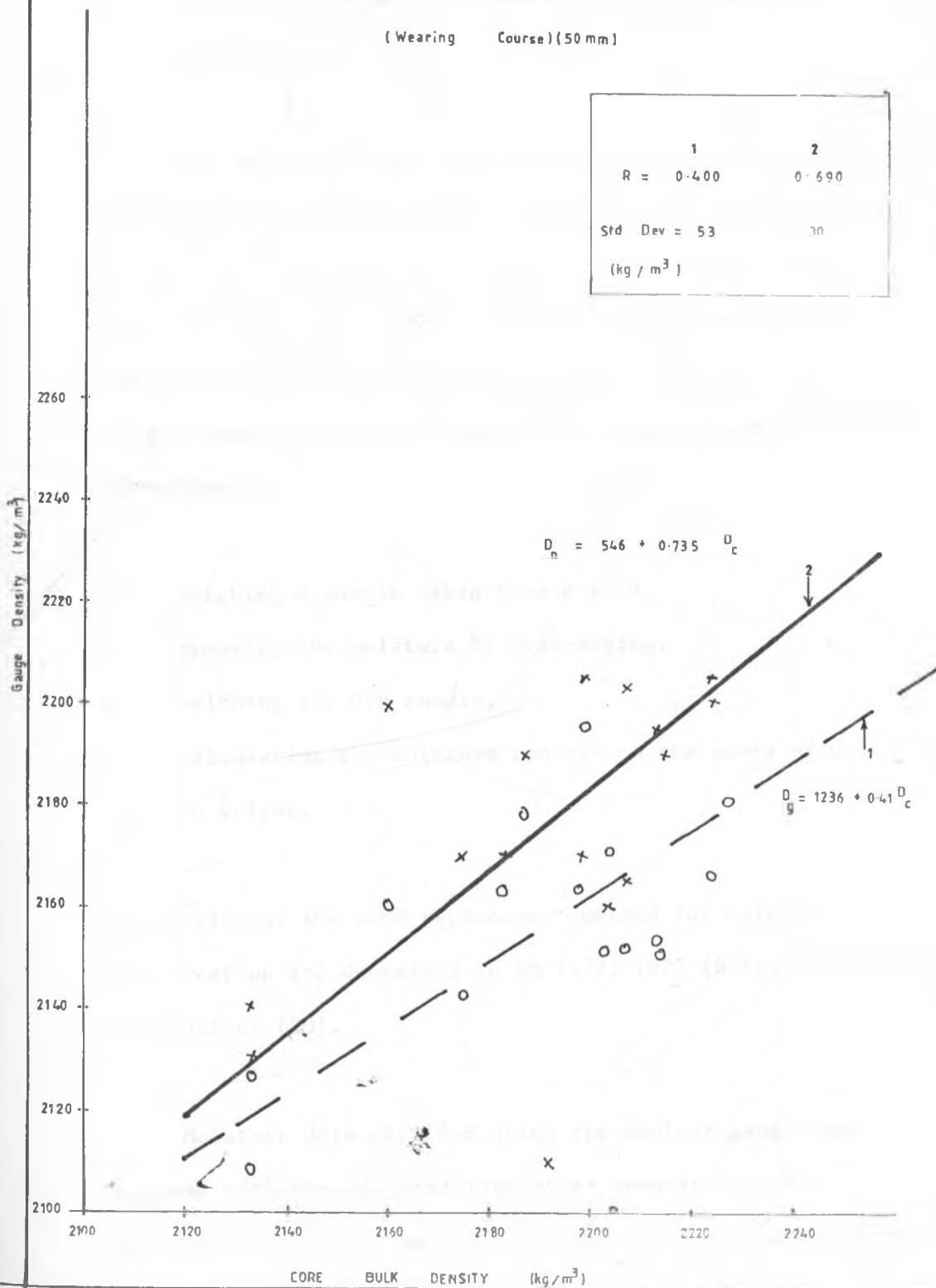
4.2.3   Comparison of moisture from sand replacement and

nuclear gauge.

Soil moisture tests were carried out on all the eight

soil types tested for density.   The test areas were sections

of the roads which were under actual construction.   Both

sand replacement and nuclear moisture determination tests

were carried out at the same spots on each material tested.

The gravimetric method of determining moisture content involves

four steps:-

1.   Weighing a sample taken from a road,

2.   removing the moisture by oven-drying,

3.   weighing the dry sample,

4.   calculating the moisture content on the basis of difference

in weight.

The details of the sand replacement method for moisture

determination are described in B5 1377: 1975 (British Standards

Institution) [30].

Moisture data obtained using the nuclear gauge were

compared with the standard laboratory oven-dry results.

The results obtained together with their corresponding calibration

and correlation curves are shown in Tables 25-32 and figures 39-54. Calibration of the nuetron probe was done by plotting count rate values versus per cent volumetric moisture content obtained by oven-drying.

From the calibration curves, it was observed that, as expected, all the plotes show a linear relationship between gauge count rates and the gravimetric moisture determination. However, scatter of the points was noticed which was significantly due to counting statistics error and to a lesser extent due to uncertainty of the oven-dry method and also due to variations of density of the soil samples. The latter, as already mentioned influences the moisture gauge results.

The statistical and relative errors calculated from the
calibration curves are shown in Table 24.

Table 24: Field Moisture data evaluation

| Material Type | Random error due to statistical fluctuations ($\acute{O}cs$ – %M) | | Accuracy |
	Low % M	High % M	(% M)
Lime treated subbase	1	2	0.73
Subgrade 1	0.9	1.1	0.82
Lime treated Basecourse	0.9	1.0	1.1
Coarse gravel	0.9	1.3	0.4
Natural gravel	1.4	1.7	1.1
Silty sand	0.8	1.5	0.71
Brown clay	0.8	1.1	0.62
Clayey sand	0.9	1.0	0.59

Table 25 :   NAIROBI-THIKA ROAD - MOISTURE DATA - Lime treated Subbase

SIGNAL COUNTS/MIN.	OVEN-DRY % M(M_{OD})	UNCALIBRATED NUCLEAR % M	($M_{OD}-M_{UN}$) ΔD_1	CALIBRATED NUCLEAR	($M_{OD}-M_C$) ΔD_2
198	15.8	19.0	-3.2	14.6	+1.2
204	14.9	19.1	-4.2	16.4	-1.5
206	17.7	21.9	-4.2	17.0	+0.7
201	16.0	18.9	-2.9	15.5	+0.5
204	16.7	20.4	-3.7	16.4	+0.3
200	15.4	19.5	-4.1	15.2	+0.2
196	14.2	18.5	-4.3	14.0	+0.2
199	15.0	18.5	-3.5	14.9	+0.1
206	17.5	22.3	-4.8	17.0	+0.5
206	17.5	21.9	-4.4	17.0	+0.5
204	16.4	22.2	-5.8	16.4	0
203	16.9	22.4	-5.5	16.1	+0.8
200	16.2	22.0	-5.8	15.2	+1.0
196	15.2	22.0	-6.8	14.0	+1.2
204	15.5	23.0	-7.5	16.4	-0.9
212	18.6	22.5	-3.9	18.9	-0.3
212	18.5	22.3	-3.8	18.9	-0.4
213	19.1	24.2	-5.1	19.2	-0.1
215	19.1	23.6	-4.5	19.8	-0.7
215	19.2	23.7	-4.5	19.8	-0.6
210	17.7	21.7	-4.0	18.5	-0.8
208	16.8	20.3	-3.5	17.6	-0.8

NAIROBI - THIKA RD.   MOISTURE   CALIB.   CURVE   FIG. 39

Lime treated subbase

$CR = 150.363 + 3.268\% M_{OD}$

NAIROBI - THIKA RD.   LIME   TREATED   SUBBASE   FIG. 40

MOISTURE   CORRELATION   CURVES

$\% \ Mg = 6.5 + 0.882 \ \% \ M_{OD}$

$\% M_{C.C} = 1.813 + 1.105 \ \% \ M_{OD}$

Correl. coeff.   R = .782   .9173

std. Der. s(%m)   = 1.8   .73

GAUGE % MOISTURE
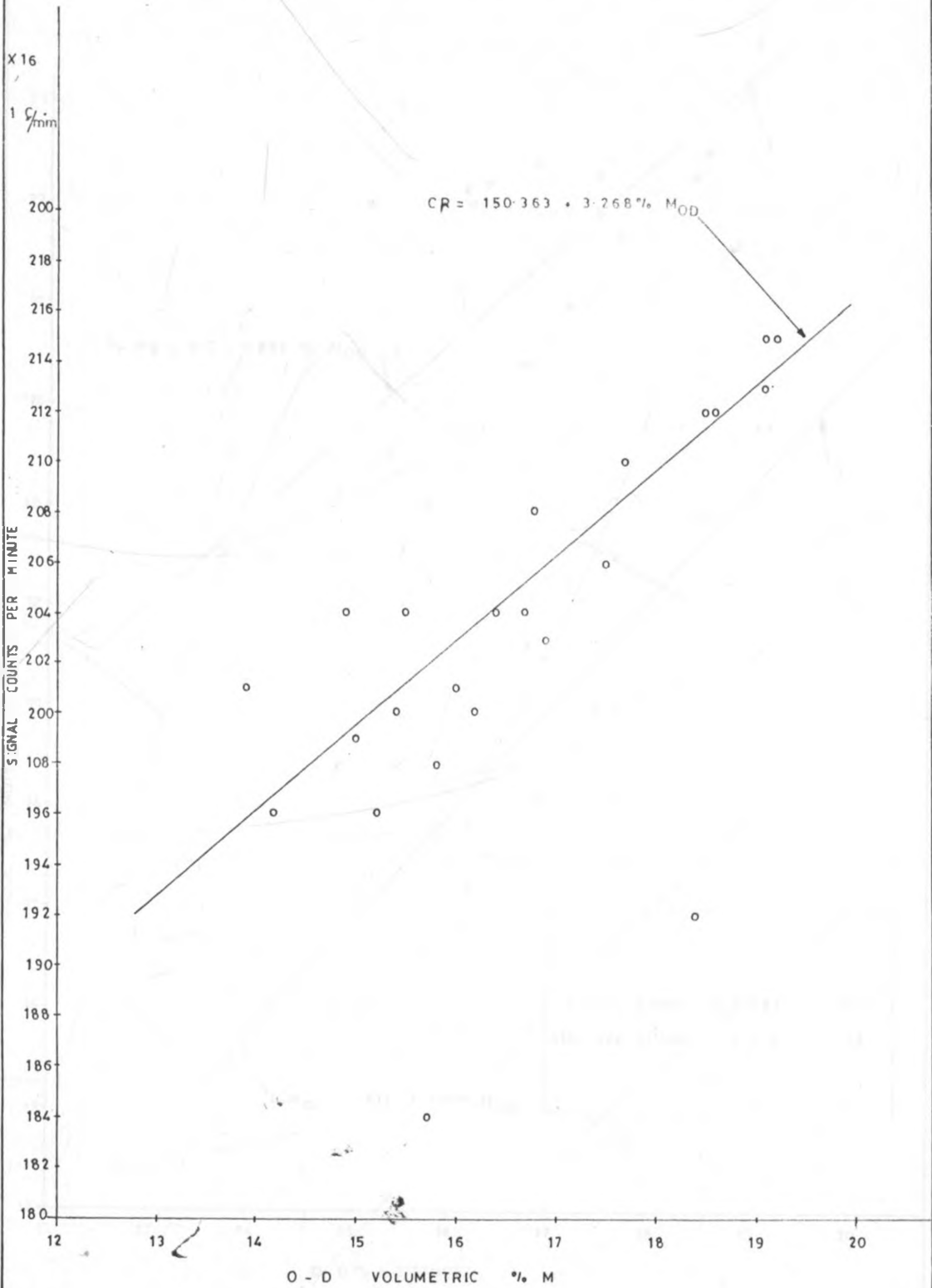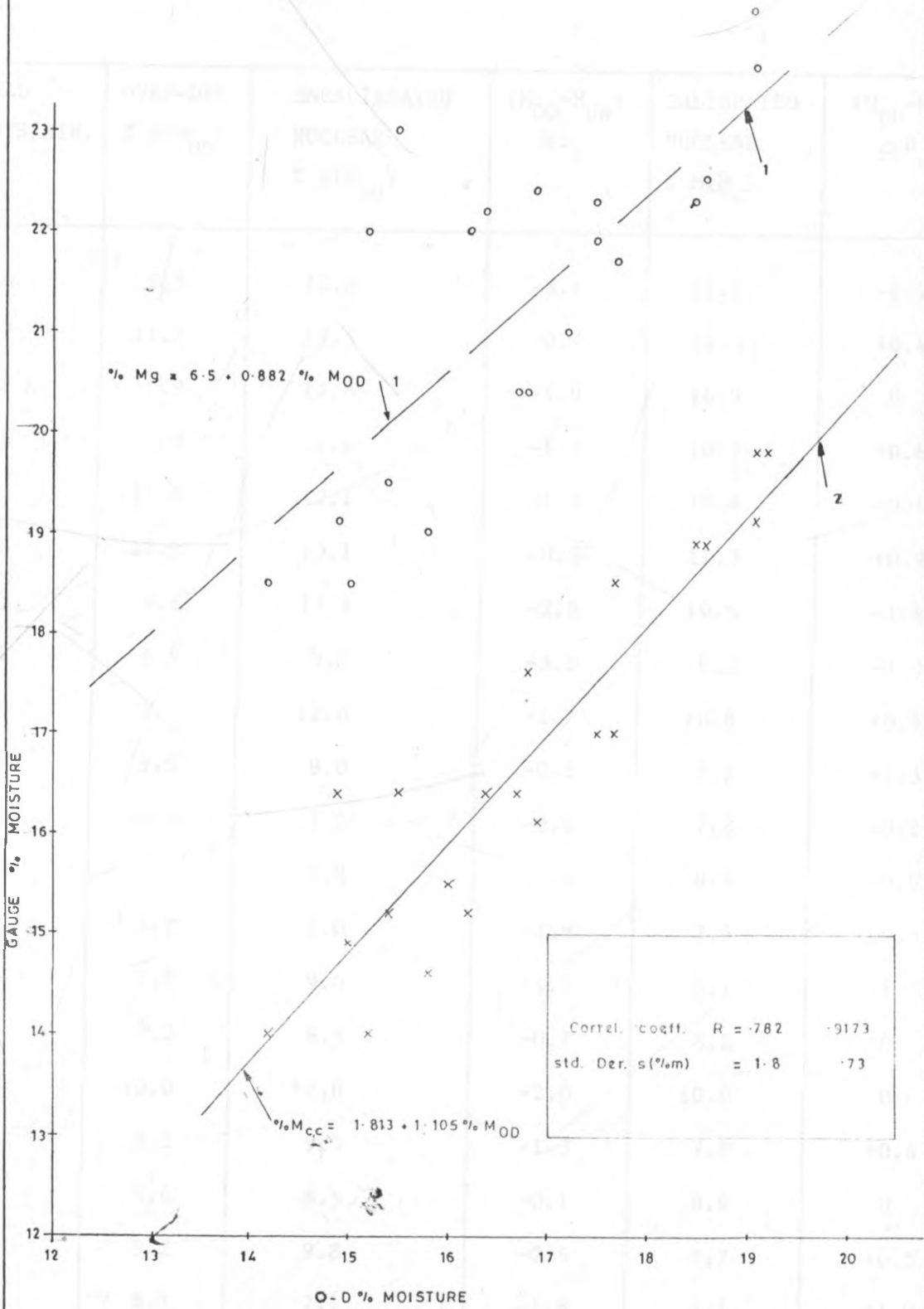
O - D % MOISTURE

Table 26 : BURA-GARISSA ROAD - MOISTURE DATA - Subgrade 1

SIGNAL COUNTS/MIN.	OVEN-DRY % M(M_{OD})	UNCALIBRATED NUCLEAR % M(M_{OD})	(M_{OD}-M_{UN}) $\triangle D_1$	CALIBRATED NUCLEAR % M(M_C)	(M_{OD}-M_C) $\triangle D_2$
146	9.5	12.6	-3.1	11.2	-1.7
147	11.7	12.4	-0.7	11.3	+0.4
148	10.9	12.8	-1.9	10.9	0
136	10.9	12.6	-1.7	10.3	+0.6
141	10.9	12.1	-1.2	10.8	+0.1
148	12.2	13.1	-0.9	11.3	+0.9
143	9.5	12.4	-2.9	10.9	-1.4
111	6.9	9.9	-3.0	8.2	-1.3
142	11.1	12.8	-1.7	10.8	+0.3
110	9.5	9.0	-0.5	8.2	+1.3
100	7.1	7.7	-0.6	7.3	-0.2
112	7.4	9.3	-1.9	8.3	-0.9
102	7.2	9.0	-1.8	7.5	-0.3
116	7.5	9.0	-1.5	8.7	-1.2
111	8.2	8.9	-0.7	8.2	0
132	10.0	12.0	-2.0	10.0	0
106	8.2	9.5	-1.3	7.8	+0.4
115	8.6	8.5	-0.1	8.6	0
116	9.2	9.8	-0.6	8.7	+0.5
97	8.1	7.1	-1.0	7.1	+1.0

TBRP   MOISTURE   CALIBRATION   CURVE :   SUBGRADE   1   FIG. 41

$CR = Gg \; 434 + 5.924 \; \%M$

COUNTS / MIN

O - D   VOLUMETRIC % MOISTURE
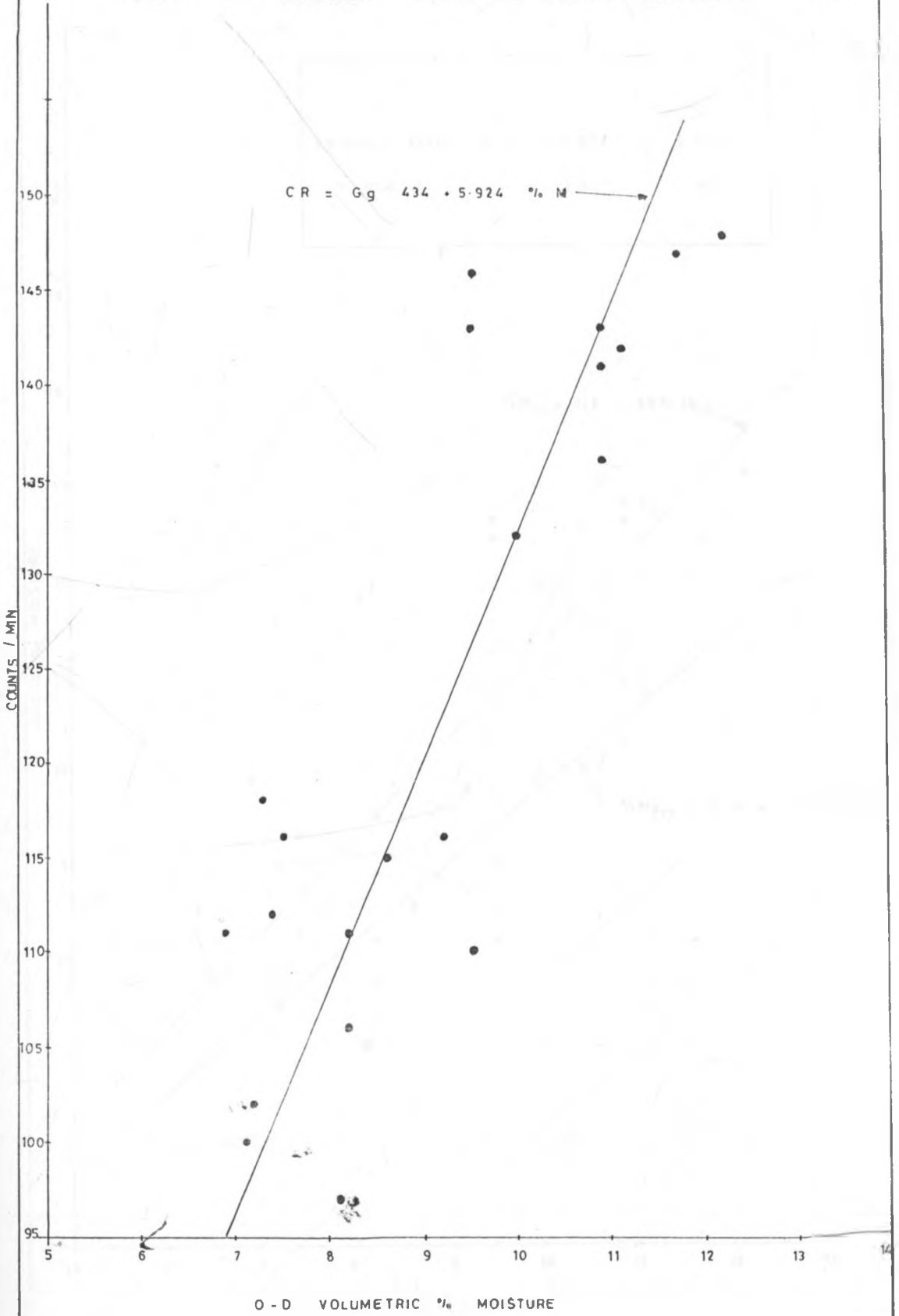
FIG 42   T 8 R P   MOISTURE   CORRELATION   CURVES   (SUBGRADE 1)

Correl.   coeff.   R =   0·832   0·863

S (°/₀m)   =   1·6   ·82

$°/₀ M_{c.c} = 1·3 + ·99 °/₀ M_{O.D}$

$°/₀ Mg_{c.c} = 2·0 + ·785 °/₀ M_{OD}$

GAUGE °/₀ MOISTURE
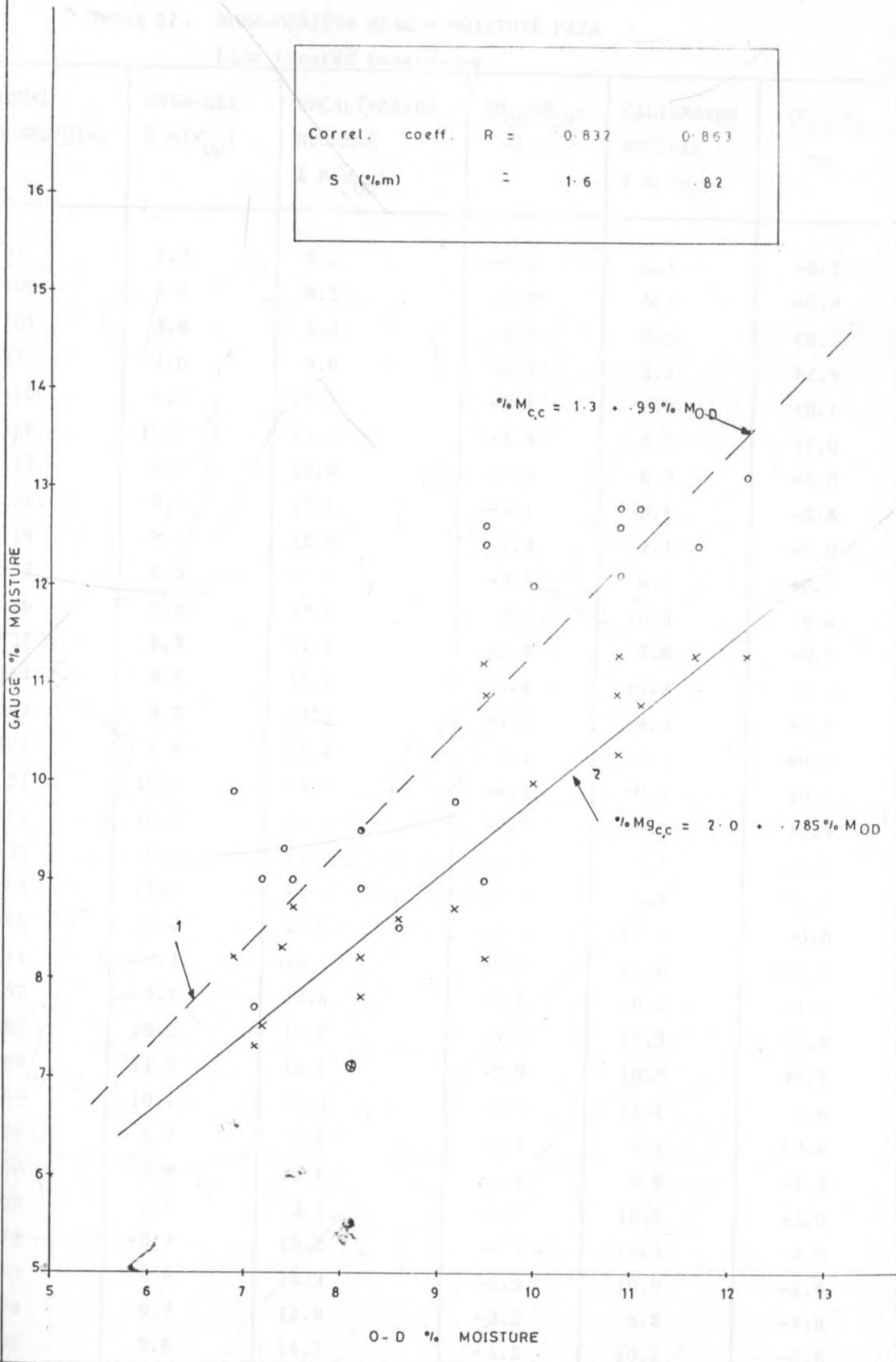
O - D °/₀ MOISTURE

Table 27 :   BURA-GARISSA ROAD - MOISTURE DATA

Lime treated basecourse

SIGNAL COUNTS/MIN.	OVEN-DRY % M(M_{OD})	UNCALIBRATED NUCLEAR % M(M_{OD})	(M_{OD}-M_{UN}) ΔD_1	CALIBRATED NUCLEAR % M (M_C)	(M_{On}-M_C) ΔH_2
97	5.0	8.2	-3.2	5.1	-0.1
100	5.6	8.5	-2.9	5.4	+0.2
101	5.8	8.2	-2.4	5.5	+0.3
97	7.6	9.0	-1.4	5.1	+2.5
110	6.4	9.5	-3.1	6.3	+0.1
148	10.6	13.0	-2.4	9.6	+1.0
115	8.7	10.6	-1.9	6.7	+2.0
136	8.0	12.1	-4.1	8.6	-0.6
119	9.1	11.4	-2.3	7.1	+2.0
132	8.3	11.8	-3.5	8.2	+0.1
156	9.5	13.2	-3.7	10.3	-0.8
137	8.3	12.1	-3.8	8.6	-0.3
161	9.5	15.1	-5.6	10.8	-1.3
145	9.5	13.5	-4.0	9.3	+0.2
122	7.8	10.4	-2.6	7.3	+0.5
157	10.5	14.7	-4.2	10.4	+0.1
141	10.5	13.3	-2.8	9.0	+1.5
156	10.4	15.1	-4.7	10.3	+0.1
148	11.3	14.2	-2.9	9.6	+1.7
166	10.4	15.0	-4.6	11.2	-0.8
171	12.3	16.1	-3.8	11.6	+0.7
152	8.9	13.4	-4.5	10.0	-1.1
167	10.5	15.7	-5.2	11.3	-0.8
160	11.2	15.1	-3.9	10.7	+0.5
165	10.1	15.0	-4.9	11.1	-1.0
108	6.7	9.6	-2.9	6.1	+0.6
150	7.9	12.8	-4.9	9.8	-1.9
159	8.6	13.5	-4.9	10.6	-2.0
178	10.7	15.2	-4.5	12.3	-1.6
153	9.8	14.3	-4.5	10.0	-2.0
139	9.7	12.9	-3.2	8.8	-1.6
155	9.6	14.1	-4.5	10.2	-0.6
175	10.8	17.3	-6.5	12.0	-1.2
160	9.9	15.5	-5.6	10.7	-0.8

FIG. 43

TBRP   MOISTURE   CALIBRATION   CURVE

LIME   STABILISED   BASE   COURSE

$CR = 39 + 11.3$ % M_{OD}

BURA GARISSA RD. Lime treated Base - course FIG. 44
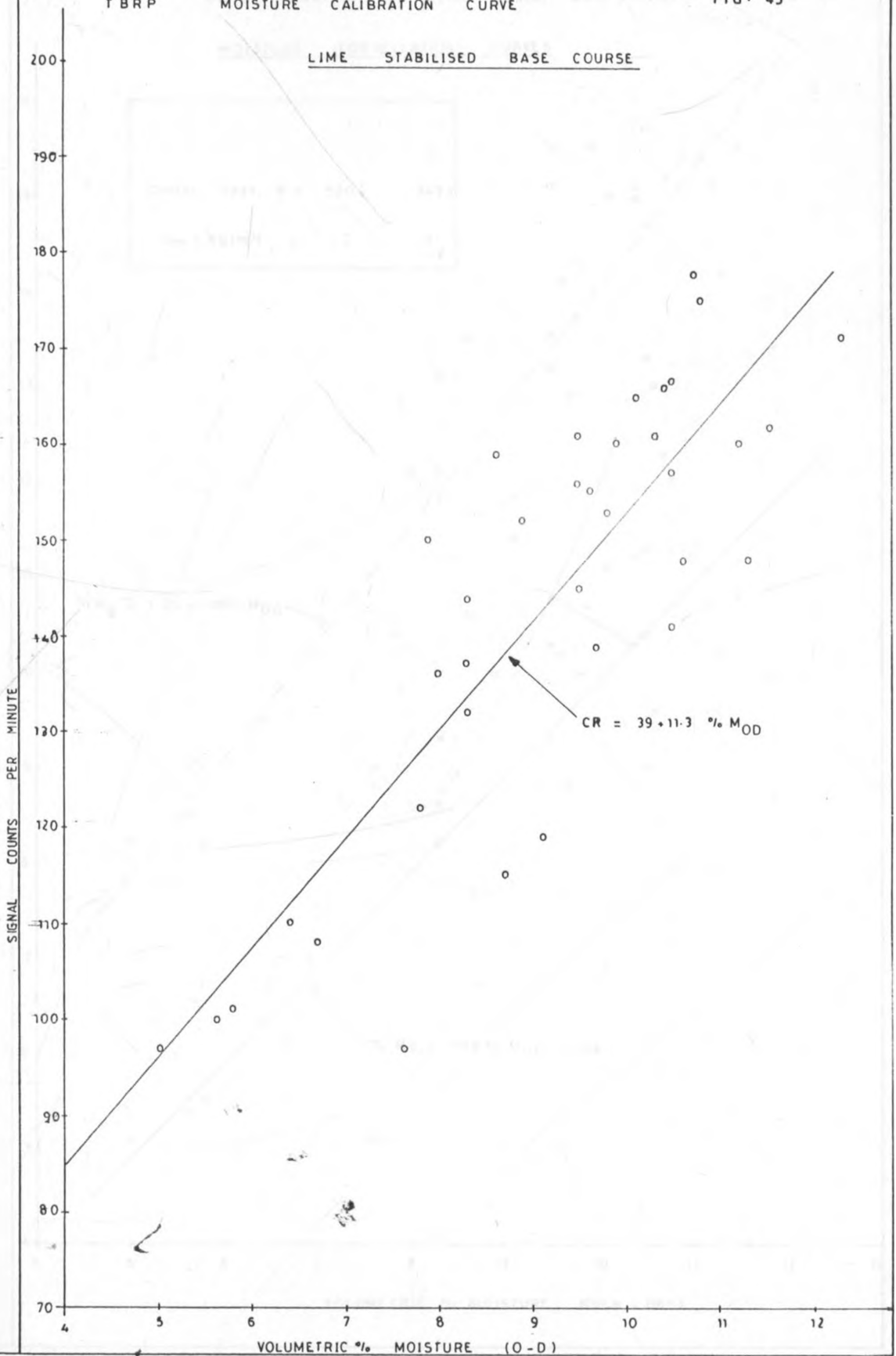
MOISTURE CORRELLATION CURVES

Correl. coef. R = ·9002 · 8434

S_m (Kg/m^3) = 1·3 1·1

$\%M_g = 1·25 + 1·58\% M_{OD}$

①

②

$\% Mg_{c,c} = ·996 \% M_{OD} - 0·05$

GAUGE % MOISTURE

VOLUMETRIC % MOISTURE (OVEN - DRY)
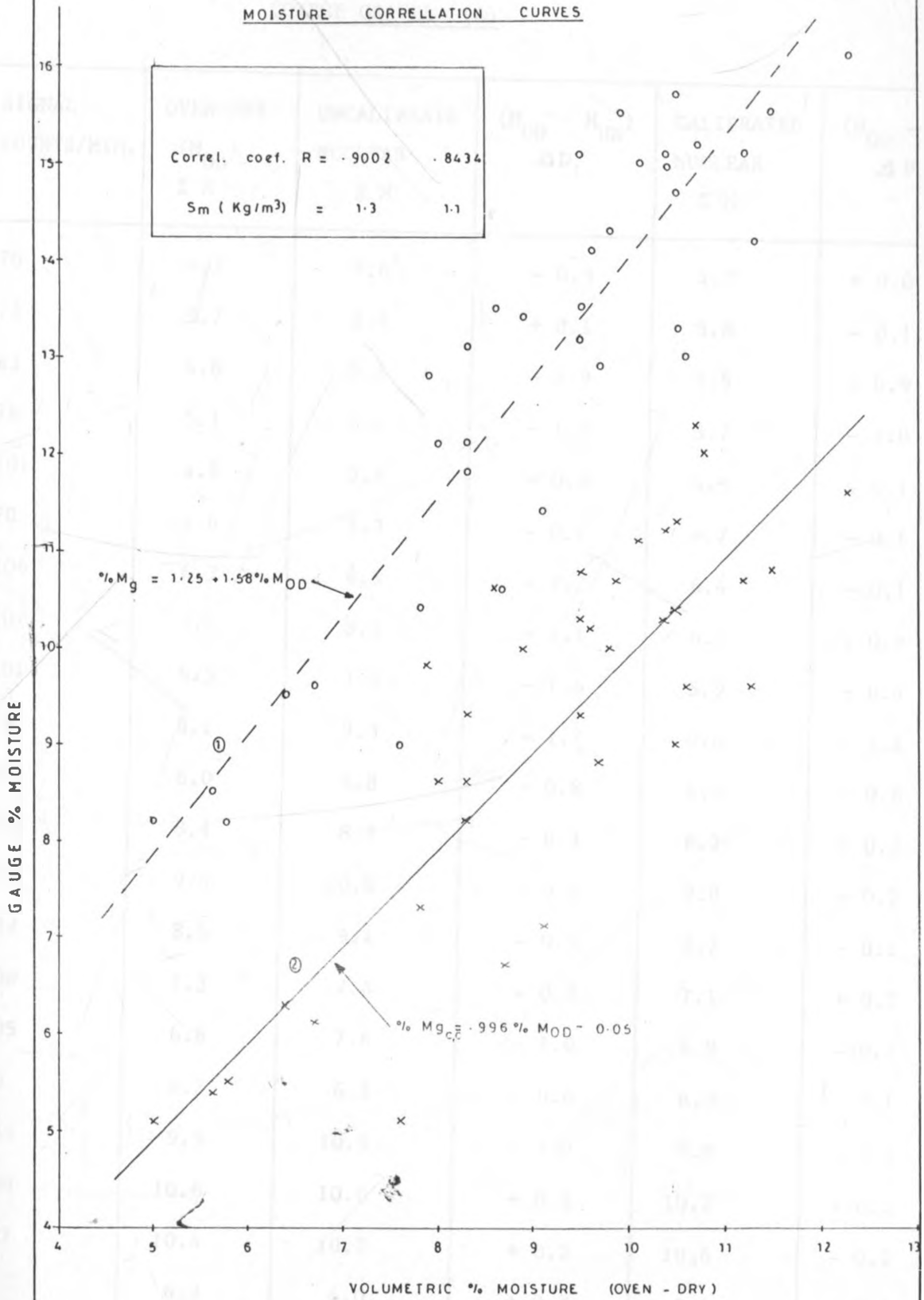
Table 28: LODWAR–KAKUMA ROAD – MOISTURE RESULTS

COARSE GRAVEL   (A)

SIGNAL COUNTS/MIN.	OVEN-DRY (M_{OD}) % M	UNCALIBRATE NUCLEAR % M	$(M_{OD} - M_{UN})$ ΔD_1	CALIBRATED NUCLEAR % M	$(M_{OD} - M_C)$ ΔD_2
70	4.7	5.6	− 0.9	4.7	+ 0.0
73	5.7	5.6	+ 0.1	5.8	− 0.1
83	4.6	6.5	− 1.9	5.5	− 0.9
79	5.1	6.1	− 1.0	5.2	− 1.0
101	4.8	5.4	− 0.6	4.9	− 0.1
70	4.6	5.3	− 0.7	4.7	− 0.1
106	6.3	8.5	− 2.2	6.4	− 0.1
107	7.4	8.5	− 1.1	6.5	+ 0.9
101	6.3	7.9	− 1.6	5.9	+ 0.4
118	8.1	9.3	− 1.2	8.6	− 1.2
110	8.0	8.8	− 0.8	8.2	− 0.8
110	8.4	8.7	− 0.3	8.2	+ 0.2
125	9.6	10.0	− 0.4	9.8	− 0.2
117	8.5	9.4	− 0.9	8.7	− 0.2
100	7.3	7.6	− 0.3	7.1	+ 0.2
105	6.6	7.6	− 1.0	6.9	− 0.3
80	6.2	6.2	+ 0.0	6.3	− 0.1
133	9.5	10.5	− 1.0	9.8	− 0.3
130	10.6	10.0	+ 0.6	10.2	+ 0.4
127	10.4	10.2	+ 0.2	10.6	− 0.2
82	6.3	6.0	+ 0.3	6.4	− 0.1
103	7.1	8.2	− 1.1	7.2	− 0.1
127	7.5	10.2	− 2.7	8.3	− 0.8

FIG 45   COARSE   GRAVEL   CAL. CURVE   (A)

COUNTS   PER   MIN.   Vs.   O-D %   MOISTURE

$CR = 34 + 9.6\% M_{OD}$

O D % VOLUMETRIC MOISTURE
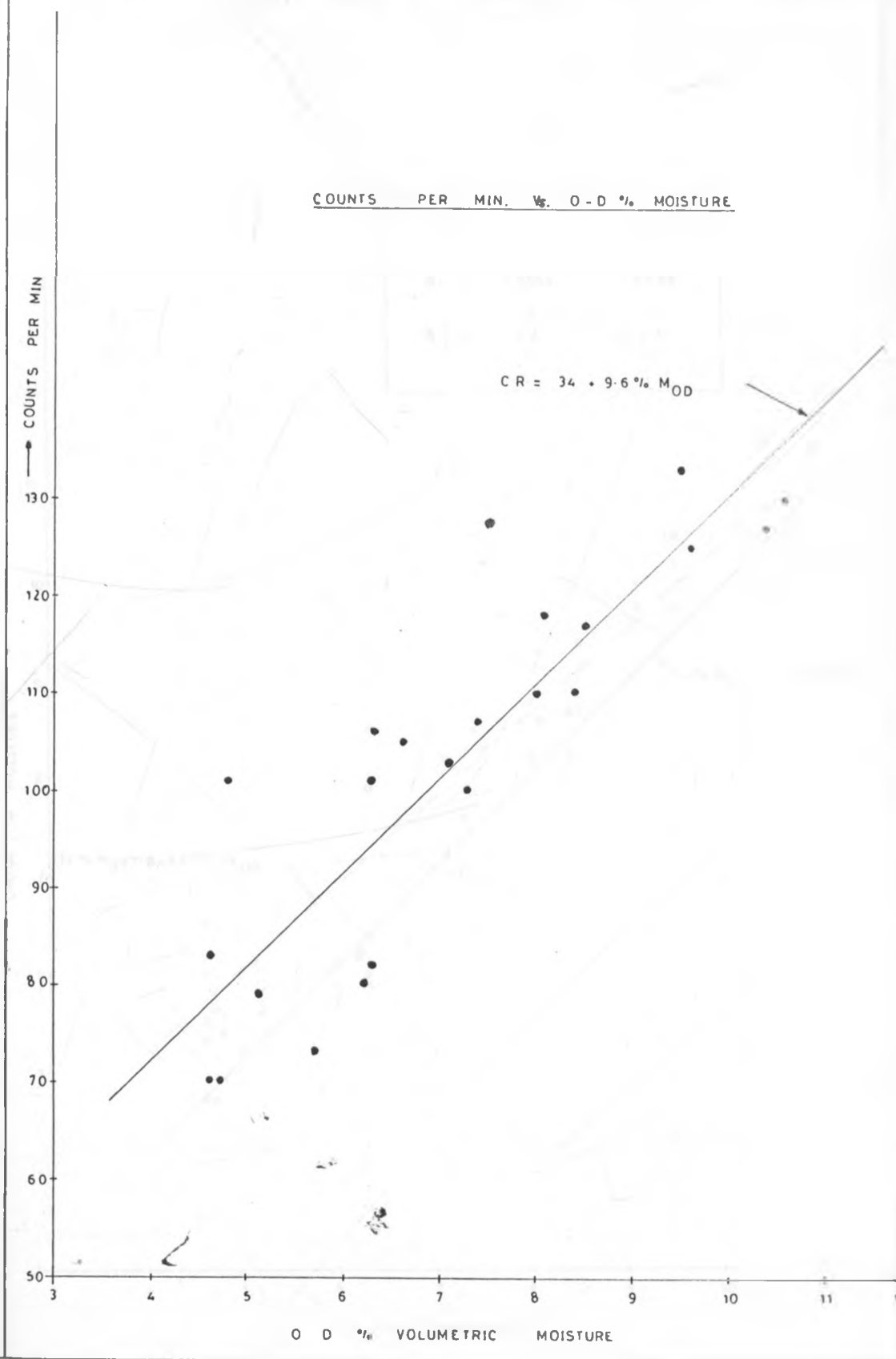
FIG. 46 COARSE GRAVEL (A) CORRELATION CURVE

Table 29:   MOISTURE RESULTS

NATURAL   GRAVEL   (B)

SIGNAL COUNTS/MIN.	OVEN-DRY (M_{OD}) % M	UNCALIBRATE NUCLEAR % M	$(M_{OD} - M_{UN})$ ΔD_1 3-4	CALIBRATED NUCLEAR % M	$M_{OD} - M_C)$ ΔD_2 3-6
77	5.2	5.8	− 0.6	4.5	+ 0.7
77	5.1	5.9	− 0.8	4.5	+ 0.6
78	5.1	6.0	− 0.9	4.7	− 0.9
88	4.3	5.9	− 1.6	6.3	− 1.6
84	6.1	6.0	0.1	5.6	+ 0.5
83	5.6	6.0	− 0.4	5.5	+ 0.1
95	7.8	7.6	0.2	7.4	+ 0.4
84	6.4	5.8	0.6	5.6	+ 0.8
110	8.8	9.8	− 1.0	9.4	− 0.6
95	7.4	6.6	+ 0.8	7.4	+ 0.0
85	7.8	5.9	+ 1.9	6.8	+ 1.0
125	9.4	13.9	− 4.5	12.2	− 2.8
121	12.3	11.0	+ 1.3	11.6	+ 0.7
118	8.8	11.9	− 3.1	11.1	− 2.3
100	9.2	9.6	− 0.4	8.2	+ 1.0
123	10.5	12.2	− 1.7	11.9	− 1.4
120	11.3	13.4	− 2.1	11.4	− 0.1
115	11.0	10.1	0.9	10.6	+ 0.4
101	8.6	9.0	− 0.4	8.4	+ 0.2
100	9.2	8.0	+ 1.2	8.2	+ 1.0
88	5.9	6.9	− 1.0	6.3	− 0.4
120	12.0	10.4	1.6	11.4	+ 0.6
110	10.1	9.4	+ 0.7	9.8	+ 0.3

FIG. 4·7   FIELD   MOISTURE   CALIBRATION   CURVE   (NATURAL   GRAVEL   (B))

$$CR = 48·9 + 6·244\% M_{OD}$$

COUNTS PER MIN

VOLUMETRIC % MOISTURE

FIELD   MOISTURE   CORRELATION   CURVES   (NATURAL   GRAVEL   B)

FIG. 4B

	1	2
Correl. coeff. R =	0.8199	0.9105
S (% m) ≡	1.6	1.1

$\% M_g = 0.07 + .9962 \% M_{OD}$

$\% M_g = 1.13 + 0.911 \% M_{OD}$

COUNT   RATIO

VOLUMETRIC   %   MOISTURE   (OVEN - DRY)
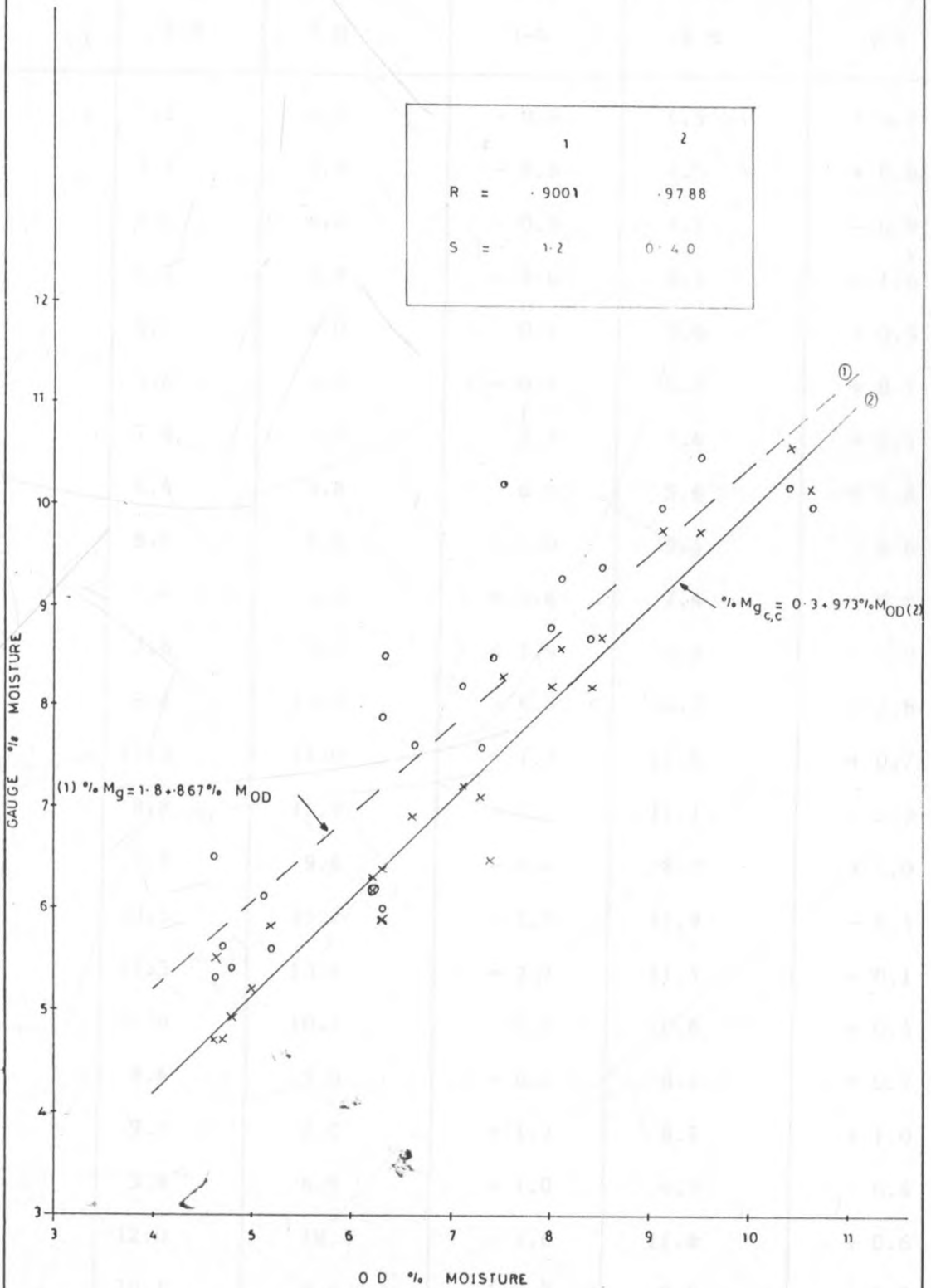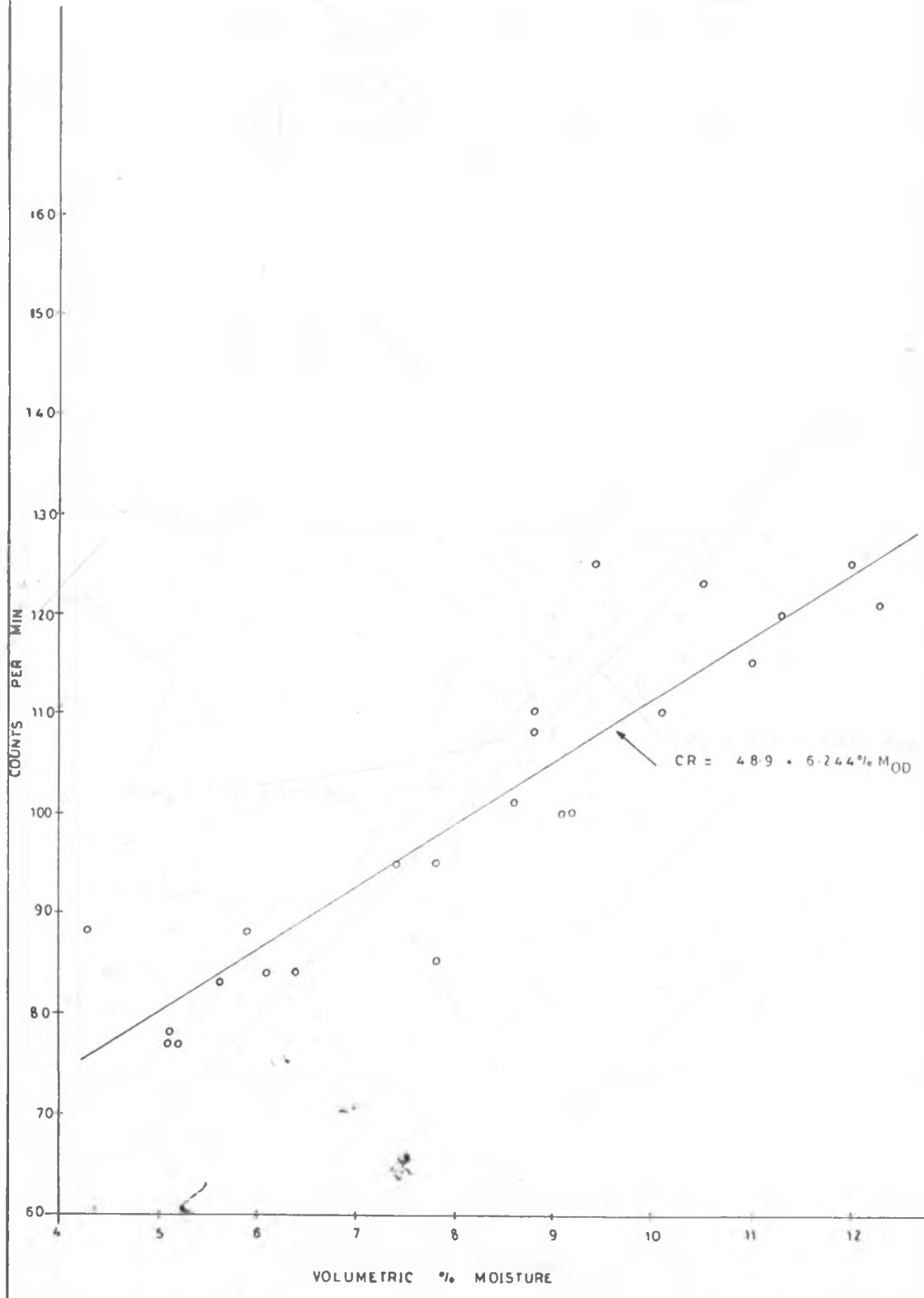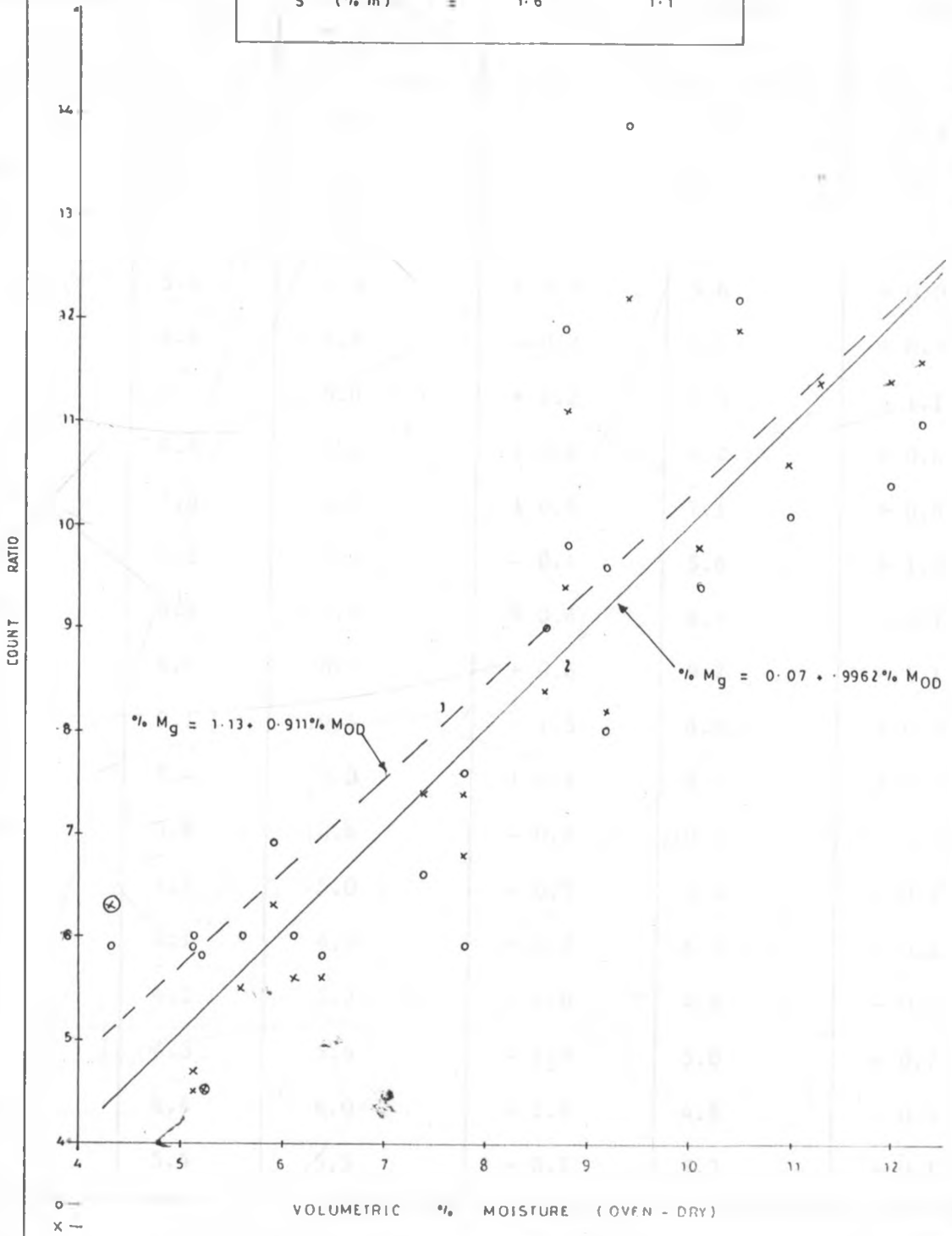
o —
x —

Table 30:   MOISTURE RESULTS

SILTY SAND   (C)

SIGNAL COUNTS/MIN.	OVEN-DRY (M_{OD}) % M	UNCALIBRATE NUCLEAR % M	$(M_{OD} - M_{UN})$ ΔD_1	CALIBRATED NUCLEAR % M	$(M_{OD} - M_C)$ ΔD_2
57	4.1	5.8	- 1.7	3.8	+ 0.3
60	4.2	5.6	- 1.4	4.1	+ 0.1
55	5.0	3.6	+ 1.4	3.6	+ 1.4
75	5.6	3.3	+ 2.3	5.6	+ 0.0
60	4.6	4.8	- 0.2	4.1	+ 0.5
92	6.2	5.0	+ 1.2	7.3	- 1.1
81	6.8	6.2	+ 0.6	6.2	+ 0.6
90	7.6	6.7	+ 0.9	7.1	+ 0.5
75	7.2	7.6	- 0.4	5.6	+ 1.6
108	8.2	7.6	+ 0.6	8.9	- 0.7
115	8.6	8.0	+ 0.6	9.7	- 1.1
107	9.1	10.6	- 1.5	8.8	+ 0.3
110	9.4	9.0	+ 0.4	9.2	+ 0.2
119	9.8	10.4	- 0.6	10.1	- 0.3
73	4.7	5.0	- 0.3	5.4	- 0.7
62	4.1	4.9	- 0.8	4.3	- 0.2
64	4.2	5.2	- 1.0	4.4	- 0.2
69	4.3	5.6	- 1.3	5.0	- 0.7
68	4.4	6.0	- 1.6	4.9	- 0.5
72	5.4	5.5	- 0.1	5.3	+ 0.1

FIG. 49

FIELD MOISTURE CALIBRATION CURVE
(SILTY SAND (C))

$CR = 20 + 9.9 \ \% M_{OD}$

VOLUMETRIC % MOISTURE
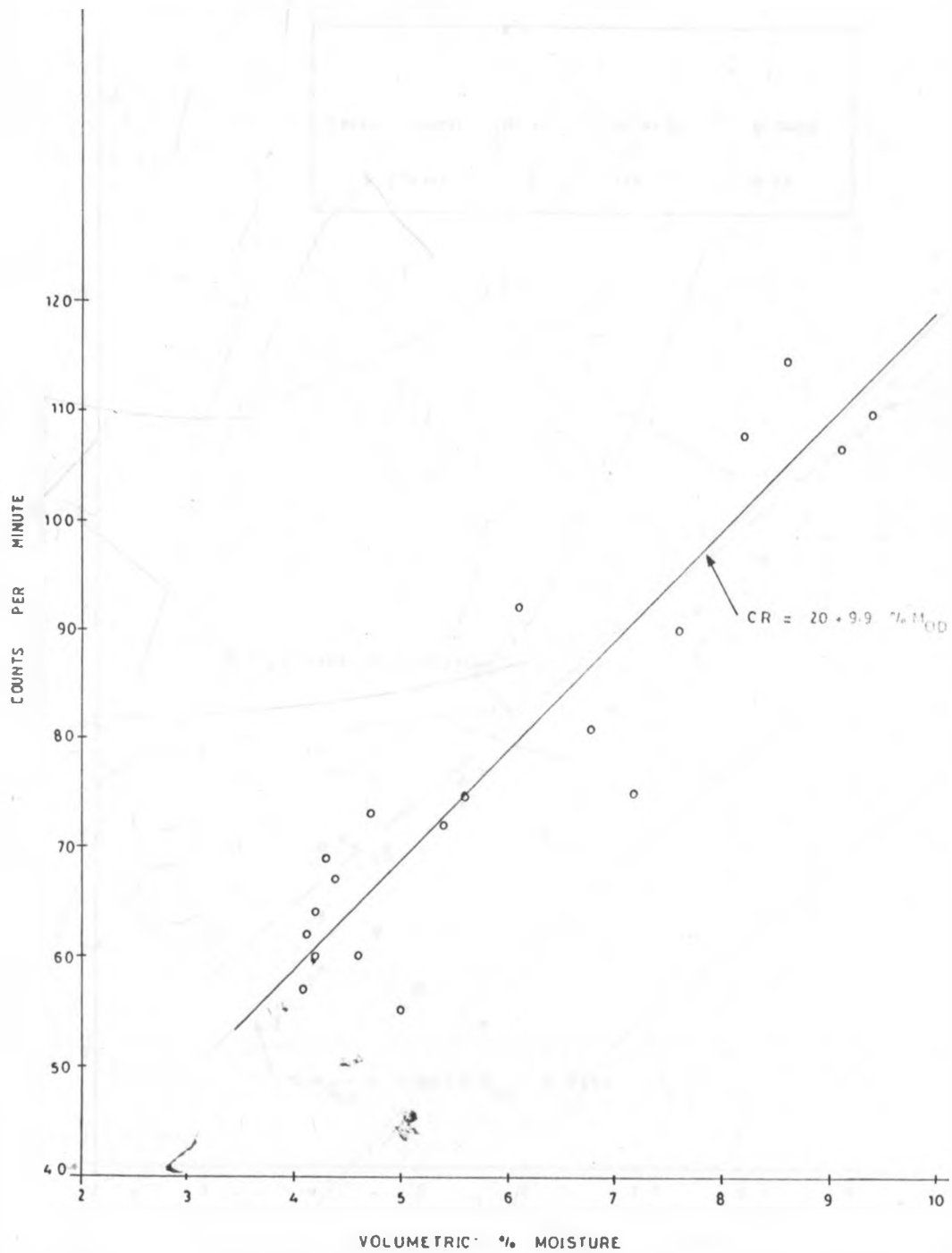
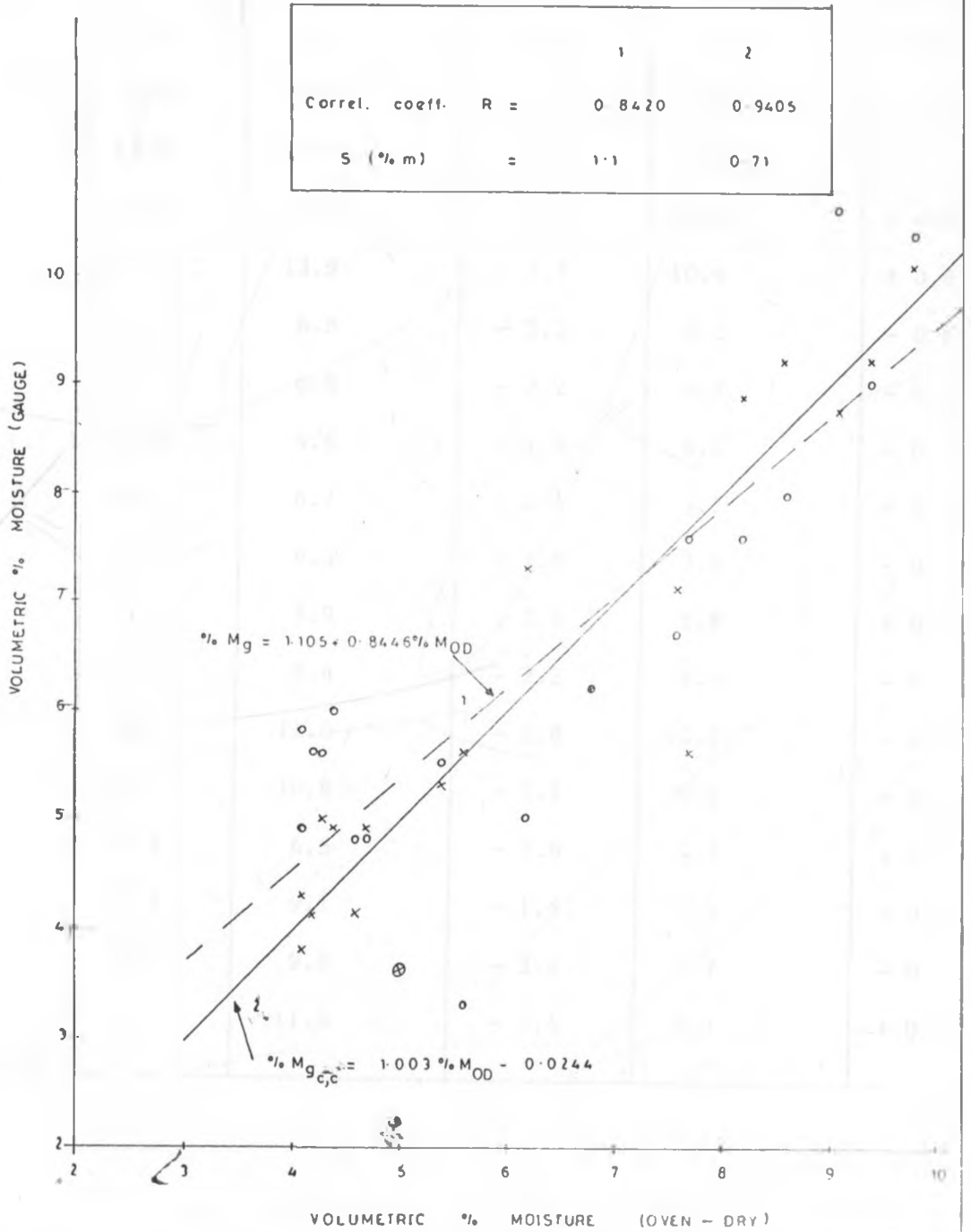FIG. 50   FIELD   MOISTURE   CORRELATION   CURVES.   (SILTY SAND (C))

Table 31:   MOISTURE RESULTS

BROWN CLAY (D)

SIGNAL COUNTS/MIN.	OVEN-DRY (M_{OD}) % M	UNCALIBRATE NUCLEAR % M	$(M_{OD} - M_{UN})$ ΔD_1 3-4	CALIBRATED NUCLEAR % M	$(M_{OD} - M_C)$ ΔD_2 3-6
68	5.6	7.5	− 1.9	4.9	− 0.7
100	6.8	8.5	− 1.7	8.3	− 1.5
135	12.0	14.8	− 2.8	12.0	− 0
122	11.0	13.3	− 2.3	10.6	+ 0.4
120	11.0	13.9	− 2.9	10.4	+ 0.6
70	4.5	6.8	− 2.3	5.1	− 0.6
68	4.6	6.8	− 2.2	4.9	− 0.3
61	3.8	4.8	− 1.0	4.1	− 0.3
51	4.3	6.7	− 2.4	3.1	+ 0.9
58	4.4	6.3	− 1.9	3.8	+ 0.6
49	3.7	5.9	− 2.2	2.8	+ 0.9
105	7.2	9.4	− 2.2	8.8	− 0.4
118	8.2	11.0	− 2.8	10.2	− 2.0
97	9.1	10.8	− 1.7	8.0	+ 1.1
63	4.9	6.5	− 1.6	4.3	+ 0.6
89	7.7	9.1	− 1.4	7.1	+ 0.6
95	6.4	9.8	− 3.4	7.7	− 0.7
98	9.2	11.6	− 2.4	8.1	+ 0.9

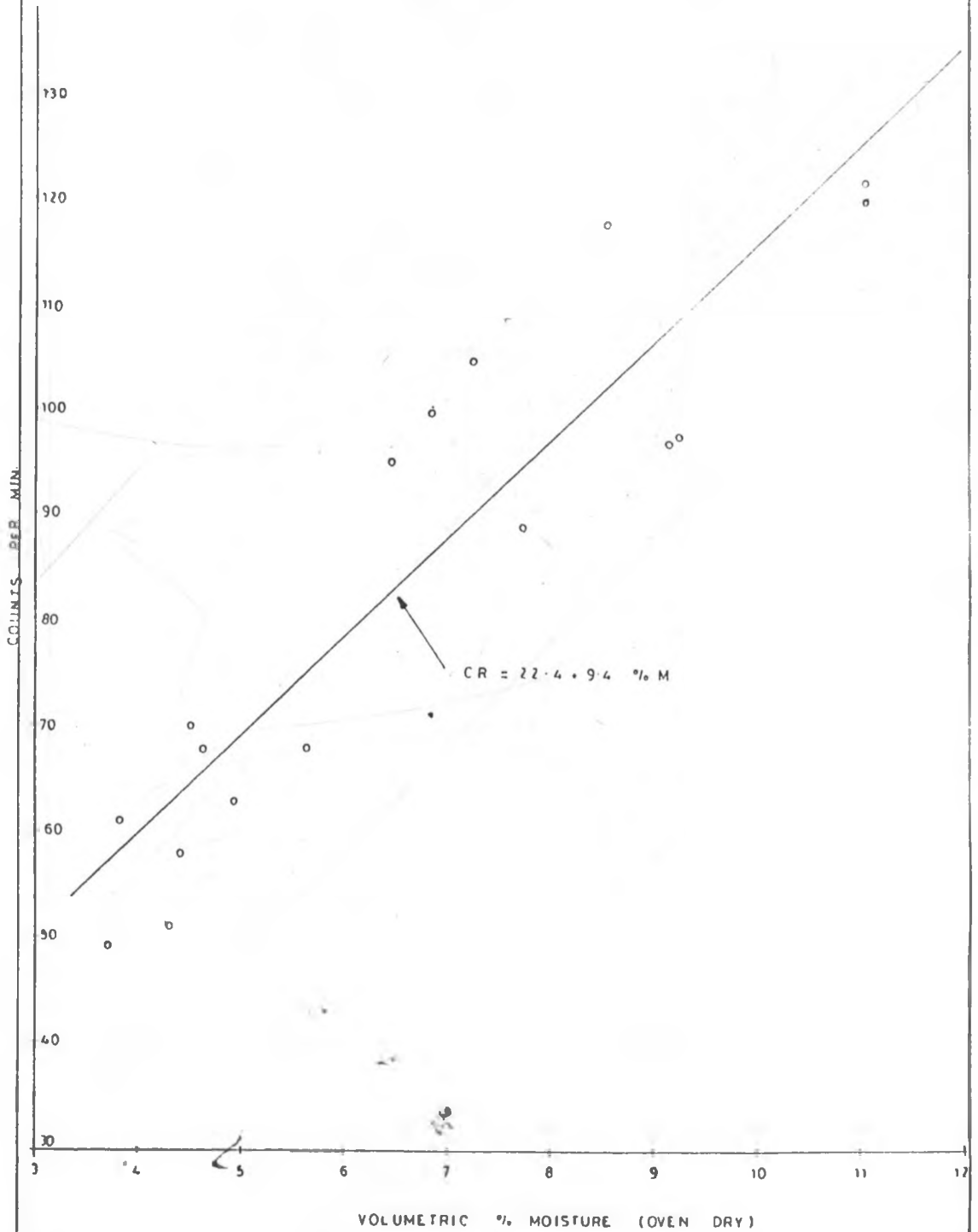FIG.51 FIELD MOISTURE CALIBRATION CURVE (BROWN CLAY SILT)

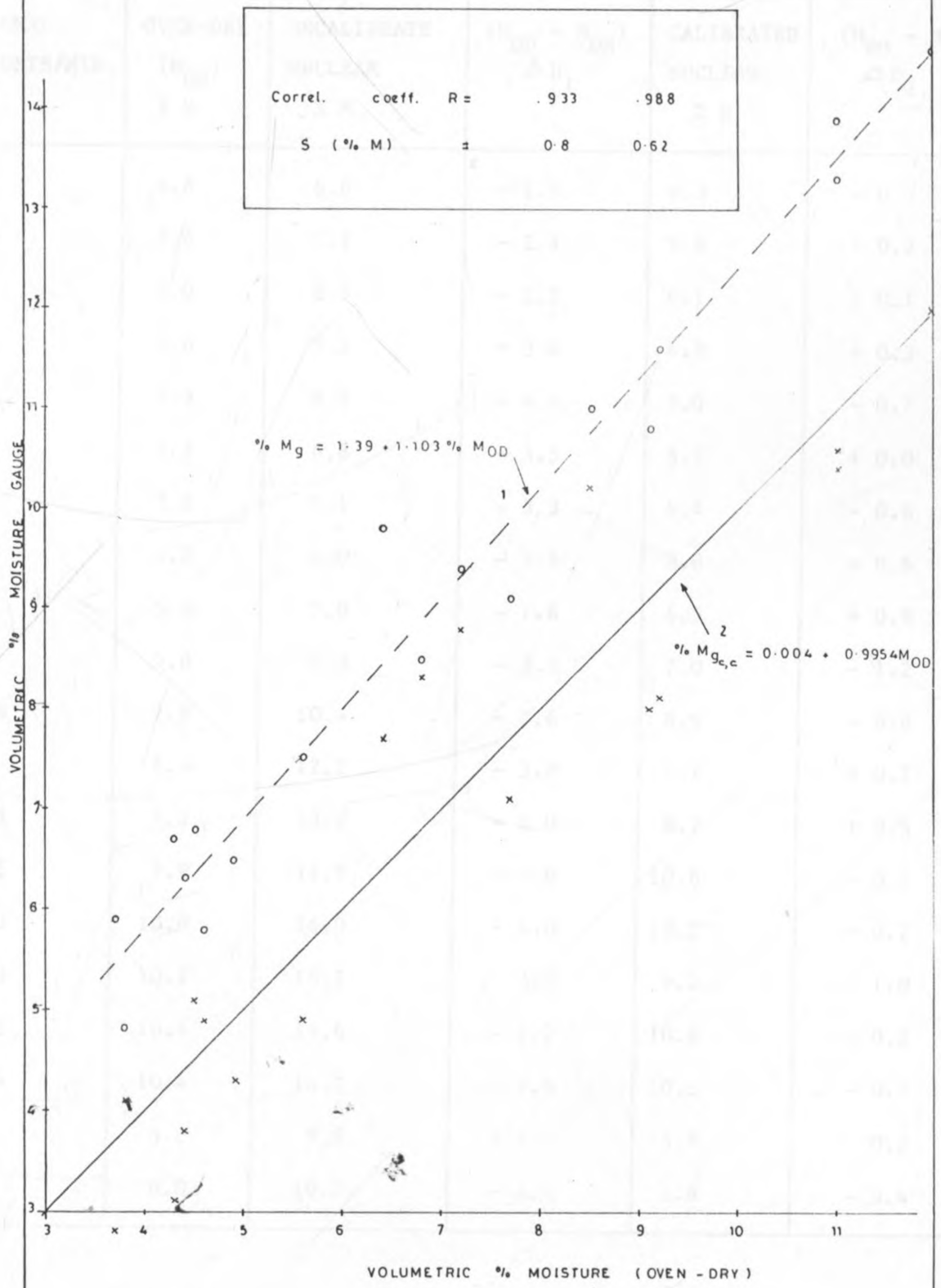FIG. 52 FIELD MOISTURE CORRELLATION CURVES (BROWN CLAY (D))

Table 32:   MOISTURE RESULTS

MATERIAL E

SIGNAL COUNTS/MIN.	OVEN-DRY (M_{OD}) % M	UNCALIBRATE NUCLEAR % M	$(M_{OD} - M_{UN})$ ΔD_1	CALIBRATED NUCLEAR % M	$(M_{OD} - M_C)$ ΔD_2
60	4.8	6.6	− 1.8	4.3	− 0.5
75	5.6	7.7	− 2.1	5.8	− 0.2
78	6.0	8.5	− 2.5	6.1	− 0.1
60	4.6	8.2	− 3.6	4.3	+ 0.3
67	5.3	9.5	− 4.2	5.0	− 0.7
50	3.3	6.8	− 3.5	3.3	+ 0.0
61	3.8	7.1	− 3.3	4.4	− 0.6
53	4.2	8.0	− 3.8	3.6	+ 0.6
62	5.4	7.0	− 1.6	4.5	+ 0.9
88	5.8	9.3	− 3.5	7.0	− 1.2
104	7.8	10.4	− 2.6	8.6	− 0.8
95	8.4	12.2	− 3.8	7.7	+ 0.7
105	9.2	13.2	− 4.0	8.7	+ 0.5
125	9.9	14.9	− 5.0	10.6	− 0.7
120	10.0	14.0	− 4.0	10.2	− 0.2
110	10.2	14.1	− 3.9	9.2	− 1.0
125	10.4	14.6	− 4.2	10.6	− 0.2
124	10.4	14.2	− 3.8	10.5	− 0.1
76	5.6	9.8	− 4.2	5.8	− 0.2
82	6.0	10.0	− 4.0	6.4	− 0.4

FIG 53

FIG. 53   FIELD   MOISTURE   CALIBRATION   CURVE

(CLAYE   SAND (E))

$CR = 15.89 + 10.26\% \, MOD$
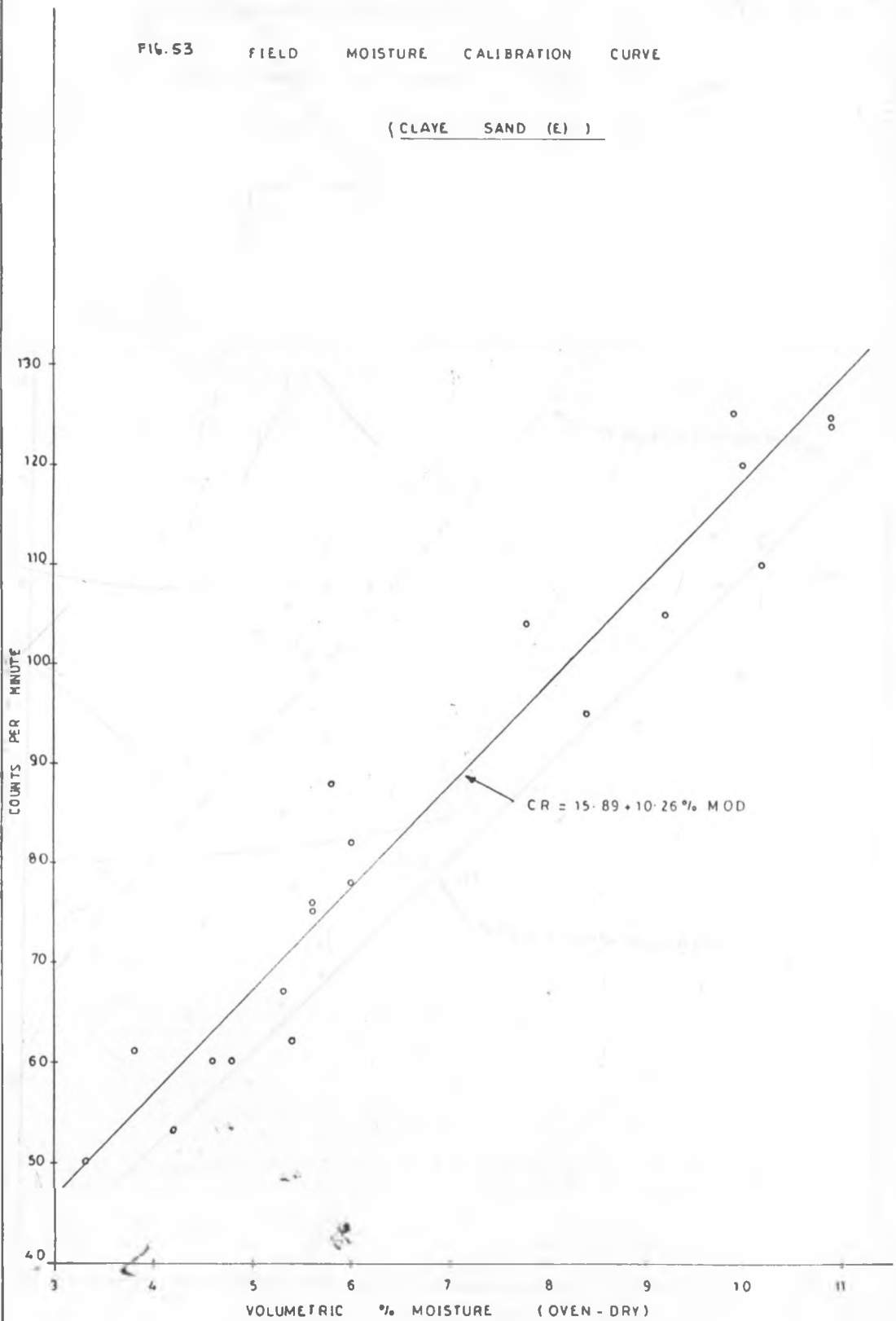
FIELD   MOISTURE   CORRELLATION   CURVES   (CLAYEY   SAND (E)).   FIG. 54

Correl. Coeff. R = 0·9451 (1)   0·9719 (2)

(%m) = 0·8   ·59

$\% M_g = 2·1 + 1·1871 \% M_{OD}$

$\% M_{g,c} = 1·00 \% M_{OD} - 0·006$

VOLUMETRIC % MOISTURE [GAUGE]

Volumetric % Moisture (Oven — Dry)
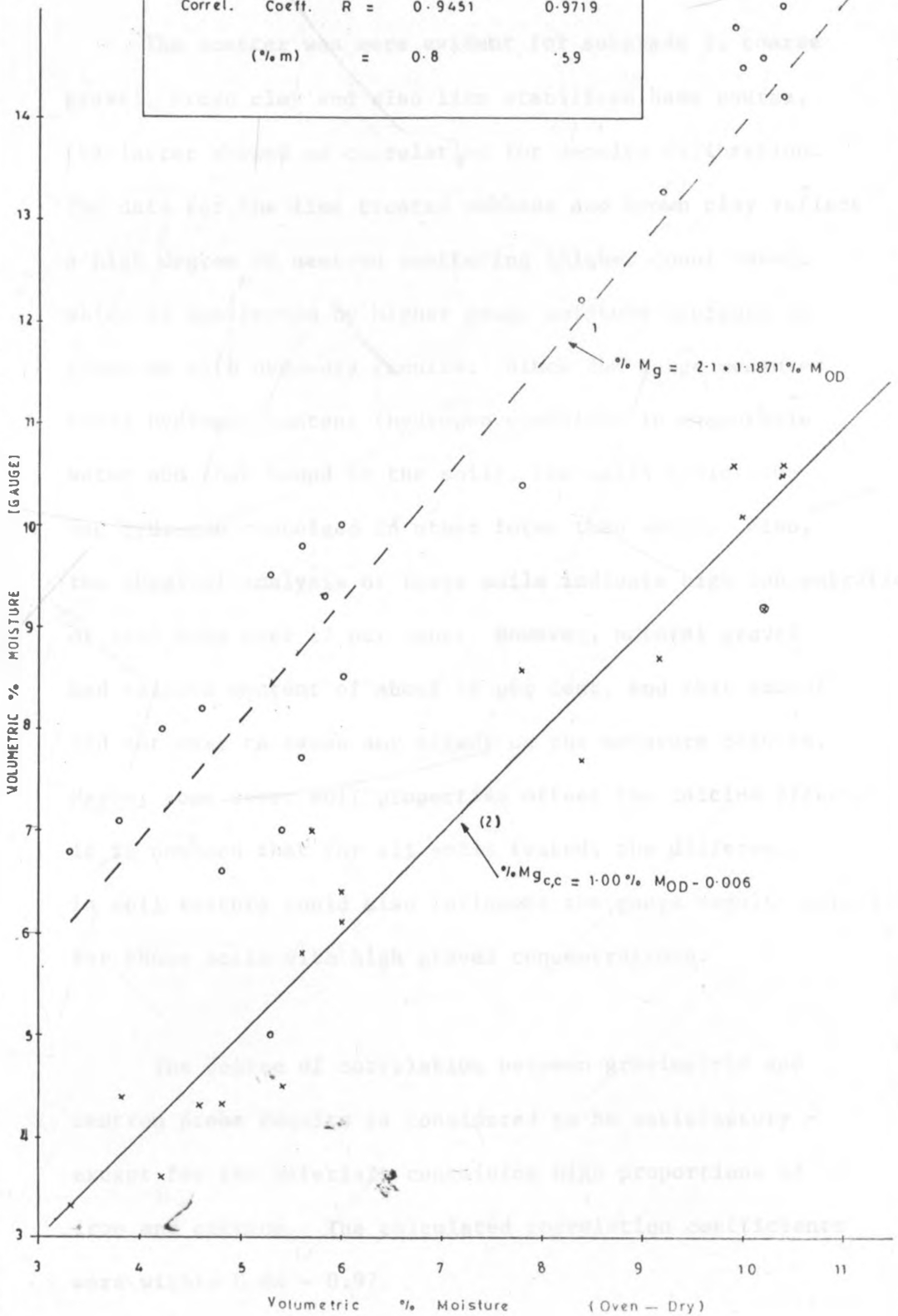
The scatter was more evident for subgrade 1, coarse gravel, brown clay and also lime stabilised base course, the latter showed no correlation for density calibration. The data for the lime treated subbase and brown clay reflect a high degree of neutron scattering (higher count rate), which is manifested by higher gauge moisture contents as compared with oven-dry results. Since the gauge measures total hydrogen content (hydrogen contained in evaporable water and that bound in the soil), the soils could have had hydrogen contained in other forms than water. Also, the chemical analysis of these soils indicate high concentration of iron even over 12 per cent. However, natural gravel had calcium content of about 14 per cent, and that amount did not seem to cause any effect on the moisture results. Maybe, some other soil properties offset the calcium effect. It is noticed that for all soils tested, the difference in soil texture could also influence the gauge results especially for those soils with high gravel concentrations.

The degree of correlation between gravimetric and neutron probe results is considered to be satisfactory - except for the materials containing high proportions of iron and calcium. The calculated correlation coefficients were within 0.84 - 0.97.

Also, the nuclear gauge measures the average content of

a relatively large volume of material, whereas the oven-dry

samples represent only 150 to 200 gms of soil. The differences

are considered to account for the major portion of the observed

variations when comparing moisture contents determined by

these methods. Although oven-dry is the widely accepted

standard method for measurement of moisture, there are sources

of error that must be considered. Interferences are present

in the form of sample decomposition and water of crystallization.

Moisture or gases may be absorbed between the time the sample

is taken and the time it is weighed.

CHAPTER   FIVE

5.0   CONCLUSIONS

5.1   General

The results obtained in this investigation indicated
clearly that before the gauge can be employed for density and/
or moisture measurement on site, initial calibrations should
be carried out on each material likely to be encountered. This
can be achieved either in the laboratory using mould of
material or on the site by comparing in-situ measurements
with the standard sand replacement method. The latter procedure
(field calibration) while producing probably more scattered
results, would possibly have the advantage of obtaining
larger density range, more calibration samples and an adjustment
for the effect of density gradients on the site. The overall
conclusions drawn from this work can be summarised as follows:-

5.2   Laboratory Calibration

Relatively small magnitudes of error were found in the
laboratory density calibration curves, however, a deviation
from the manufacturer's calibration curve was recognised.
The larger errors were believed to be due to the measurement

particularly on loose soil (natural gravel and silty sand) even after compaction. Also, the determination of the exact soil volume as tested by the sand replacement method was subject to error due to difficulties in levelling the top surface of calibration model.

The deviation of the calibration curves from the factory plot is believed to be due to the differences in chemical composition between the soil materials and the materials used by the manufacturer (Troxler laboratories). Though laboratory calibration is feasible, a great deal of work is involved and may not be a worthwhile procedure for routine calibration of gauge for every new soil material.

5.3 Field Calibration

Using Troxler's calibration, the density results, in most cases, were deviated from those obtained by sand replacement method with systematic errors which confirmed the laboratory results. The data were markedly affected by the type of material, that is, chemical composition and soil texture. In order to obtain reliable results using the nuclear method, the gauge should be calibrated before attempting the measurements on a specific soil. The errors given in the results analysis were calculated after eliminating this effect by performing

an individual calibration for each soil tested.

It can be concluded that calibration on 20-25 sand replacement samples taken for test on each soil type should be sufficient. A correction for soil hydrogen content on the sample for gamma attenuation will further improve the results.

5.4 FIELD TESTS

5.4.1 SOIL

Both the two methods sand replacement and nuclear gauge which were used in-situ for density determination were subject to errors. From sand replacement tests, the source of error could be due to inaccurate calculation of the volume of excavated soil, whereas the gauge errors are due to statistical fluctuations of the counts, soil texture and in-depth density differences within the same compacted layer.

Standard deviations for the gauge values when measuring dry density of the various soils were within 17-46 kg/m^3 (1.1% - 2.3%) with respect to the mean density range. The standard deviation values presented affect the way in which the gauge should be used in the field.

The sand replacement tests are relatively time consuming
and the results are obtainable in 24 hours after sampling,
whereas, the gauge results can be obtained on spot within
few minutes. Thus, more tests may be performed in a given
area within a specified time. Having more results, the
compaction of a given area will be better defined.

5.4.2 ASPHALT CONCRETE

The density results of the 50 mm thick layer read
directly from the gauge in its backscatter mode had relatively
no correlation with the core density values. However, after
calibration or the use of nomographic method of density
adjustment, the results improved appreciably. The average
standard deviations for the density results obtained from
the calibration curve and from nomograph were respectively
33 kg/m^3.

On the basis of preliminary results for asphalt concrete
density measurement by nuclear method, it may be concluded
that the readings from the gauge with additional use of
a nomograph could be used in the field without prior calibration.
However, more tests should be done on more types of asphaltic
concrete wearing courses in order to confirm the above
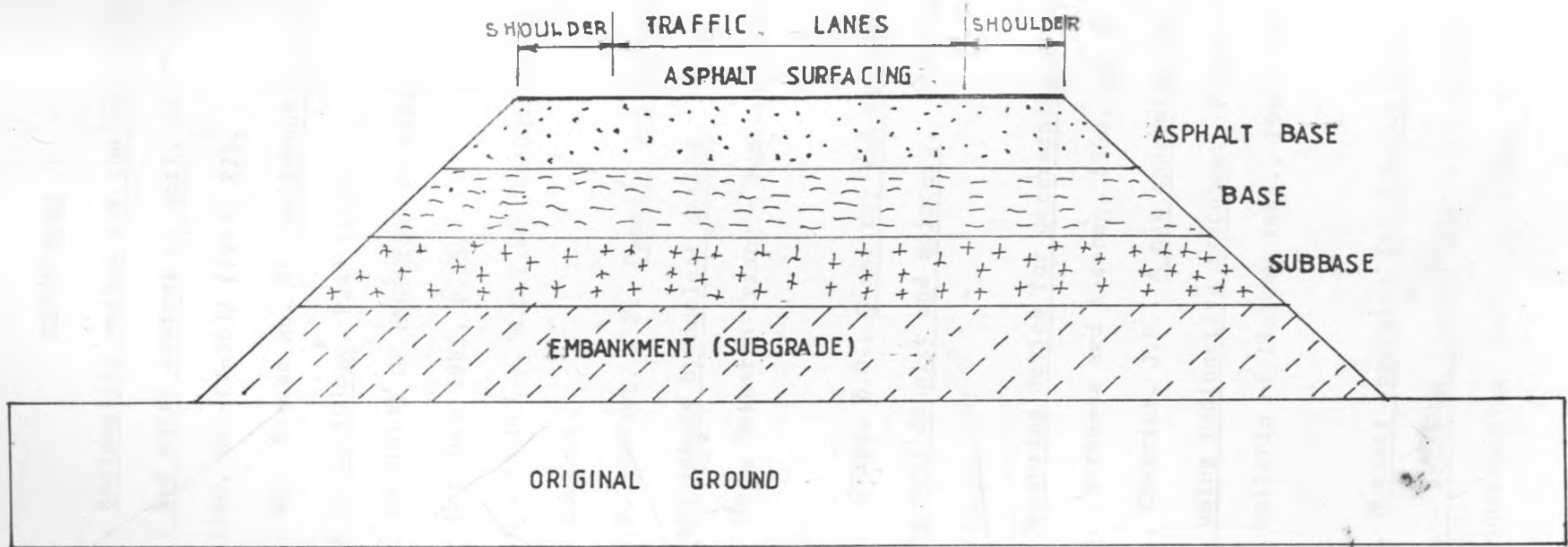conclusion.

5.5 MOISTURE

The majority of the results obtained from the gauge
reading were systematically higher than those from oven-dry
method. This can implicate that hydrogen content in the
soil in the form other than water (bound or absorbed water,
interlayer water, hydrates and hydroxy water and from organic
matter) is biasing the results, since, they additionally
cause the slowing down of neutrons. Thus, for moisture
determination by the gauge, calibration for different types
of soil should be done prior to use of the gauge. The accuracy
of moisture determination expressed as relative standard
deviation is unacceptably high since the time of measurement
was only one minute (due to the contractor's time limitation)
which was the reason. The error due to counting statistics
contributes most to the total error. The contribution to
the total error for low moisture contents exceeds 4 per
cent and for higher moisture contents, it exceeds 2 per cent.
By increasing the counting time upto 4 minutes, the error
due to counting statistics would decrease by 50 per cent
and this would improve accuracy.

For a given hydrogen content, different count rates
were obtained for different soils. The significantly lower
data were for subgrade 1 and also for silty sand, brown

clay and clayey sand.   The reason for this could be the
presence of elements on the site which highly absorb thermal
neutrons as rare earth elements.   Unfortunately, it was
not possible to determine these elements and confirm the
above statement.   Since soil is often heterogeneous, one
can expect the changes in neutron absorbing elements from
one point to another and therefore the moisture determination
does not seem to be very accurate.   It could be that the
tested soils have a volcanic origin and may have rare earth
elements.

SHOULDER | TRAFFIC. LANES | SHOULDER

ASPHALT SURFACING.

ASPHALT BASE

BASE

SUBBASE

EMBANKMENT (SUBGRADE)

ORIGINAL GROUND

ROAD SECTION

REFERENCES

1. Stein, G., <u>Radiometers method for the determination of density and water content of soil</u>, Int. Colloquium Leipzig, 1960, AEC-tr-5632 (1963) 275.

2. IAEA Tech. Rep. Series No. 91 "<u>Guidebook on nuclear techniques in hydrology</u>, P.43 (1983).

3. Patel, M., INSTITUTE OF ENGINEERS OF KENYA. Kenya Engineer - May/June 1985, P.15.

4. Rendel, M.G., (S.S.E.), M.O.T.&C. (Materials branch) - personal contact.

5. Gardner, R.P., Robert, K.F., <u>Density and moisture content measurements by nuclear method</u>. Final report on project 10-5, Research Triangle Inst., Durham, N.C. (1967).

6. Meigh, A.C., Skipp, B.O., <u>Gamma ray and neutron methods of measuring soil density and moisture</u>. Geotechnique, 1960, <u>10</u>, 110/26.

7. Hauss, W., <u>Measuring device for determining compaction embarkments</u>. Strasses and Autoban, 1963, <u>14</u>, (1), 7/9.

8. Alezard, G., Chevrier, J.P., <u>A new apparatus for density measurement using radioactive isotopes</u>. France Min. of Transp., Bulletin of liaison labs., 1965, (13) 10/6.

9. Lewis, W.A., <u>Nuclear apparatus for density and moisture measurements - study of factors affecting accuracy</u>. Rds. & Rd. construction, 1965, <u>43</u>, (506), 37/43.

10.   IAEA Technical Rep. Series No. 112, <u>Neutron soil</u>

      <u>moisture gauges</u> IAEA (1970).

11.   Smith, R.E., <u>Nuclear soil-moisture correlation</u>. Hwy.

      Res. Record No. 438, Hwy Res. Board, Washington (1973),

      p.45/53.

12.   Hoffmeyer, C.K., <u>Control of compaction by nuclear</u>

      <u>density meters</u>. Ohio River Division Labs., U.S. Army

      Corps. of Engrs. (1958).

13.   Carlton, P.F., <u>Application of nuclear soil meters</u>

      <u>to compaction control for airfield pavement construction</u>.

      Symposium on nuclear methods for measuring soil density

      and moisture. ASTM Spec. Tech. Pub. No. 293(1961).

14.   Hughes, C.S., Anday, M.C., <u>Correlation and conference</u>

      <u>on portable nuclear density and moisture systems</u>.

      Hwy. Res. Record No. 112 (1967), p. 239-279.

15.   Kuhn, S.H., <u>The effects of type of material on nuclear</u>

      <u>density measurements</u>. Hwy. Res. Rec. No. 66 (1965),

      p. 1-14.

16.   Gunderman, W.G., <u>Current status of nuclear testing</u>

      <u>of moisture and density of soils and related materials</u>.

      Presented at the 4th annual Symposium Eng. Geology

      and soils Eng., Univ. of Idaho, Moscow, April 19-21,

      1966.

17.   Ballard, L.F., Gardner, R.P., <u>Density and moisture</u>

      <u>content by nuclear methods</u>. Interim rep. NCHRP No. 14,

      (1965), p. 32.

18.   Couchet, P., Determination of the calibration curve
        for the neutron moisture meter by chemical soil analysis.
        Isotopes & Rad. Techniques in Soil Physics and Irrigation
        Studies. Proc. Panel FAO/IAEA, Symp. Istanbul,
        June 12-16, 1967, p. 67-82.

19.   Mchenry, J.R., Gill, A.C., The influence of bulk density,
        slow neutron absorbers and time of calibration of
        the neutron moisture probe. Isotopes and Radiation
        Tech. in Soil Physics and Irrigation Studies. IAEA/FAO
        Symp. Istanbul, June 12-16, 1967, p. 83-97.

20.   Jensen, P.A., Somer, A. Scintillation techniques
        in soil moisture and density measurements. Isotopes
        & Rad. Tech. in Soil Physics and Irrigation Studies.
        IAEA/FAO Symp. Istanbul, June 12-16, 1967, p. 31-46.

21.   Lal, R., The effect of soil texture and density on
        the neutron probe calibration on some tropical soils.
        Int. Inst. of Tropical Agriculture, Ibadan, Nigeria, 1975.

22.   Sherwood, P.T., The measurement of in-situ densities
        of cement bound materials. TRRL Lab. Rep. No. 1109
        (1983).

23.   Ahuja, L.R., Williams, R.D., Use of a surface gamma-
        neutron gauge to measure bulk density, field capacity
        and macroporosity in the top soil. Water quality
        and Watershed, Agriculture Research Service,
        U.S. Dept. of Agri. Durant, Oklahoma, IAEA-SM-267/15,
        (1985).

24. James, G.W., <u>A field evaluation of nuclear gauge</u> <u>calibration methods Part 1</u>. Aust. Rd. Const. Authority, Rep. No. 38J286 (1985).

25. Christaller, G., Thies, R., <u>Two new designs of two-source</u> <u>soil moisture gauges</u>. Laboratory of Nuclear Radiation Measurement, Berlin (West), IAEA-SM-267/31 (1985).

26. Cameron, J.F., <u>Nucleonic soil density and moisture gauges</u>. Nuclear Enterprises Limited, Edinburgh, U.K., SM-112/6.

27. Glasstone, E., Edlund, M.C., <u>The elements of nuclear reactor</u> <u>theory</u>. Van Nostrand, New York (1957).

28. Troxler Electronic Labs., 3400-B Series Instruction Manual. Surface Moisture-Density gauges. Research Triangle Park, N.C., U.S.A. (1980).

29. Rewitz, E., Etkin, H., Hazan, A., <u>Soil Sci. Am. J., 46</u>, (1982), 461.

30. BRITISH STANDARD INSTITUTION. BS 1377:1975, <u>Methods of test</u> <u>for soils for Civil engineering purposes</u>. London.

31. BRITISH STANDARDS INSTITUTION. BS 598:1985, <u>Sampling and</u> <u>examination of bituminous mixtures for roads and other paved</u> <u>areas</u>, Part 3. Methods for design and physical testing. London.

32. King, L.G., <u>Gamma-ray attenuation for soil-water-content</u> <u>measurements using ^{241}Am</u>. Isotope and Radiation Techniques in soil Physics and irrigation Studies, Symp., Istanbul, 12-16 June, (1967), SM-94/20.